

**Design and Optimization of an Injectable Biomaterial for
Vocal Fold Augmentation**

A Thesis

Submitted By

Rosario Friedman

In Partial Fulfillment of the Requirements for the Degree of
Master of Science in Mechanical Engineering

TUFTS UNIVERSITY

May 2013

Advisor: Gary Leisk

Abstract

The vocal cords, located in the larynx, are used to create sound. When tissues in the vocal fold are damaged, the associated muscles become atrophied, or other problems arise in the larynx, and it often becomes difficult or impossible to speak. There are many forms vocal fold damage can take, such as nerve damage, muscle atrophy, or superficial scarring from cancer removal, and many treatment options are available, however there is no ideal solution for loss of voice as treatments administered differ depending on the underlying pathology. One of the most commonly used treatments, known as vocal fold augmentation injection, involves injecting a supportive material behind the vocal cords to push them toward the center of the larynx, decreasing the size of the gap between the cords in order to create sound, and making it easier to talk. While this treatment is preferred over more invasive options like laryngeal framework surgery, an augmentation material does not currently exist that meets all of the needs of this application: a long lasting, safe material that matches the viscoelasticity of the vocal fold, is easy to inject, is available off-the-shelf and augments the vocal fold sufficiently. A silk-based biomaterial solution is proposed in this thesis research, and various silk formats investigated for use in vocal fold augmentation injections. Materials are evaluated and down-selected based on rheological properties, degradation time, and *in vivo* safety, as well as ease of delivery and preparation that must be performed by surgeon administering the treatment.

Acknowledgements

I would like to thank my advisor, Dr. Gary Leisk, for all of his help and support during my time at Tufts. I would also like to thank my thesis committee members Dr. Thomas Carroll (also our consulting physician), and Dr. Luisa Chiesa for taking the time to review this project, as well as Dr. Kaplan and Dr. Omenetto for their advice and support.

A huge thank you to Ben Partlow for helping me set up experiments and interpret results, and for being on call for questions about rheology. Thank you to the members of G810 and 2100 at 200 Boston Avenue. Tim Lo (you taught me everything there is to know about silk processing), Nereus Patel, Gabe Perrone, Ethan Golden, Jodie Moreau, Roberto Elia, and everyone else: thank you for all the help you have given me and for making my time at the lab extremely enjoyable. I would also like to thank the Devices and Implants minigroup for their input and support throughout this project, and Milva Ricci, who is really just the greatest.

Lastly I would like to thank my family for all of their support, especially my grandma Billy, who has made my education possible.

Table of Contents

ABSTRACT	2
ACKNOWLEDGEMENTS	3
TABLE OF CONTENTS	4
LIST OF FIGURES	7
LIST OF TABLES	11
1. INTRODUCTION	13
2. BACKGROUND	16
2.1 VOCAL FOLD ANATOMY	16
2.2 GLOTTIC INSUFFICIENCY	20
2.3 TREATMENTS FOR GLOTTAL INSUFFICIENCY	21
2.3.1 <i>Vocal Fold Augmentation Injections</i>	22
2.3.2 <i>Injection Laryngoplasty</i>	23
2.3.3 <i>Thyroplasty</i>	25
2.4 VOCAL FOLD AUGMENTATION INJECTION MATERIALS	26
2.5 MATERIAL SPECIFICATIONS AND CUSTOMER NEEDS	31
2.6 SILK AS A BIOMATERIAL.....	36
2.7 SILK STRUCTURE AND PROPERTIES	37
2.8 SILK SOLUTION PROCESSING	39
2.9 POST-PROCESSING TECHNIQUES	42
2.9.1 <i>Injectable Silk Porous Foams</i>	43
2.9.2 <i>Shear Induced Silk Hydrogels</i>	44
2.9.3 <i>Sonicated Silk Hydrogels</i>	46
2.9.4 <i>Vortexed Silk Hydrogels</i>	47

	5
2.9.5 <i>pH Induced Silk Hydrogels</i>	47
2.9.6 <i>Silk Electrogels</i>	49
2.9.7 <i>Silk Additive Gels</i>	51
2.9.8 <i>Temperature Considerations</i>	52
2.9.9 <i>Hybrids and Combinations</i>	53
3. EXPERIMENTAL METHODS	54
3.1 REGENERATED SILK FIBROIN SOLUTION PROCESSING.....	54
3.2 REGENERATED SILK FIBROIN SOLUTION CONCENTRATION AND BOIL TIME.....	55
3.2.1 <i>RSF Solution Concentration Modeling</i>	57
3.2.2 <i>Compressive Injection Force Testing</i>	59
3.3 RHEOLOGICAL MEASUREMENTS	60
3.4 DEGRADATION STUDIES	63
3.5 POST-PROCESSING METHODS	64
3.5.1 <i>Vortexed Gels</i>	64
3.5.2 <i>Sheared Gels</i>	64
3.5.3 <i>Silk Electrogels</i>	65
3.5.4 <i>Silk Electrogels with additives</i>	66
3.5.5 <i>Additive Gels</i>	70
4. RESULTS AND DISCUSSION	71
4.1 VORTEXED GELS.....	73
4.2 SHEARED GELS	82
4.2.1 <i>Rheology</i>	82
4.2.2 <i>Delivery</i>	89
4.3 SILK ELECTROGELS.....	90
4.3.1 <i>Time Dependent Rheology</i>	90

4.3.2 Silk Electrogels with Sodium Chloride.....	95
4.3.3 Silk Electrogels with Ethanol	102
4.3.4 Degradation	106
4.3.5 Delivery.....	108
4.4 ADDITIVE GELS.....	111
4.4.1 Rheology.....	112
4.4.2 Degradation	113
4.5 INJECTABLE SILK FOAMS.....	114
4.6 SONICATED GELS	114
4.7 PH GELS	115
5. CONCLUSIONS	116
5.1 RHEOLOGY	116
5.2 DEGRADATION	117
5.3 DELIVERY	118
5.4 COMPARISONS OF ALL PROPERTIES	120
6. FUTURE WORK.....	124
6.1 FURTHER TESTING OF ESTABLISHED CONSTRUCTS	124
6.1.1 Silk Electrogels.....	125
6.1.2 Additive Gels	127
6.1.3 Sheared Gels	128
6.1.4 Hybrid Materials.....	130
6.2 ALTERNATIVE APPROACH	131
APPENDIX.....	133
APPENDIX I: SHEAR FLOW CALCULATIONS	133
REFERENCES.....	135

List of Figures

Figure 1: Glottal anatomy and placement [6, 7].	16
Figure 2: Vocal fold anatomy (adapted from [8]).	17
Figure 3: (A) Contraction of the lateral cricoarytenoid muscle rotates the arytenoids medially, adducting the vocal folds. (B) Contraction of the interarytenoid muscle adducts the arytenoids. (C) Contraction of the posterior cricoarytenoid muscles rotates the arytenoids laterally, opening the airway. (D) Contraction of the thyroarytenoid muscles adducts the vocal folds and allows for vocal pitch modification (adapted from[5]).	18
Figure 4: Vibration in a healthy glottis. (A) Coronal view of the vocal fold. 1) Closed vocal fold, subglottal pressure builds up. 2) Lower surface of the vocal cords separate due to rising subglottal pressure. 3) Only upper surfaces are in contact. 4) Air is released as the vocal folds separate. 5, 6) Airflow continues, elastic recoil of the vocal folds and Bernoulli's forces cause the lower surfaces of the vocal cords to draw inward. The mucosal wave propagates superiolaterally. 7) Airflow slows, and the lower lips close. 8) In a zipper like closure, the free edge of the vocal folds close from bottom to top and posterior to anterior. Adapted from [12]. (B) Theory behind stroboscopic aliasing for visualization of vocal fold vibrational modes.	20
Figure 5: Various forms of vocal fold damage. (A) Vocal fold paresis, or weakening of the laryngeal muscles, presents as bowing in the vocal cord on the atrophied side. (B) Vocal fold paralysis, which presents as one immobile cord. (C), (D) Vocal fold polyps and granulomas, which prevent full glottal closure, and may require removal, which often causes scarring on the vocal fold.	21
Figure 6: Vocal fold augmentation injection procedure [1].	23
Figure 7: Injection laryngoplasty procedure [5, 8, 15, 16].	24
Figure 8: Thyroplasty implant placement and medializing effect on the right vocal cord (adapted from [5, 16]). (A) Thyroplasty Incision Site[16]. (B) Silastic® Implant. (C) Gore-Tex® Implant.	26
Figure 9: Structure of native silk fibers [47].	37
Figure 10: Silk fibroin composition and molecular behavior (adapted from [46, 52]).	39
Figure 11: Post-processing techniques for various silk constructs. Adapted from [25, 26].	42

Figure 12: Suggested shear gelation mechanism in natural silk fiber spinning [60].	45
Figure 13: (A) Sonication procedure for creating silk hydrogels (adapted from [26]). (B) Silk fibroin chain interactions induced by sonication [61]	46
Figure 14: (A) Time delayed gelation response of 20%w/v RSF solution at different sonication times. (B) Time delayed gelation response of RSF solutions sonicated for 15 s at various concentrations of silk, and varied pH levels [61].	47
Figure 15: The natural silk spinning process [31].	48
Figure 16: E-Gel formation procedure.	49
Figure 17: E-Gel formation mechanisms [66].	51
Figure 18: Temperature dependence of RSF solution self-assembly rate [49].	53
Figure 19: Silk solution processing [26].	55
Figure 20: Mechanical compression testing for maximum applied force.	56
Figure 21: Shear flow model.	58
Figure 22: (A) Instron test setup. (B) Test needle/catheter. (C) Actual needle/catheter.	59
Figure 23: Averaged maximum compressive load required to maintain a 135.2 mm ³ /s flow rate (8.5 mm/s plunger compression rate) as determined by mechanical testing.	60
Figure 24: Rheometer setup and mechanisms [67].	61
Figure 25: E-Gelling setup.	66
Figure 26: NI-DAQ and thermocouple setup.	68
Figure 27: Typical complex shear modulus curve for silk constructs.	71
Figure 28: Standard G', η , and ζ curves for silk	72
Figure 29: Vortexed gel rheology: Complex shear modulus comparisons between RSF solutions of varying concentration and V _t (3 samples per construct).	74
Figure 30: Rheological comparisons between initial vortexed gels and human vocal fold mucosa (3 samples per data point).	76

Figure 31: Vortexed gel rheology: secondary complex shear modulus comparisons of 8% w/w RSF with varying vortexing times (3 samples per construct).....	77
Figure 32: Rheological comparisons between secondary vortexed gels and human vocal fold mucosa (3 samples per data point).....	79
Figure 33: Sheared gel rheology: complex shear modulus comparisons between 7% RSF solutions injected through various needles (2 samples per construct). ...	82
Figure 34: Rheological comparisons between sheared gels (various needles) and vocal fold mucosa (2 samples per data point).....	84
Figure 35: Sheared gel rheology: complex shear modulus comparisons of RSF solutions sheared by injection through a 27G needle with and without a catheter (3 samples per construct).	86
Figure 36: Rheological comparisons between 27G needle sheared gels (with and without a catheter) and vocal fold mucosa (3 samples per data point).	88
Figure 37: Proposed sheared gel delivery mechanism.....	89
Figure 38: E-Gel rheology: complex shear modulus of RSF solutions and E-Gels as a function of solution age (3 samples per construct per time point).....	91
Figure 39: E-Gel rheology: complex shear modulus comparisons between E-Gels and RSF solutions of different boiling times (48 samples or more per construct).	92
Figure 40: Rheological comparisons between RSF solutions, 10 minute - 25 volt E-Gels, and vocal fold mucosa (48 samples or more per data point). (A) Storage modulus. (B) Dynamic viscosity. (C) Damping ratio.	93
Figure 41: Initial temperature testing for salinated E-Gels: 7 % w/w 15mb RSF + 0.9% w/v NaCl temperature over time during electrogelation (average of 3 trials).	96
Figure 42: Maximum temperature (over a two-minute gelation period) vs. salinity for salinated E-Gels (average over 3 trials per data point).	97
Figure 43: Salinated E-Gel rheology: complex shear modulus comparisons between different levels of salinity in E-Gels (3 samples per construct).	98
Figure 44: Rheological comparisons between salinated E-Gels and vocal fold mucosa (3 samples per data point). (A) Storage modulus. (B) Dynamic viscosity. (C) Damping ratio.	100

Figure 45: Percentage of silk solution converted to a hydrogel upon electrogelation with various concentrations of salt (3 samples per construct). ..	101
Figure 46: E-Gels with ethanol: complex shear modulus comparisons (3 samples per construct).	103
Figure 47: Rheological comparisons between E-Gels with ethanol and vocal fold mucosa (3 samples per data point).	105
Figure 48: Percentage of silk solution converted to a hydrogel upon electrogelation with various concentrations of ethanol (3 samples per construct).	106
Figure 49: Enzymatic degradation of E-Gels (3 samples per construct).	107
Figure 50: Proposed <i>in vivo</i> gelation mechanism for E-Gels.	109
Figure 51: Proposed E-Gel delivery mechanism: needle geometries.	110
Figure 52: Progression of salt gels over time (2 samples per construct).	112
Figure 53: Enzymatic degradation of salt gels (average of 3 samples).	113
Figure 54: Rheological comparisons between current materials, silk materials and vocal fold mucosa.	116
Figure 55: <i>In vivo</i> degradation of existing vocal fold materials and <i>in vitro</i> degradation of silk materials.	118
Figure 56: Alternative approach for using silk in vocal fold augmentations.....	132

List of Tables

Table 1: Comparisons between vocal fold augmentation materials and vocal fold tissue.	31
Table 2: Material Specifications [1].....	35
Table 3: List of possible silk material formats.....	43
Table 4: Parameters altered and tests performed for various silk constructs.....	73
Table 5: Comparisons for different silk formats based on ease of delivery.	120
Table 6: Comparisons between silk material formats based on customer needs.	121

Design and Optimization of an Injectable Biomaterial
for Vocal Fold Augmentation

1. Introduction

Damage to the vocal folds (also known as vocal cords) can lead to difficulty speaking, a weak or raspy voice, or total loss of speech. These conditions are both physically and socially debilitating and can severely diminish a patient's quality of life. Vocal fold damage often presents in the form of vocal fold paralysis, muscle atrophy, or vocal fold scarring. These conditions can be caused by a number of things, including nerve damage (which often occurs during neck or chest surgery), old age, and superficial damage caused by the removal of cancer or other growths on the vocal cords. In some cases, damage can be so severe that the amount of air required to speak causes shortness of breath or exhaustion, making speech a painful and inefficient method of communication. Spoken word is the most critical form of information exchange in human society, and being unable to speak is a severe disability. While there is the possibility of using sign language or written communications, these are not commonly used forms of expression, and do not adequately replace speech.

Treatments are available to reduce or reverse the effects of vocal fold damage, however none are an ideal or permanent solution. One commonly used method of reversing the effects of laryngeal damage is to augment the vocal fold by injecting a small amount of viscous material behind the damaged vocal cord. This pushes the vocal cord inward, closing the vocal cords slightly (which interrupts airflow and allows for higher amplitude vibrations) and making it easier to vocalize. In order to satisfy the needs of both the patient and the surgeon, materials must be easy to inject, available off-the-shelf, last a long time,

sufficiently augment the vocal fold, and match the viscoelasticity of the vocal fold (in order to vibrate in the same modes as the natural tissues). It is also important that injection materials are non-toxic and that they do not cause any inflammatory response. Materials must not expand once in place (unless expansion is minimal, consistent, and can be adjusted for upon initial injection). Post-implantation expansion could partially or fully close the airway, asphyxiating the patient.

Many materials have been used for vocal fold augmentation, including various forms of natural collagen, gelatin, and fat, as well as synthetic materials such as Teflon® and various cosmetic dermal fillers (similar to Botox®). None of these materials meet all of the customer needs. This thesis research seeks to advance treatment methods for these conditions in order to improve patient care and quality of life, and focuses on developing a silk-derived biomaterial for use in vocal fold augmentation procedures. Silk has been shown to be a useful implantation material for many applications due to bio-compatibility, a wide range of possible physical properties (varied by changing processing parameters), and tunable degradation rates. There are a wide variety of silk biomaterials that could work for this application. A selection of promising materials was chosen to investigate and evaluate based on safety, tissue property matching, ease of injection, and degradation rate. Safety was quantified by different methods for each construct (depending on the safety concerns present for that material or associated delivery mechanism). Other properties were quantified using parallel plate rheology, fluid mechanics modeling and testing, and enzymatic degradation testing. Materials were down-selected and improved upon, and it was shown that

several silk constructs show promise for this application. The following sections provide background on the problem and materials used, explain methodologies used during experimentation, review the results of these experiments, and overview conclusions drawn from collected data.

2. Background

2.1 Vocal Fold Anatomy

The vocal folds are located in the larynx, and used to create sound. Figure 2 shows the placement of the vocal folds in the larynx, and a top-down view of the glottis, the area where the vocal folds meet, as well as the surrounding structures including the esophagus, epiglottis, trachea, arytenoid cartilage, intralaryngeal spaces and true and false vocal cords (TVC, FVC). The true and false vocal cords (or TVF and FVF, respectively), are also referred to as the vocal cords and vestibular folds, as they will be referred to hereafter. [1, 3-5]

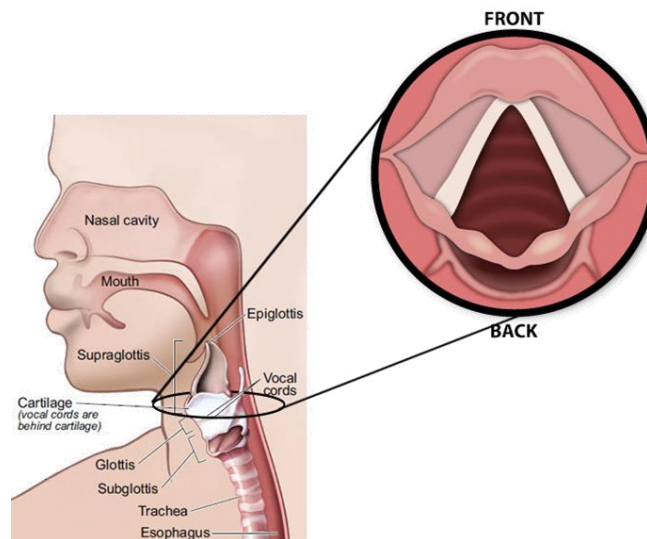


Figure 1: Glottal anatomy and placement [6, 7].

Figure 2 shows more detailed anatomy of the vocal folds and surrounding tissues. When in an open position, the trachea is exposed, and it is possible to breathe. When the vocal cords are closed, air can be passed between the vocal cords in order to create sound.

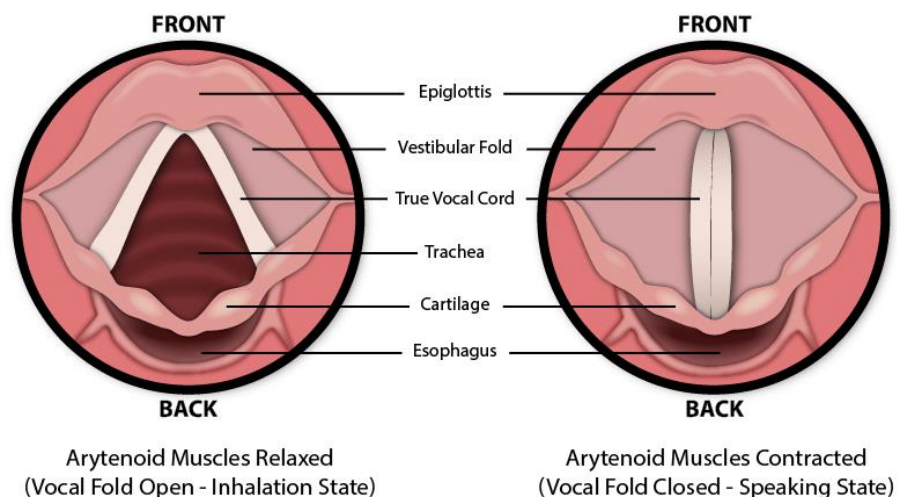


Figure 2: Vocal fold anatomy (adapted from [8]).

Musculature within and around the larynx controls the position of the vocal cords and epiglottis (as well as the surrounding tissues and cartilage), affording speech, swallowing, and airway protection. The thyroarytenoid, lateral cricoarytenoid, posterior cricoarytenoid and interarytneoid muscles are responsible for the abduction and adduction of the vocal folds, which adjusts their positioning and tension. Adduction of the vocal cords (moving them toward the center of the larynx) creates a taut parallel surface [1, 3-5]. Similarly, abduction pulls the vocal cords apart, allowing the airway to open. Figure 3 shows the anatomy of the musculature that controls vocal cord movements.

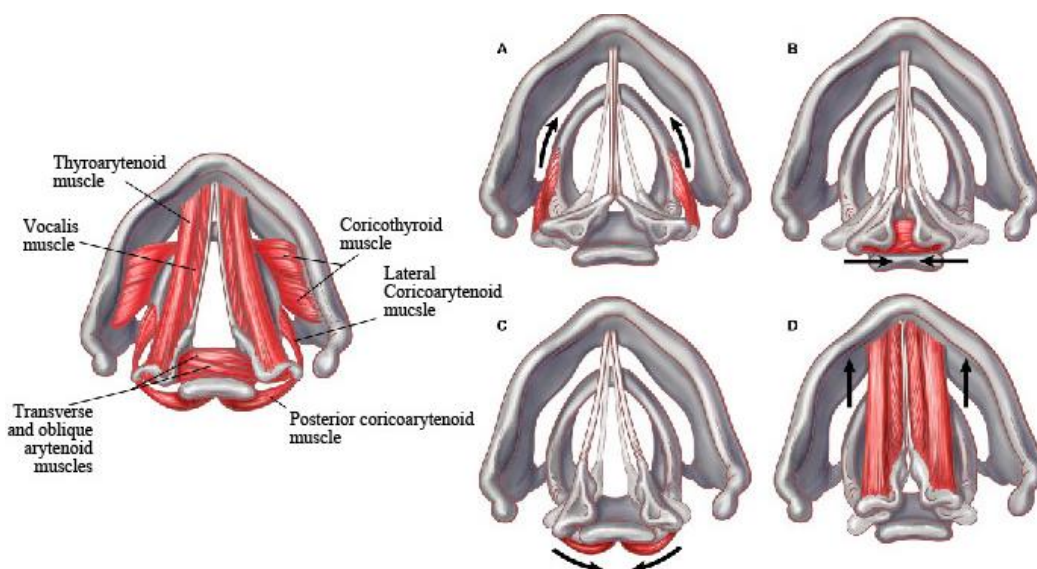


Figure 3: (A) Contraction of the lateral cricoarytenoid muscle rotates the arytenoids medially, adducting the vocal folds. (B) Contraction of the interarytenoid muscle adducts the arytenoids. (C) Contraction of the posterior cricoarytenoid muscles rotates the arytenoids laterally, opening the airway. (D) Contraction of the thyroarytenoid muscles adducts the vocal folds and allows for vocal pitch modification (adapted from[5]).

When air is passed between adducted vocal cords, the medial surfaces of the true vocal cords (the lamina propria, superficial to the thyroarytenoid muscle) oscillate. The amplitude of this vibration can be influenced by the distance between the vocal cords, the tension on the vocal cords, and the differential pressure between the trachea and supraglottal cavity. Changing the tension on the vocal cords temporarily stiffens or softens the tissue surfaces, changing the natural frequency of the vibratory surface. Vibrations created in the glottis are amplified in the pharyngeal, nasal, and oral cavities, and can be modified by contracting muscles in the face and neck to manipulate the shape of the vocal tract. This manipulation can alter harmonic frequencies and overtones, which affect the quality of the sound produced, and allow for articulation of speech. The pressure differential (difference between the pressure in the lungs and pressure

above the vocal cords) required to create and sustain oscillations of the vocal cords is known as the phonation threshold pressure. [9-11]

In a normal, healthy vocal fold, vocal cord adduction pulls the vocal cords almost perfectly parallel, the space between the cords is minimal, and the right and left vocal cords are evenly taut. This means a low phonation threshold pressure, and allows for clear, even vibrations. In order to measure the vibratory properties in a specific patient's vocal fold, a technique called stroboscopy can be used. This technique is performed by inserting a trans-oral or trans-nasal scope (with a strobe light and camera on the end) into the larynx, then monitoring a video feed as the patient phonates. When the frequency of the strobe approaches that of the vibrating vocal fold material, it is possible to see the motion of the vocal cords in what appears to be slow motion. This occurs because of a phenomenon known as aliasing, which occurs when the sampling rate at which data is collected is too low, and a false wave is observed, as explained in Figure 4B. Stroboscopy can be used to assess the degree of damage to a vocal fold, or to identify a specific region of the vocal cord that may be damaged [10, 11].

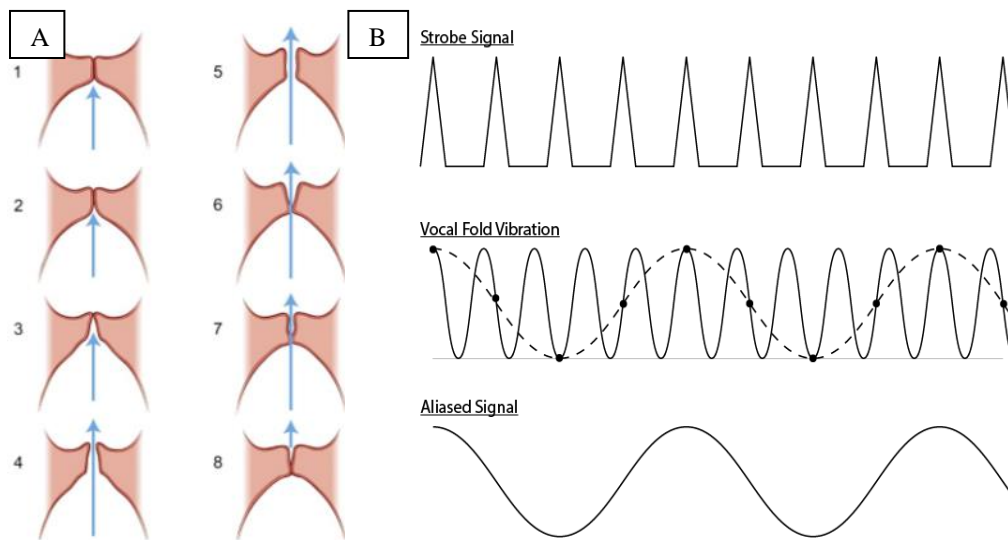


Figure 4: Vibration in a healthy glottis. (A) Coronal view of the vocal fold. 1) Closed vocal fold, subglottal pressure builds up. 2) Lower surface of the vocal cords separate due to rising subglottal pressure. 3) Only upper surfaces are in contact. 4) Air is released as the vocal folds separate. 5, 6) Airflow continues, elastic recoil of the vocal folds and Bernoulli's forces cause the lower surfaces of the vocal cords to draw inward. The mucosal wave propagates superiolaterally. 7) Airflow slows, and the lower lips close. 8) In a zipper like closure, the free edge of the vocal folds close from bottom to top and posterior to anterior. Adapted from [12]. (B) Theory behind stroboscopic aliasing for visualization of vocal fold vibrational modes.

2.2 Glottic Insufficiency

Damage to the glottis, vocal fold, or surrounding musculature can occur in a variety of ways including nerve damage from neck or chest surgeries, scar tissue from laryngeal injury (such as intubation), damage from previous vocal fold surgeries (such as cancer, granuloma, or polyp removal), and various forms of paralysis (cord immobility) and paresis (cord weakness). Superficial damage to the true vocal cords can cause scar tissue to form, which alters the vibratory properties of the tissue, interrupting the modes of vibration present in the tissues. In some cases, scarring can be severe enough to cause total loss of voice [1].

Other injuries and conditions present in the form of thyroarytenoid/lateral cricoarytenoid muscle atrophy. Each of these conditions can cause glottic insufficiency, meaning that a gap persists during vibration at the glottis and an inappropriate amount of air is escaping during phonation [5]. Figure 5 shows a vocal fold with various types of damage to the right side of the vocal fold. It can be seen in the figure that, in the cases of vocal fold paralysis and paresis, the right vocal cord is neither taut nor centered, leaving a large gap between the vocal cords. This drastically increases the phonation threshold pressure, making it extremely difficult (or impossible) for the patient to speak [1, 13, 14].

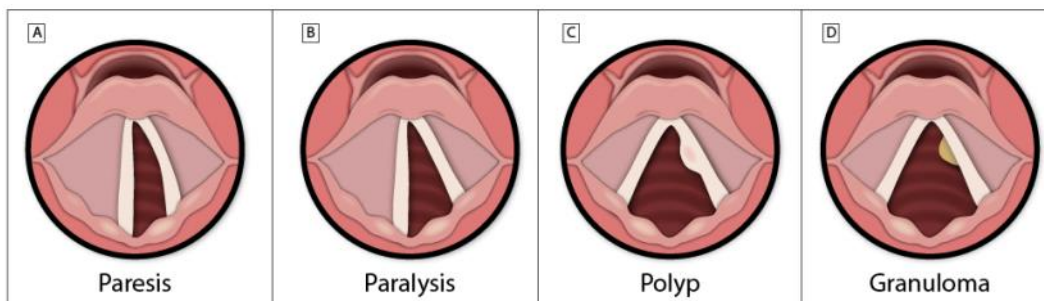


Figure 5: Various forms of vocal fold damage. (A) Vocal fold paresis, or weakening of the laryngeal muscles, presents as bowing in the vocal cord on the atrophied side. (B) Vocal fold paralysis, which presents as one immobile cord. (C), (D) Vocal fold polyps and granulomas, which prevent full glottal closure, and may require removal, which often causes scarring on the vocal fold.

2.3 Treatments for Glottal Insufficiency

A class of treatments is available for patients with severe vocal fold damage called vocal fold augmentation procedures. Vocal fold augmentation includes a variety of techniques that involve inserting an augmentation material into the tissues behind the vocal cord on the damaged side. The added volume pushes the remaining tissue toward the center of the vocal fold, reducing the gap between the

vocal cords, and lowering phonation threshold pressure (medialization). This treatment can be administered in many ways, and is typically performed by an otolaryngologist [13]. Deep vocal fold augmentation can restore the ability to speak when damage stems from muscle atrophy or paralysis, however a superficial injection would be ideal to repair damage to the superficial lamina propria (or layers of mucosal tissue that surround the vocal cords). A superficial injection must match the viscoelasticity of the vocal fold mucosa in order to vibrate properly and improve the patient's speech capacity. Currently, no material exists to replace the lamina propria in the setting of scar. Autologous fat is used but with variable success and difficulty in placement.

2.3.1 Vocal Fold Augmentation Injections

The most commonly used method of vocal fold augmentation is an injection of a gel-like augmentation material from inside the larynx. Figure 6 shows a basic schematic of vocal fold augmentation injection procedures and material placement on an awake patient in the office. Although also performed under general anesthesia in the operating room, these injections are often administered through an actuating channel laryngoscope, comprised of a cylindrical casing with a camera, light, and cannula (through which a catheter and needle can be threaded). The needle is inserted deep in the muscle of the true vocal cord, and the added volume of the material medializes the vocal cord by pushing the true vocal cord on the damaged side closer to the center of the larynx. Injections can be administered via a trans-oral or trans-nasal route (Figure 6) [13]. Both the trans-oral and trans-nasal techniques have the benefit of being an office-visit procedure,

meaning that the only necessary anesthesia is topical or local, sterility is less of a concern, and there is no need to use an operating room (which decreases the cost of the procedure significantly for both the hospital and the patient). This procedure is also significantly less time consuming than a procedure that requires an operating room. Vocal fold augmentation injection procedures are relatively painless for the patient; however there is some discomfort in the case of a trans-oral injection, as often times the scope resting on the back of the patient's tongue can trigger the gag-reflex. Ideally, all injections could be done trans-nasally, however the small scope and catheter sizes coupled with difficulty of visualization and the high viscosity of the augmentation materials used make the injections difficult for the surgeon to execute with control [1].

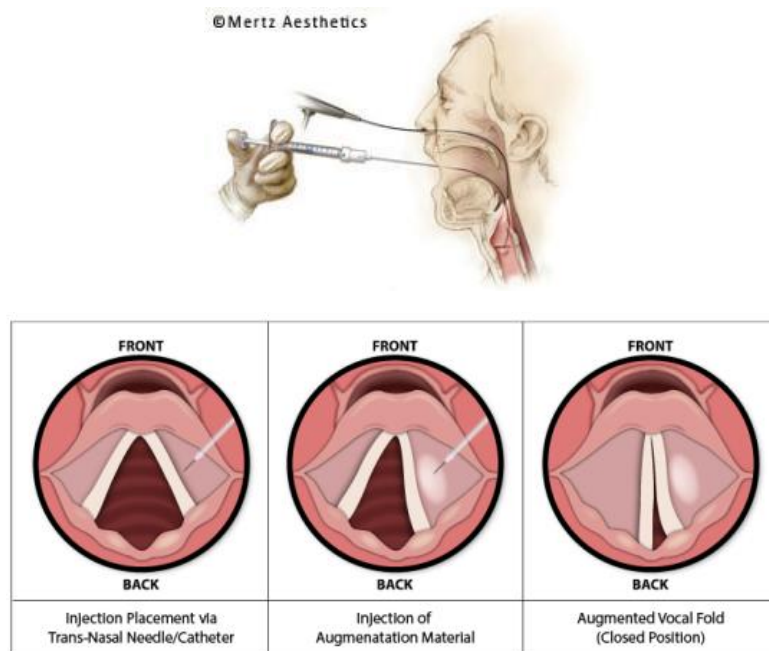


Figure 6: Vocal fold augmentation injection procedure [1].

2.3.2 Injection Laryngoplasty

Vocal fold augmentation injections can also be performed by inserting a large

needle (22 gauge) into the vocal fold from the outside of the larynx. The needle is pushed gently through the skin, and passes through the thyroid cartilage, as shown in Figure 7. The benefit of this procedure is that a much larger needle can be used than in vocal fold augmentation injections, meaning a much stiffer material can be injected. Stiffer materials tend to be stronger, stay in place better, and last longer than their softer counterparts. One drawback of this procedure is the transcutaneous path of the needle, which leads to plugging of the needle with a cartilage core. Local anesthetic can be used, keeping recovery time relatively short. The main drawback of this procedure is poor visibility for the surgeon of the depth of the needle tip within the vocal fold tissue. It is difficult to have a sense of the exact placement of the tip of the needle within the vocal fold, making optimal placement of the augmentation material very difficult, and reducing the percentage of desirable patient outcomes [1, 13]. If the material is placed too superficially and is not a rheological match for the vibration layer then the patient's voice could be made worse.

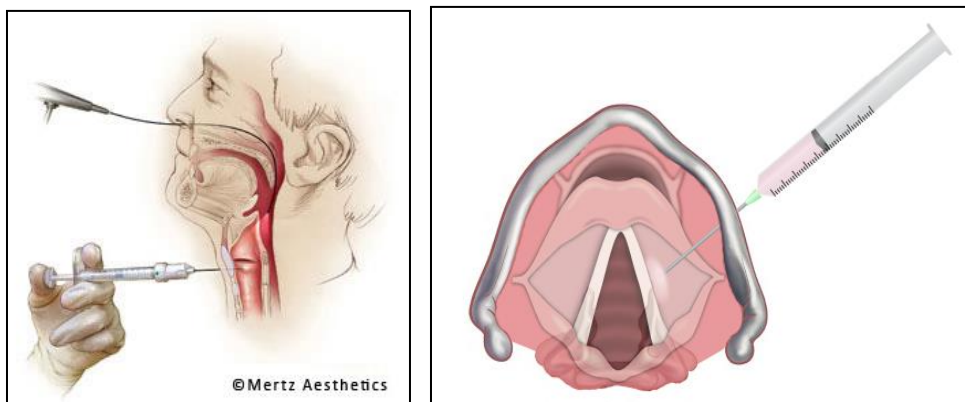


Figure 7: Injection laryngoplasty procedure [5, 8, 15, 16].

2.3.3 Thyroplasty

The last (and most invasive) option is to augment the vocal fold via open surgery through the neck. This method, known as a thyroplasty or medialization laryngoplasty procedure, involves inserting a stiff augmentation material behind the vocal fold through an incision in the neck [14]. Figure 8 shows the incision site and implant placement for thyroplasty vocal fold augmentation procedures. First, the patient is sedated and given a local anesthetic. A small incision is made in the skin, and the surgeon then drills or cuts a hole in the thyroid cartilage, and places the implant on the inside of the cartilage, pushing the vocal fold toward the center of the glottis [17]. There are two commonly used types of implants for this procedure. The first is solid piece of flexible plastic (typically made of Silastic®, a silicone based plastic) that comes in various shapes and sizes and locks into the space left by the excised portion of the thyroid cartilage (Figure 8B). The other commonly used thyroplasty implant is a thin strip of material (typically Gore-Tex®) that is folded upon itself and layered into the vocal fold until the associated vocal cord is satisfactorily medialized (Figure 8C) [12]. Once the implant has been placed, the sedated patient is asked to attempt phonation in order to test the placement of the implanted augmentation material. The implant can be adjusted if necessary, and once the desired results have been achieved, the incision is closed [18]. This procedure requires use of an operating room (sterility is critical). The incision site and cartilaginous damage will also mean a more painful recovery, and higher risk of infection than exists for injection techniques [1, 17].

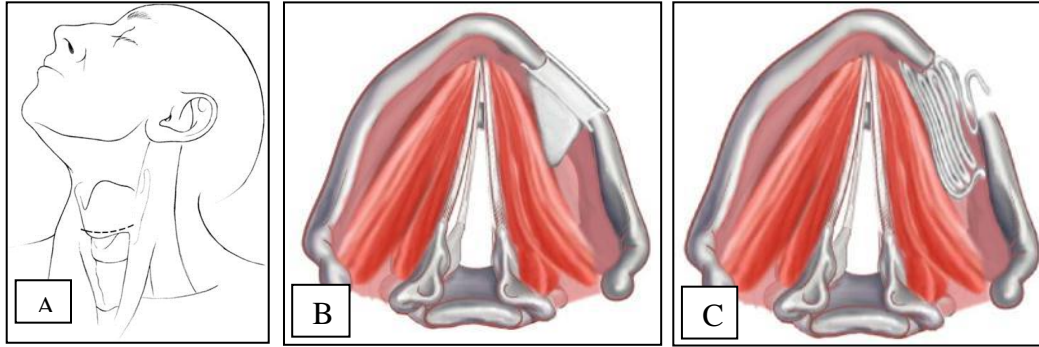


Figure 8: Thyroplasty implant placement and medializing effect on the right vocal cord (adapted from [5, 16]). (A) Thyroplasty Incision Site[16]. (B) Silastic® Implant. (C) Gore-Tex® Implant.

2.4 Vocal Fold Augmentation Injection Materials

The tissue of the vocal fold is covered by mucosal tissues [12]. In the vocal region, this mucosal tissue is a stratified squamous epithelium overlying a basement membrane covering the lamina propria (vibratory layer). For the purposes of this paper we refer to this stratified structure as mucosa but it is more complex than typical mucosa that lines all internal organs and cavities that come into contact with the outside world. For example, the areas of the digestive tract that come into contact with food are lined with mucosal tissue, as are the inside of the mouth, female reproductive organs, and nasal tract however they do not have an underlying vibratory layer [19]. The mechanical properties of this tissue are extremely important for choosing an augmentation material. Ideally, while the implanted augmentation material must to be stiff enough to medialize the vocal cord, it will also match the vibratory properties of the vocal fold mucosa. This implies that an augmentation material used for superficial injections for scar repair should have viscoelastic properties that match those of the lamina propria

of the vocal fold; whereas materials used to augment the entire vocal fold in a deep fashion should rheologically match the thyroarytenoid muscle. The same material could likely be used for both deep and superficial injection if it was rheologically similar to the lamina propria. Materials will also ideally permanently augment the vocal fold, but not incur any immunogenic responses from the body. Finding a material that meets all the criteria for this treatment is difficult, and many different materials have been tried and tested [1, 13, 20].

The first material attempted for vocal fold augmentation was paraffin wax, implanted in 1911 by injection laryngoplasty to medialize a paralyzed vocal cord. This caused significant inflammatory response, leaked from the injection site, and migrated from its original placement in the vocal fold [14]. Complications like these cause significant discomfort to the patient, and eliminate the effectiveness of the implant. Inflammatory responses can also be quite dangerous, as swelling in the vocal fold and surrounding tissues can cause the airway to close, asphyxiating the patient.

In the 1950's, bovine based gelatin materials (Gelfoam®, Surgifoam®) emerged as augmentation materials to be used with injection laryngoplasty. While both of these materials cause less inflammation than paraffin, they tend to resorb quickly and are highly viscous, requiring the use of a pressurized syringe and large gauge needle for injections. These materials are considered very safe, however are not often used today, as newer materials have been developed that are easier to handle and last longer [13, 14].

In the 1960's it became popular to use Teflon® (Polytetrafluoroethylene) as an augmentation material in a paste form (for injection laryngoplasty) and as a solid piece or Gore-Tex® strip (for thyroplasty procedures). Teflon® paste is quite viscous, and requires significant force and a large gauge needle to complete an injection laryngoplasty. While Gore-Tex® thyroplasty procedures and Teflon® paste have proven very effective at vocal cord medialization and were long considered a gold standard in vocal fold augmentation, the paste was eventually determined to incite the development of granulomas (growths or nodules caused by the body attempting to wall off foreign material within tissues) five to ten years post injection. Use of PTFE (Polytetrafluoroethylene, or Teflon®) based augmentation materials has since been discontinued. [13, 14, 20]

In the 1980's and 1990's, bovine collagen, autologous collagen, cadaveric collagen and autologous fat surfaced as augmentation materials. While none of these cause inflammation in the larynx, unfortunately, they all tend to resorb fairly quickly. One benefit to collagen derived materials is that they are relatively low viscosity, making them easier to inject, and they also have ideal mechanical properties for vibratory properties and sufficient augmentation. Bovine collagen is the easiest and cheapest material to come by, but there is a small chance that the body will be hypersensitive to the material, so a skin test must be performed before injection to ensure the injection won't cause any laryngeal swelling. Autologous collagen is time consuming, painful, and difficult to harvest. One milliliter of the material used for injection is derived from 5 cm² of the patient's own skin, and takes approximately 3 months to process before it can be injected.

Cadaveric collagen, such as Cymetra™ and Alloderm™ have similarly excellent mechanical and rheological properties, and are much easier to obtain than autologous collagen, however the efficacy of the augmentation is still limited to a few months, and there is a slight chance of disease transmission. Autologous fat is similar in nature to collagen materials, but has even better mechanical properties and requires a harvest site. The resorption time of autologous fat is very unpredictable, and can be as little as three months, however, it is considered a permanent deep augmentation material by many laryngeal surgeons who know how to handle it properly [13, 14].

In recent years several synthetic materials have been developed as vocal fold augmentation materials, many of which are also used as dermal fillers and cosmetic augmentation materials. Cosmoderm® and Cosmoplast® are lab grown collagen materials, which have the same properties as autologous or cadaveric collagen, but do not require painful harvesting or carry a risk of transmission. Other synthetic materials include Hyaluronic Acid (Hyalaforn®, Restylane®), and carboxymethylcellulose (Radiesse® Voice Gel), both of which are easily injectable. Carboxymethylcellulose lasts only two to three months, and Hyaluronic Acids can last from six months up to two years [12-14].

Efforts to create a longer lasting vocal fold augmentation materials have resulted in viscous materials that combine hydroxylapatite particles with a quickly resorbing carboxymethylcellulose carrier gel (Radiesse® Voice). This material has been shown to last up to two years (18 months on average), and demonstrates

improved viscoelastic, inflammatory, and migratory properties compared with previously used materials.

Table 1 shows comparisons between each of these vocal fold augmentation materials based on duration (or how long the material will be effective *in vivo*), viscoelasticity (as defined by rheological properties), implantation method, injectable viscosity, and immune response when implanted in the body.

Table 1: Comparisons between vocal fold augmentation materials and vocal fold tissue.

Material	Duration	Viscoelasticity	Implantation Method*	Injectable Viscosity	Immune response
Paraffin	N/A	Poor	IL	High	Yes
Bovine Collagen (Zyplast, GAX Collagen)	6 Months	Good	IL	Low	Possible
Bovine Based Gelatin (Gelfoam, Surgifoam)	4-6 Weeks	Good	IL	High	Little/None
Autologous Collagen	6 Months	Good	IL	Low	None
Cadaveric Collagen (Cymetra)	2-3 Months	Good	IL	Low	None
Autologous Fat	4 Months-2 Years	Excellent	IL	High	None
Teflon	Permanent	Poor - Very High	IL, Th	Very High	Severe
Hydroxylapatite (Radiesse Voice)	18 Months	Poor - High	VFI	Very High	None
Carboxymethylcellulose (Radiesse Voice Gel)	2-3 Months	Very Good	VFI	Low	None
Hyaluronic acid (Restylane, Perlane, Hyalaform)	4-6 Months up to 1 Years	Excellent	VFI	Low	None

*Abbreviations: IL = Injection Laryngoplasty, Th = Thyroplasty, VFI = Vocal Fold Injection Augmentation [13, 14, 20-24].

While newer vocal fold augmentation materials have been generally successful in restoring speech capability to patients, results are often short lived, and materials are often difficult to inject. There is a need for an improved material for augmentation injections that can both be delivered easily (allowing for a more comfortable experience for the patient) and remains structurally sound for a long enough period of time to adequately improve quality of life for the patient.

2.5 Material Specifications and Customer Needs

The most commonly preferred vocal fold augmentation method is a trans-nasal or

trans-oral injection. This preference is based on the minimally invasive approach, relatively low amount of pain and discomfort for the patient, and the office visit nature of the procedure [1]. This approach also has the advantage of optional trial injections. The surgeon can inject a simple saline solution into the vocal fold, then have the patient attempt to speak in order to gauge the effect of an implant before placing a more permanent material. Saline solution is easy to inject, and only lasts a few hours. Carboxymethylcellulose is short acting enough that patients can test drive the augmentation over 6 weeks or so. This allows for an initial idea of how helpful an implant will be, and allows the surgeon to make adjustments in placement or quantity of the injection without causing much discomfort to the patient [2]. While the vocal fold augmentation injection procedure has many benefits over other procedures, there is often a tradeoff with the quality of the material when compared with longer lasting materials used in more invasive approaches.

In order to have a successful augmentation, it is important that the injected material be stiff enough to push the vocal fold forward, cohesive enough that it will not migrate or be resorbed by the body, and yet have a low enough viscosity that it can be injected through the small gauge needle and catheter compatible with a trans-nasal scope without excessive amounts of force from the surgeon. A material that is low viscosity during injection and stiffer once implanted would greatly improve the vocal fold augmentation process, as it would eliminate the main drawback of trans-oral injections, making a less painful and invasive option available to patients without compromising the quality of the augmentation

material or the ease of implantation for the surgeon. Being able to perform the visualization and injection through the same scope is easier for the patient as it involves only one tube in one orifice.

Table 2 shows the material specifications for this project. Each category has a marginal and ideal value, which describe the preferred properties of the material. Properties are rated with an importance scale of 1-5, where 1 is a property of critical importance, and 5 a desirable quality. Ideally, the material will be injectable through a trans-nasal path. This means that an augmentation material must be able to pass through a 27G needle with and 16G catheter (approximately 10" long). If the material is too viscous to pass through this system, using a more traditional trans-oral vocal fold augmentation injection (25G needle) or transcutaneous injection laryngoplasty would be acceptable (22G needle). The force of injection refers to the pressure the surgeon must exert on the plunger of the syringe in order to cause the material to flow through the catheter and needle. This range was determined by testing (described later on), and was found to be between 15 and 25 Newtons. *In vivo* stiffness refers to the properties of the material once implanted in the vocal fold, which should closely match those of the vocal fold mucosa. Currently used materials tend to be stiffer than the vocal fold mucosa, so if the material cannot match the stiffness of the vocal fold exactly, it should be within the range set by current materials. Safety concerns are high priority, and include pH, salinity, and temperature. Ideally, all of these values will match physiological levels, however if necessary, pH, salinity, and temperature levels can be varied slightly to achieve better material properties, as long as no

damage is caused to the tissues, and no pain is felt by the patient. Post-injection expansion is another safety concern, and a very important property of any vocal fold augmentation material. If a material expands after injection, it is possible that the airway will be forced shut, and the patient could be asphyxiated. Ideally, the material will not expand at all, however often times slight expansion is unavoidable. In this case, it is important for the surgeon to know exactly how much a given material will swell so that they can compensate for post-injection expansion when placing the material. Additionally, the material must be removable by surgery should something go wrong with the implant, whether it be post-injection expansion, inflammatory or allergic response, or any other dangerous complication. Inflammatory and allergic responses should be non-existent or extremely mild. If possible, doping the augmentation material with antibiotics or other drugs would reduce recovery times and chances of infection, however this is not a critical property for success. Materials should have tunable degradation rates, but be capable of lasting permanently. In order to make the procedure worthwhile for the patient, the augmentation should last for at least six months. The material should also be easy for the surgeon to prepare. Ideally, a pre-filled syringe of the material will be ready for implantation “off-the-shelf”, meaning that no extra steps are necessary to prepare the material before injection. It is possible the material would need to be heated, mixed, or treated by some other method pre-injection. This is acceptable, however preparation should be kept to a minimum. The cost per injection should be equal to or lower than that of current materials, both for the patient and the hospital. This includes the injection

material itself (as well as the syringe, needle and catheter required to inject it), the time it takes to prepare and administer the injection, and any extra equipment the hospital must purchase in order to use the material. Satisfying all of these conditions, either marginally or ideally will result in a viable vocal fold augmentation injection material.

Table 2: Material Specifications [1].

Importance Factor*	Specification	Marginal	Ideal
2	Delivery	Injection Laryngoplasty (22G Needle) or Trans-Oral VFI	Trans-Nasal VFI (27G Needle + 10" 16G Catheter)
1	Force of Injection	15 N-25 N	20 N
1	In vivo Stiffness	Stiffer than vocal fold mucosa, Analogous to Current Materials	Equal to vocal fold mucosa
1	Safety: pH	Slightly outside Physiological (5-8)	Physiological (7.38-7.42)
1	Safety: Salinity	Slightly Above Physiological	Physiological (.9%w/v NaCl)
1	Safety: Temperature	No patient discomfort or burns	No detectable temperature difference
2	Post-Injection Expansion	Compensated	None
1	Removability	Removable via surgery	Removable via surgery
1	Inflammatory Response	Minimal	None
4	Drug delivery	None	Can be doped with drugs
2	Duration	6 months	Tunable, up to permanent
5	Preparation	May require pre-procedural treatments	Off-the-shelf injection material
3	Cost	Equal to current options	Lower than current options
5	Required Equipment	Custom Device	Existing Equipment

* Importance factors range from 1 to 5, 1 being of critical importance and 5 being a non-critical but desirable quality.

2.6 Silk as a Biomaterial

One material that could work well for use in vocal fold augmentation injections is a silk-derived biomaterial. Silk produced by the *Bombyx Mori* Silkworm has been used for centuries in many applications, primarily for textiles and as suture thread. In recent years *Bombyx Mori* silk has been investigated for use as a biomaterial in tissue scaffold engineering, implant, cell culture, and controlled drug release applications [25-33]. Silk has many unique characteristics that make it a promising biomaterial: it is biocompatible, does not induce inflammatory responses in the body, and is FDA-approved for some applications (Allergan Medical, Inc.) [26, 34]. Degradation rates *in vivo* can be controlled, and range from days to years [32, 33, 35, 36], it can be functionalized with bioactive compounds if it is necessary to embed antibiotics or growth factors [37-42], is stable at reasonably high temperatures (up to 170 °C) [25, 43], and when implanted as a hard construct acting as a replacement for metal, does not impede MRI imaging. The most important aspect of silk is the ability of natural fibers to be broken down and regenerated in many different forms to create a wide variety of material formats with extraordinary mechanical properties. Changing processing parameters can vary properties significantly, allowing a wide range of constructs to be created and tuned to a specific application [26, 33, 44]. These properties make silk a promising material for use in vocal fold augmentation injections.

2.7 Silk Structure and Properties

Bombyx Mori silk is composed of two main proteins: sericin and fibroin. Natural silk fibers consist of two inner filaments of fibroin surrounded by glue-like sericin proteins, as shown in Figure 9. Fibroin protein accounts for most of the strength in natural silk, and sericin allows the silkworm to bind the fibers together into a cocoon. Each fibroin filament is approximately $10\mu\text{m}$ in diameter, and is composed of smaller fibrils, less than $1\mu\text{m}$ in diameter. Each fibril is made up of approximately 1,000 microfibrils, each of which has a diameter of $100\text{-}150\text{ \AA}$. Microfibrils are composed of fibroin polymer chains, assembled into an organized structure (conformation). For biopolymer processing, sericin proteins are typically removed, and the fibroin protein is used for biomedical applications. [25-27, 43, 45-47]

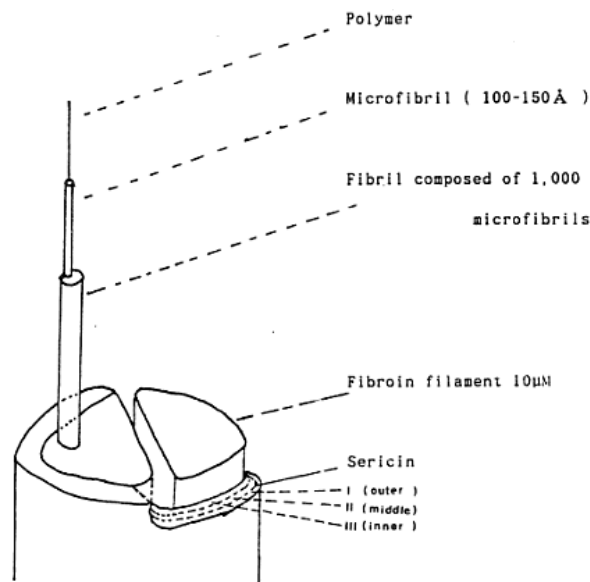


Figure 9: Structure of native silk fibers [47].

Fibroin protein has a primary structure of heavy and light chains, with molecular weights (or unit polymer chain lengths) of 325 and 25 kDa, respectively [43]. As

it is currently understood, the heavy fibroin chain (responsible for the majority of the strength in silk fibroin) is composed of repetitive amino acid chains, which mimic the behavior of block copolymers. Figure 10 shows the protein chain sequence of *Bombyx mori* silk, and the different conformations and structures found in silk fibroin. This protein sequence is primarily comprised of hydrophobic blocks, with a few mildly hydrophilic blocks dispersed throughout the sequence, and highly hydrophilic blocks at the ends of each chain. This organization of molecules allows for the formation of various secondary structures and conformations, such as random coil, α -Helix, and β -Sheet crystalline conformations (also shown in Figure 10) [43, 46, 48-50]. Figure 10 shows the protein chain sequence of *Bombyx mori* silk, and the different conformations and structures found in silk fibroin. Each of these states has its own specific properties, and the presence and quantity of each conformation determines the material properties of the larger silk construct [46, 48, 51]. β -Sheet silk accounts for most of the natural strength in crystalline (solid) silk constructs. Many different factors can affect chain interactions and behaviors, as well as conformation content in a larger construct including physical forces, chemical interactions, and charge interactions.

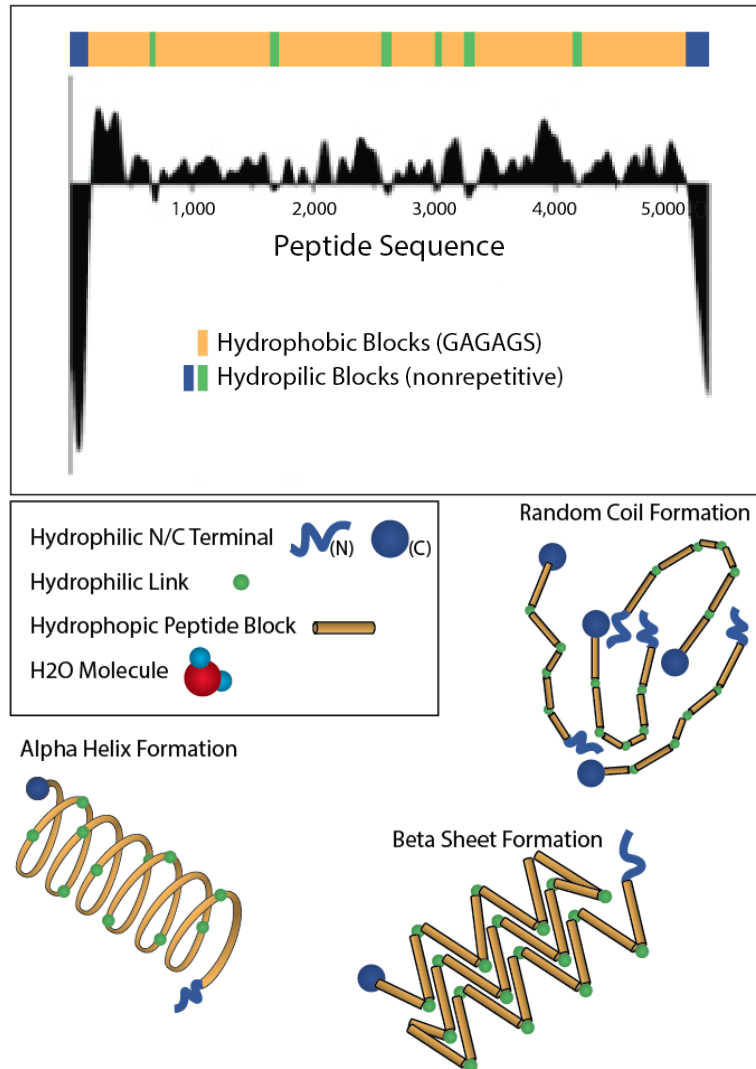


Figure 10: Silk fibroin composition and molecular behavior (adapted from [46, 52]).

2.8 Silk Solution Processing

A series of steps are taken to convert silk cocoons into an aqueous solution of regenerated silk fibroin to be used as a basis for most silk biomaterial formats. The sericin coating on native silk fibers has been shown to cause irritation and immunogenic responses *in vivo*, therefore it is important to remove these proteins when using silk as an implantable biomaterial. Sericin can be removed by washing native silk fibers in a slightly caustic bath. The preferred detergent for

silk processing is sodium carbonate. Once sericin proteins have been extracted from the fibers, pure fibroin strands remain. These strands can be dissolved in various chaotropic solvents, however the most commonly used is Lithium Bromide (LiBr). Once the proteins have been dissolved, the solvent can be washed out by dialyzing the solution with water using a membrane which allows exchange of water and LiBr, but not silk proteins. After this step, solutions can be centrifuged to remove impurities, yielding a pure regenerated silk fibroin (RSF) solution.

By treating and processing RSF solutions with different additives, conditions, and techniques it is possible to create many silk constructs including films, foams, hydrogels, porous constructs, and solid constructs. A selection of these silk material formats can be seen in Figure 11. The constructs shown have a range of properties. Silk Electrodes (the first construct listed) are created by applying a voltage to silk solution, which causes a thick, sticky hydrogel to form. Silk foams are created by freeze-drying silk solution at specific temperatures under a strong vacuum. These materials can be made soft or stiff by varying processing parameters. Solid silk constructs are manufactured by dissolving silk foams in an organic solvent called 1,1,1,3,3,3-hexafluoro-2-propanol (HFIP), then setting the mixture by submerging the material in a methanol bath. The methanol and HFIP are then leached out by water, and a hard pure silk construct remains. These constructs can be used for a variety of applications, including bone screws and plates, plastic substitutes, or bone tissue engineering scaffolds. Silk films mimic the properties of materials such as Cellophane™ and polyethylene plastic

wrap. Thickness, flexibility and surface patterns can be altered by varying processing techniques. These constructs are also used for tissue engineering applications, as well as for making dissolvable, flexible circuitry. Porous scaffolds can be created by adding a porogen (particulate matter) to silk, letting the silk gel, then washing out the porogen. Salt is the most commonly used porogen, although polymethylmethacrylate spheres have been explored as well for more uniform pore sizes and distributions. Porous scaffolds are primarily used for tissue engineering applications. Regenerated silk fibers can be created by heating a silk electrogel then extruding or drawing fibers from the solution (which becomes less viscous upon heating). Regenerated fiber strength approaches that of natural silk, and has the benefit of drug delivery capabilities. For example, regenerated silk sutures with embedded antibiotics could be created. The last material listed is a non-woven mat created by a method known as electrospinning. Silk solution is mixed with a thickening agent, and injected slowly through a highly charged needle. A distant grounded plate is placed below the needle, and as the solution is injected, nano-fibers are pulled to the ground plate at extremely high velocity. This technique yields nano-fibrous non-woven mats, which provide an ideal cell culture surface. Due to this affinity for cellular adhesion, these constructs are used frequently in tissue engineering applications.

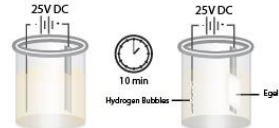
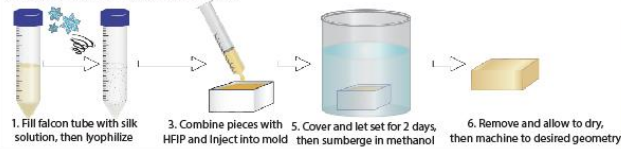

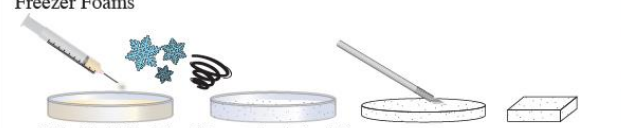


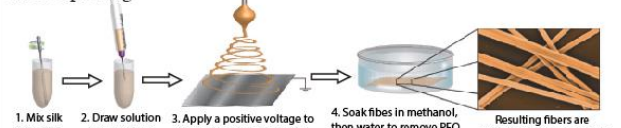
Construct	Uses
<p>E-Gels</p>  <p>Apply a voltage across a bath of silk solution</p>	<ul style="list-style-type: none"> • Adhesives • Augmentation
<p>Solid Silk Constructs</p>  <ol style="list-style-type: none"> 1. Fill falcon tube with silk solution, then lyophilize 2. Combine pieces with HFIP and inject into mold 3. Cover and let set for 2 days, then submerge in methanol 4. Remove and allow to dry, then machine to desired geometry 	<ul style="list-style-type: none"> • Bone Screws • Bone Plates • Tissue engineering
<p>Films</p>  <ol style="list-style-type: none"> 1. Fill a dish with solution 2. Place inside humidity controlled chamber and allow to dry 3. Remove dish from humidity chamber and extract film 4. Cast on a patterned surface for other effects 	<ul style="list-style-type: none"> • Corneal replacements • Biodegradable circuitry and sensors
<p>Freezer Foams</p>  <ol style="list-style-type: none"> 1. Fill a dish with silk solution 2. Freeze and lyophilize solution 3. Cut foam to desired size 	<ul style="list-style-type: none"> • Augmentation • Tissue scaffold Engineering
<p>Porous Scaffolds</p>  <ol style="list-style-type: none"> 1. Add silk solution to a beaker 2. Add porogen. Rotate for even distribution 3. Allow silk to gel 4. Remove porogen 5. Allow scaffold to dry 	<ul style="list-style-type: none"> • Augmentation • Tissue scaffold Engineering
<p>Regenerated Fibers</p>  <ol style="list-style-type: none"> 1. Create an E-Gel 2. Heat Egel and draw out strands of silk 3. Steam draw silk strands 	<ul style="list-style-type: none"> • Drug-doped silk fibers • Sutures • Woven scaffolds
<p>Electrospinning</p>  <ol style="list-style-type: none"> 1. Mix silk with PEO 2. Draw solution into a syringe 3. Apply a positive voltage to the syringe to initiate a jet 4. Soak fibers in methanol, then water to remove PEO <p>Resulting fibers are under 800nm in diameter</p>	<ul style="list-style-type: none"> • Cell culture scaffolds • Tissue engineering

Figure 11: Post-processing techniques for various silk constructs. Adapted from [25, 26].

2.9 Post-Processing Techniques

There are many silk constructs that have promising properties for vocal fold augmentation injections. The most promising constructs are silk hydrogels (created using various processing techniques) and silk foams. Both of these

material formats can have the desired rheological and compressive properties (with the appropriate processing), and many types of silk gels and foams can be injected or formed *in vivo*. Silk materials used for this application should have rheological properties that closely match those of the vocal fold mucosa, be safe to inject directly into the tissues of the vocal fold, degrade slowly *in vivo*, and be easily deliverable. They should also have compressive strength substantial enough to sufficiently augment the vocal fold, and be easily removable, if necessary. The following is a list of silk formats that have potential for this application.

Table 3: List of possible silk material formats.

	Materials	Processing Methods
Foams	Freezer Foams	Freeze and Lyophilize
Hydrogels	Sheared Gels	Inject through small needle
	Sonicated Gels	Add high frequency vibrational energy
	Vortexed Gels	Add low frequency vibrational energy
	pH Gels	Add small amount of strong acid
	Electrogels	Apply voltage
	Additive Gels	Add cross-linking or coagulation agent

2.9.1 Injectable Silk Porous Foams

Porous silk foams can be made by a variety of techniques. The preferred technique is to create a foam from regenerated fibroin solution by freezing the solution for several days, then lyophilizing (freeze-drying) the frozen solution at sub-zero temperatures under vacuum until all water has been sublimated from the silk structure [26, 53-55]. The preference for this technique is due to the aqueous

processing. This means that no harsh chemicals are used, and the silk can be doped with live enzymes or bacteria when in a solution state (without these additives being damaged during processing). It is also possible to create a silk hydrogel by mechanisms such as electrogelation, sonication, or the addition of low pH additives, then lyophilize this construct to produce a foam. Other techniques include porogen leaching and gas foaming techniques [55]. Each of these processes leaves a porous pure RSF construct, which can then be treated with methanol or by water annealing to induce β -Sheet structure in order to improve mechanical properties and make constructs insoluble in water [56, 57]. An injectable foam technique that was a focus of this thesis research is the freezer foam technique. By varying parameters such as solution concentration, freeze time, lyophilization time, temperature and vacuum pressure, methanol treatment parameters and water annealing parameters, a wide variety of mechanical properties can be achieved [55, 57].

2.9.2 Shear Induced Silk Hydrogels

The application of shear forces to silk solution is one of the key mechanisms used by the silkworm in the natural silk spinning process [31, 48]. The silkworm uses a combination of protein concentration, change in pH, change in ionic content, and shear forces to convert silk dope from the gland of the silkworm into the silk fibers they lay down to create cocoons [31, 58]. Figure 12 shows the effects of concentration and shear on silk fiber formation. It has been hypothesized that silk fibroin in silkworm dope is in a liquid crystalline form, and has a tendency to form spherical structures (micelles) as solution is concentrated and dried. Changes

in pH and ionic content can accelerate this process. When the silkworm ejects silk dope from the oral cavity, the movement of the head in a figure-eight pattern stretches the sticky, sericin coated fibers from the points they have been anchored to. At a critical strain rate, crystallization and alignment of the molecules occurs, and the silk forms a solid, fibrous strand. This rate is dependent on the concentration of the solution, the micellar concentration in the solution, and the ionicity and pH of the solution. [31, 43, 46, 48, 50, 59]

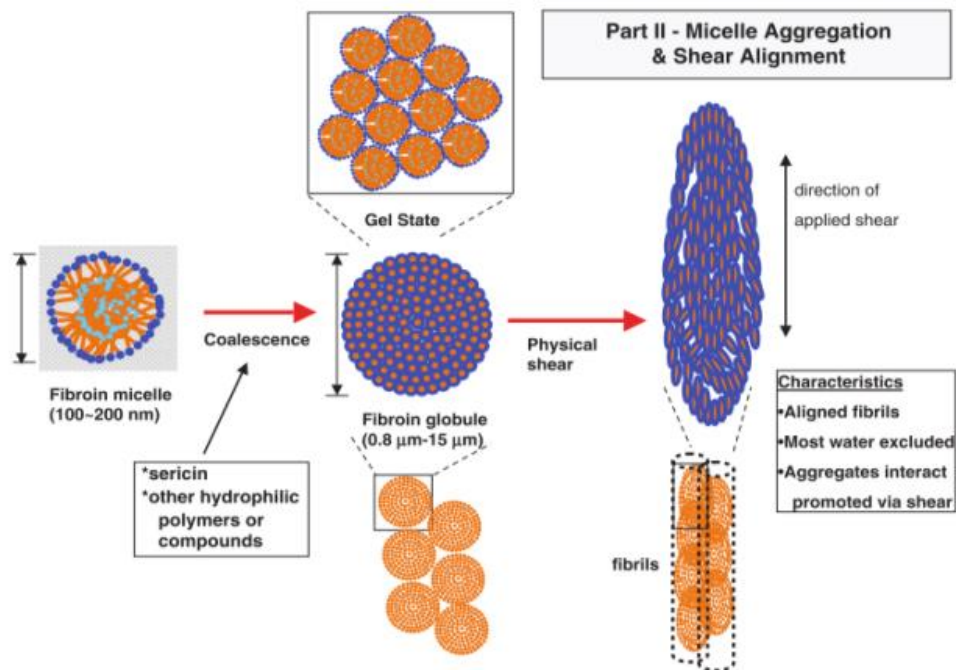


Figure 12: Suggested shear gelation mechanism in natural silk fiber spinning [60].

By applying shear forces to a regenerated silk solution, it is possible to create a hydrogel if shear rates are relatively low. Shear applied in the natural silk spinning process causes the silk to completely crystallize and form a fiber due to the fact that the solution is already in a highly concentrated, ionic, and pH lowered state, encouraging the chains to form aligned crystalline structures. In the case of regenerated fibroin solution, silk dope is a lower concentration silk protein

solution with minimal ionic content and neutral pH, meaning that the application of shear causes the formation of globules and semi-crystalline structures within the solution to form a hydrogel, but (at reasonable shear rates) does not form a solid.

2.9.3 Sonicated Silk Hydrogels

By adding high frequency vibrational energy to a RSF solution, shear forces are applied to the silk on a molecular level. By sonicating silk solution by submerging the tip of a Sonifier with a microtip into a bath of silk solution (Figure 13), it is possible to create a silk hydrogel. Sonication causes rapid acceleration of natural silk assembly mechanisms by the addition of large amounts of energy (primarily vibrational energy, but some heat). Gelation will occur more rapidly the higher the sonication power output used. [61]

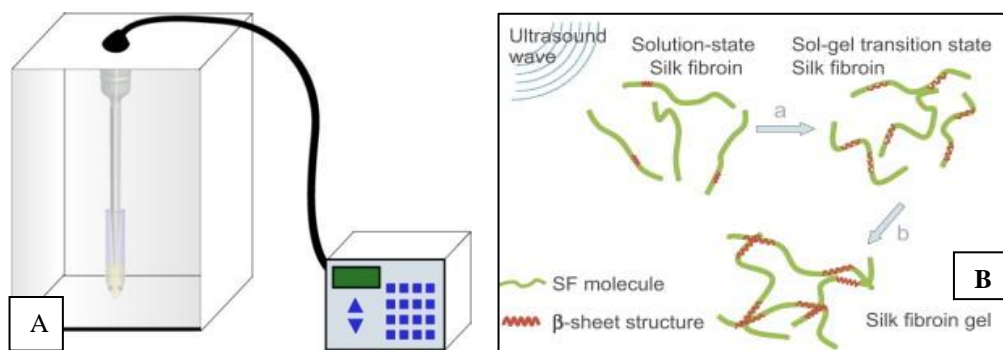


Figure 13: (A) Sonication procedure for creating silk hydrogels (adapted from [26]). (B) Silk fibroin chain interactions induced by sonication [61] .

After sonication, samples are incubated at 37 °C until self-assembly occurs. An increase in sonication time results in a decrease in assembly time, as does the addition of ions and the lowering of the RSF pH. These relationships are shown in Figure 14. By tuning the gelation time to the appropriate time scale, it would be

possible to prepare a sonicated solution, inject it into the vocal fold, then wait for gelation to occur. [61]

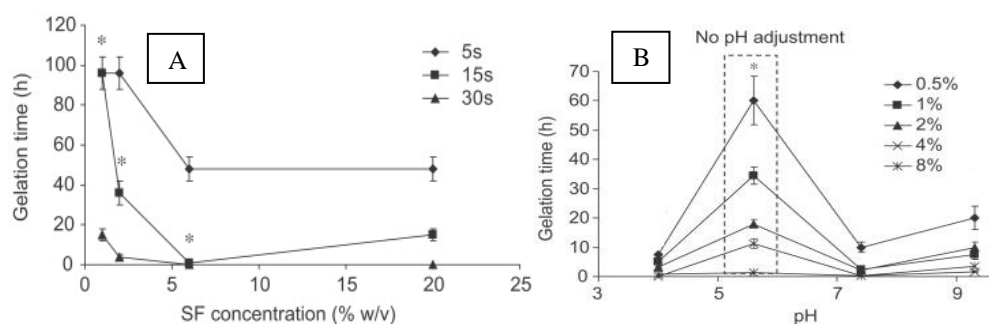


Figure 14: (A) Time delayed gelation response of 20%w/v RSF solution at different sonication times. (B) Time delayed gelation response of RSF solutions sonicated for 15 s at various concentrations of silk, and varied pH levels [61].

2.9.4 Vortexed Silk Hydrogels

As is the case with sonication, the addition of energy and molecular shearing of silk fibroin can be achieved by low frequency vibration. These gels are known as vortexed silk hydrogels, and can be tuned to possess a variety of properties by altering vibrational frequency, concentration of RSF solution, and vortexing time. As with sonication, vortexing causes accelerated self-assembly to occur. The amount of time between vortexing and self-assembly can be tuned by altering the process parameters, meaning that the solution could be vortexed, injected as a solution, then solidify on a prescribed time frame. It is important to note, however, that vortexing a solution perturbs the solution violently, causing significant foaming and bubbling to occur, as well as a slight thickening of the solution, which may make these materials difficult to inject. [26, 32, 62]

2.9.5 pH Induced Silk Hydrogels

As mentioned previously, pH is another key mechanism used by the silkworm to prepare silk dope for solidification into a fibrous form [31, 63, 64]. Figure 15

shows the silkworm gland and the various processes that take place inside it to form native silk fibers.

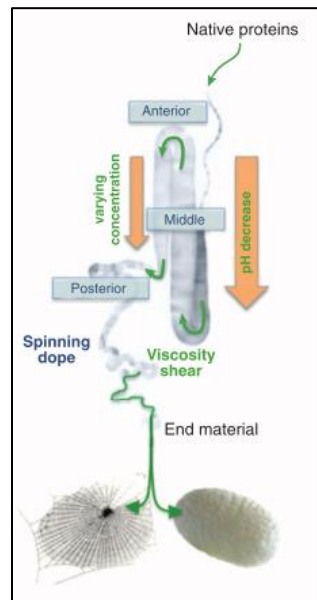


Figure 15: The natural silk spinning process [31].

When in a solution state, silk fibroin chains typically have a net negative charge. This means that when in close proximity, the chains repulse one another electrostatically, allowing the chains to maintain their natural liquid crystalline solution state. Lowering the pH in native silkworm dope eliminates or reduces the effects of these electrostatic repulsion interactions, allowing the fibroin chains to aggregate and bond, forming a hydrogel [63, 64]. Lowering the pH of a regenerated silk fibroin solution has the same effect, and a RSF hydrogel can be created by the addition of a small amount of strong acid (such as HCL) to a bath of RSF solution [26, 51]. In order for the elimination of electrostatic repulsion to take place, the pH must be lowered to a value below the isoelectric point of the solution, a pH level of approximately 4.2 for *Bombyx Mori* derived silk fibroin (note that this value is significantly lower than the accepted limits for *in vivo* use

(pH 5)). It has been found that pH induced changes in silk can be reversed by the addition of alkaline materials if exposure to low pH is brief, however longer exposures can cause a permanent denaturing of the proteins and intra-molecular hydrogen bonds will form, causing the chains to form a β -Sheet-rich structure [64].

2.9.6 Silk Electrogels

Electrogelation of silk is another method of creating hydrogels, and the material created is known as an E-gel. E-gels are processed by using a power supply and electrodes to apply a voltage across a bath of RFS, as shown in Figure 16.

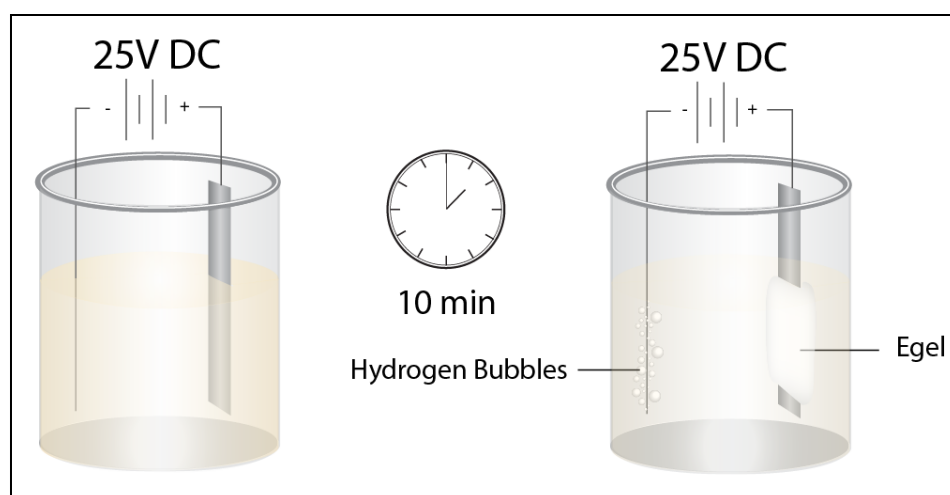
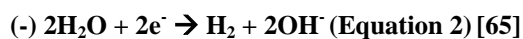
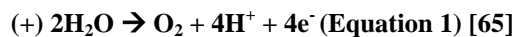


Figure 16: E-Gel formation procedure.

The conductivity of the aqueous solution allows electrolysis to occur, causing a number of events to take place. Bubbles begin to collect on both the positive and negative electrodes; hydrogen bubbles on the negative electrode, oxygen bubbles on the positive. This is due to the electrochemical reactions taking place. (+) $2\text{H}_2\text{O} \rightarrow \text{O}_2 + 4\text{H}^+ + 4\text{e}^-$ (Equation 1 and (-) $2\text{H}_2\text{O} + 2\text{e}^- \rightarrow \text{H}_2 + 2\text{OH}^-$ (Equation 2 show the governing electrochemical reactions taking place at the electrodes.



Due to the localized changes in proton concentration, the pH levels at the positive and negative electrodes diverge. When the pH at the positive electrode drops below the isoelectric point (pI) of silk (4.2) [65, 66], a protonation of the polar side chains of the silk molecules occurs, interrupting the electrostatic repulsion forces that normally keep chains from interacting, as shown in Figure 17. These changes allow a compaction of the chains to occur, as well as dissociation with the bound water in the molecules. Thus, the localized concentration of the solution is increased, intermolecular crosslinks are allowed to form, and there is an increase in inter-helical interactions. The resulting gel is highly adhesive and has excellent extensibility. This is due to the fact that, unlike most silk hydrogels, E-Gels are rich in α -Helix conformation (as opposed to β -Sheet). Another implication of the α -Helix-rich gel is that the process is reversible by heating, or by reversing the applied electric field. [65, 66]

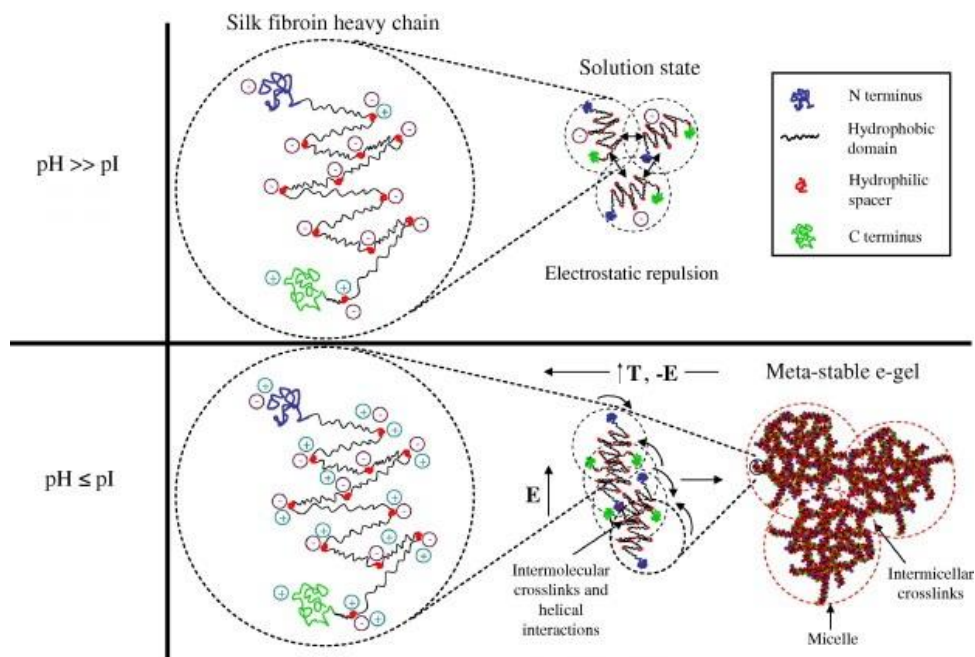


Figure 17: E-Gel formation mechanisms [66].

2.9.7 Silk Additive Gels

As with any polymeric material, many different substances can be used to cross link silk solutions. Cross-linking with the right additives can result in the formation of a hydrogel. Ideally, liquid additives could be co-injected with RSF solutions to incite a reaction which creates a gel immediately after the materials have been injected. Unless a very low viscosity (yet highly cohesive) gel is created, it is unlikely that it would be possible to inject a cross-linked hydrogel, therefore it would have to be created *in vivo*. Gelling *in vivo* with additives does not prove challenging if those additives are in a solution state, however for a powder or otherwise solid additive, injection will be more difficult. Because the gel will be formed *in vivo*, any cross-linking elements that are harmful to the body cannot be used. For example, one of the most commonly used β -sheet-inducing substances, methanol, would not be an acceptable additive for this application.

This constraint leaves only a few commonly used additives for gelling silk, including ions, silk particles, ionic or metallic nanoparticles (such as Ferro fluid or gold nano-particles), and body safe alcohols. While there are other substances that could be used to create a silk gel, these were the primary options investigated for this application.

2.9.8 Temperature Considerations

RSF solutions are inherently unstable over time, and if stored for a long enough period of time a silk solution will self-assemble into a stiff, white gel. The exact mechanism by which this occurs is yet unknown, but several factors can accelerate the process. One way to accelerate self-assembly of silk proteins is to store and RSF solution at an elevated temperature. Solutions are typically refrigerated at 4 °C when not in use. In this environment, silk solutions can last anywhere from 60 to 140 days after processing depending on boil time, concentration, solution conformation concentrations, and environmental factors. In a room temperature environment, a silk solution will self-assemble within 30-40 days (at 6-8% w/v concentrations). The higher the storage temperature, the higher the rate self-assembly of the silk proteins [49]. Figure 18 shows a plot of gelation time vs. solution concentration for at various storage temperatures. When silk constructs are partially gelled by other methods (such as vortexing) and exposed to elevated temperatures there is a decrease in assembly time. Because all constructs being injected for this application will be injected into a 37 °C environment (body temperature), it is important to keep in mind that gelation may be accelerated.

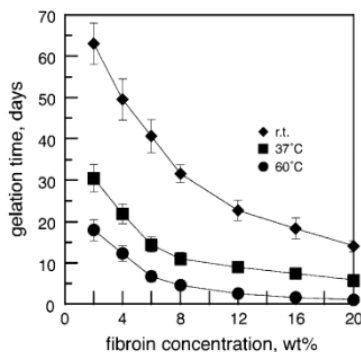


Figure 18: Temperature dependence of RSF solution self-assembly rate [49].

2.9.9 Hybrids and Combinations

The properties of silk hydrogels and foams make them promising candidates for vocal fold augmentation materials. The variety of properties that can be achieved by careful processing coupled with the tunability of *in vivo* degradation time and lack of inflammatory response make for a very promising material. Each of the previously described constructs has the potential to work for this application, however it is likely that while they satisfy one criteria, other criteria will not be met. To solve this, combinations of these materials can be investigated such as particle reinforced sheared gel, salinated E-Gels, or cross-linked forms of thinner gels.

3. Experimental Methods

Experiments were carried out to determine the best possible silk construct for vocal fold augmentation injections. Each material was characterized based on rheology, degradation, safety and delivery. Processing parameters were varied to find optimal values for each of these properties in an effort to find a material appropriate for this application.

3.1 Regenerated Silk Fibroin Solution Processing

Silk solution was processed from Japanese *Bombyx mori* silk cocoons (Tajiha Shoji Co., Ltd, Sumiyoshicho Nakaku, Yokohama), as shown in Figure 19. Cocoons were cut into even pieces and boiled in a .02M Na₂CO₃ Solution for 10, 15 and 30 minutes. Degummed fibers were then rinsed for 30 minutes in ultrapure water 3 times, and allowed to dry. All ultrapure water used for silk processing was Milli-Q distilled ultrapure water (Millipore, Inc.). Dry degummed fibers were then dissolved in 9M LiBr and incubated at 60 °C for 4 hours, then injected into 3500 MWCO Slide-A-Lyzer Dialysis Cassettes (Fisher Scientific) and dialyzed with ultrapure water (Milli-Q) for 48 hours, changing out ultrapure water every 6 hours. Upon removal from dialysis, silk solution was centrifuged twice at 11,000 rpm for 20 minutes. Temperatures inside the centrifuge were maintained at 5-10 °C. The resulting pure RSF solution was measured for protein concentration. Typical concentration measurements are performed by measuring out a specific volume of solution, drying the solution, and weighing the resulting silk film, however 10 and 15 minute boil solutions are highly viscous, and accurate volume

measurements are difficult, therefore solutions were quantified by percent weight by weight concentrations. RSF solution was pipetted onto a weigh boat and the mass of the silk solution was recorded. The solution was then incubated at 60 °C for several hours or until dry. The weight of the resulting film was recorded, and the %w/w concentration of the RSF in grams fibroin per gram of solution calculated.

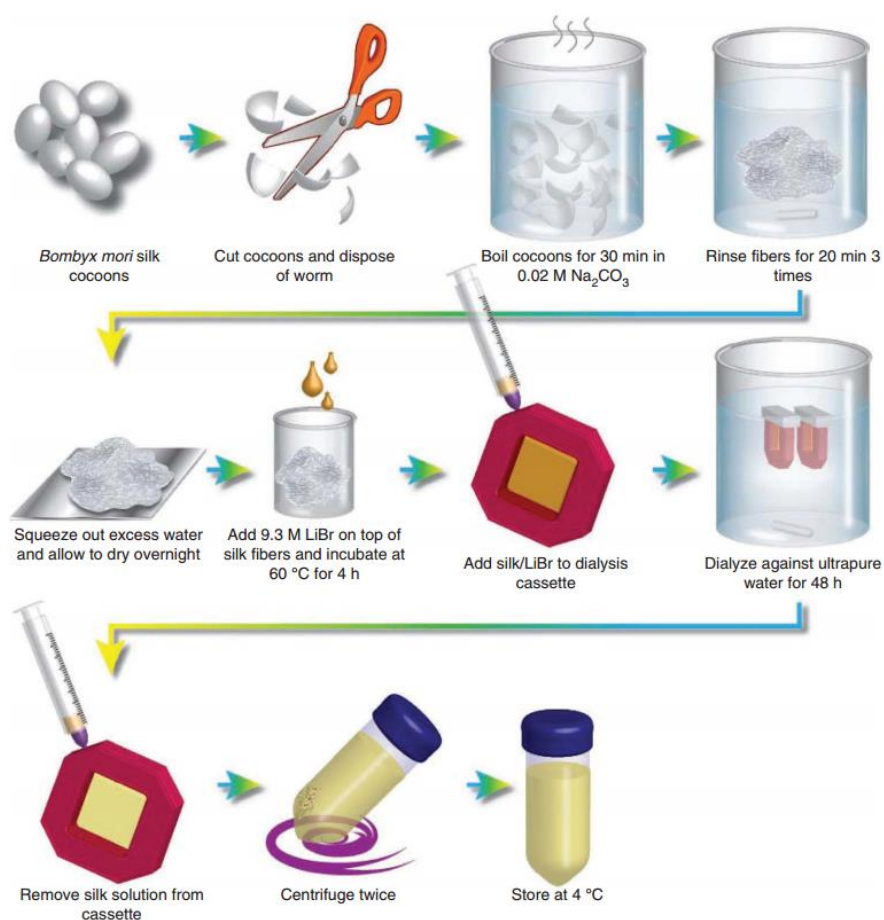


Figure 19: Silk solution processing [26].

3.2 Regenerated Silk Fibroin Solution Concentration and Boil Time

Fifteen minute-boil (15mb) silk was deemed the most appropriate choice of solution for this application, as it combines a reasonably low viscosity (unlike 10

minute-boil (10mb) silk solution), making it injectable through the trans-nasal system with enough cohesiveness that augmentation would be possible (unlike 30 minute-boil (30mb) silk solution).

RSF solution concentration was chosen based on the knowledge that a higher concentration RSF solution will yield a stronger, longer lasting, and more cohesive hydrogel. With this in mind, solution concentration was maximized based on difficulty of injection. The highest reasonable input force was determined as shown in Figure 20, by manually exerting pressure on an Instron 47913 Static load cell rated to 100 N using the thumb, forefinger, and middle finger. Pressure was exerted on the center of the face of the load cell, while holding the load cell in a way that mimics the grip used on a syringe.



Figure 20: Mechanical compression testing for maximum applied force.

Several individuals ran this experiment, and it was determined that a reasonable input force would be between 15 and 25 Newtons.

With these values in mind, a simplified viscous flow model was constructed to gauge the feasibility of silk solution injections through this system. Because fluid properties are necessary for such an approximation, rheological testing was performed on a basic 7%w/w 15mb RSF solution, which yielded a value for the dynamic viscosity of this solution.

3.2.1 RSF Solution Concentration Modeling

Basic flow calculations were based on the Hagen-Poiseuille equation. Values for silk solution viscosity were determined by rheological testing, and were plugged into the simplified model to determine the force needed to flow the solution through the system. Figure 21 shows the simplified model of the syringe-catheter-needle system, and more detailed calculations can be found in Appendix I. For simplicity, incompressibility, zero catheter extensibility, constant force, and zero shear sensitivity were assumed for all calculations. Equations are dependent on several variables: Pressure (ΔP), dynamic viscosity (μ), syringe, catheter, and needle length (L), Flow rate (Q), and syringe, catheter, and needle radius (r). Because fluid properties are necessary for such an approximation, rheological testing was performed on a basic 7%w/w 15mb RSF solution. Flow rate was calculated from a plunger compression rate of 8.5 mm/s, which was determined to be a reasonable injection speed. Calculations were performed for each segment of the system in order to verify the limiting factor. While it seems intuitive that the needle would be the most difficult to flow through due to the small inner diameter, the catheter is significantly longer, and therefore may offer more resistance.

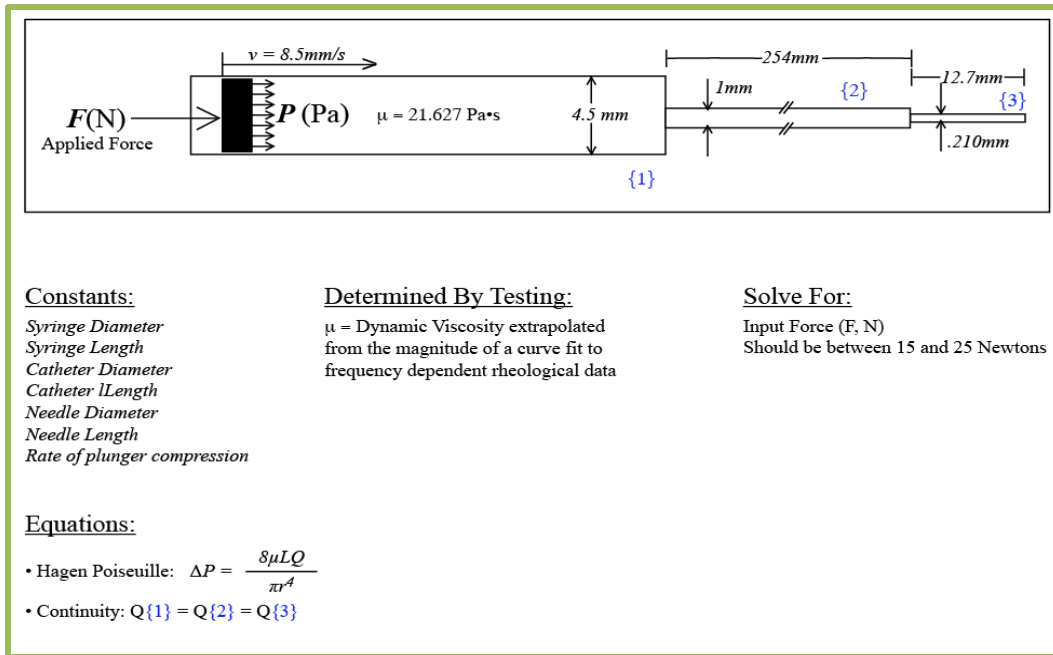


Figure 21: Shear flow model.

As expected, the needle is the limiting factor on flow in this system, however not by a significant amount. Substituting in values for a 7% w/w 15mb RSF solution, a maximum force of 26.94 N was calculated for the needle, and 23.80 N for the catheter. Both of these forces are close to the range set by project parameters, and appear to be reasonable values.

Because this model was highly simplified, it will by no means be fully accurate. The application of shear will cause an increase in β -Sheet content as the solution flows through the system, meaning that the further along the needle or catheter, the higher the solution viscosity will be. This shear sensitive behavior would be extremely difficult to approximate through a mathematical model. Because of these inaccuracies in the simplified model, mechanical testing was performed to get a better idea of what RSF solution concentration levels would be appropriate for this application, and to verify results of mathematical modeling.

3.2.2 Compressive Injection Force Testing

Mechanical testing was performed on varying concentrations of 15mb RSF solution. A needle and catheter setup with inner diameters comparable to those of the needle and catheter system to be used during the procedure was constructed by connecting 10” of 1 mm inner diameter Tygon tubing (Cole-Parmer Instrument Co., Vernon Hills, IL) to a BD 1mL luer-lok™ syringe (Fisher Scientific) and BD PrecisionGlide™ 27G x ½ Needle using plastic luer fittings. The syringe and catheter were loaded with RSF solution, and the setup was mounted in a custom acrylic fixture (shown in Figure 22).

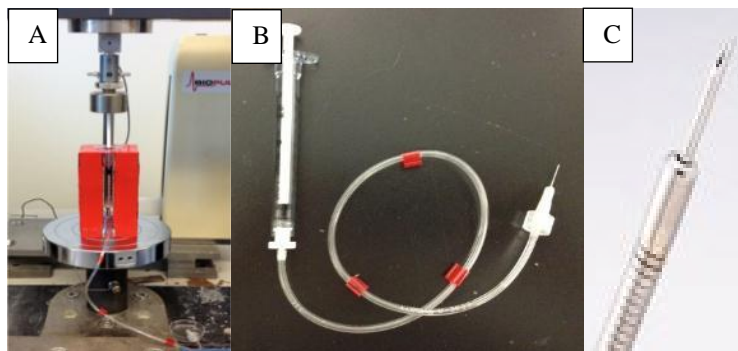


Figure 22: (A) Instron test setup. (B) Test needle/catheter. (C) Actual needle/catheter.

A compressive load was applied to the plunger of the syringe at a constant rate of 8.5 mm/sec using an Instron 3366 testing frame (Norwood MA, USA). The load observed by the load cell was recorded throughout the injection, and the maximum force from each test was calculated. Care was taken to eliminate end of test data in which the plunger may have been pressed flush with the body of the syringe, thus recording the compressive strength of the syringe and acrylic base and not the resistance of the solution. As a safety precaution, forces applied to the syringe were limited to 50 N. 15mb RSF solutions were tested at 1, 3, 5, and

7% w/w concentrations. Secondary testing included 8% w/w in order to reach input force limits of 25 N.

Figure 23 shows the results of mechanical testing performed. According to these results, an input force range of 15-25 N correlates to a concentration range of approximately 6-8% w/w RSF solution. After the definition of this range, all tests were performed using 7% w/w 15mb RSF solution. Mechanical testing also verified the results of the mathematical model, as the input force required to inject through the system was reasonably close to that calculated for injecting solution of the same viscosity through a 27G needle at the same flow rate.

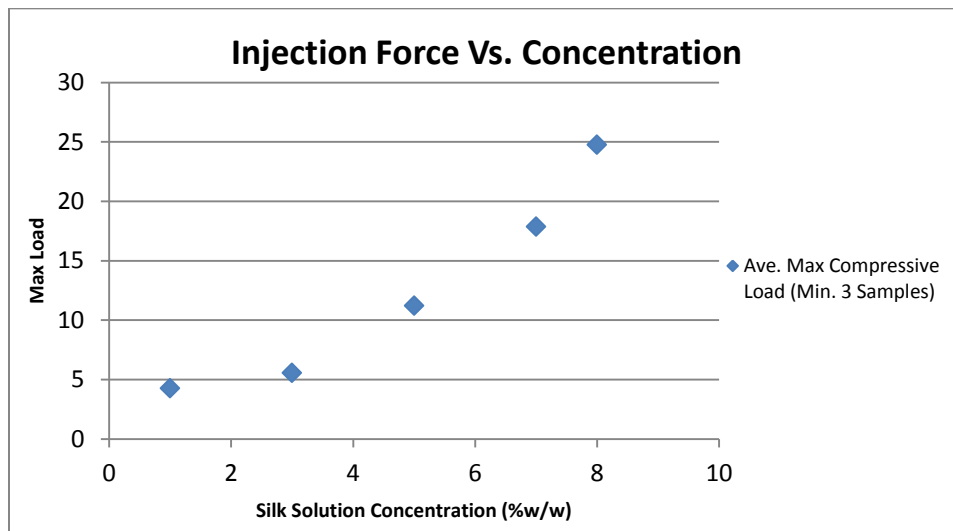


Figure 23: Averaged maximum compressive load required to maintain a 135.2 mm³/s flow rate (8.5 mm/s plunger compression rate) as determined by mechanical testing.

3.3 Rheological Measurements

Rheology is a testing method that defines the properties of viscoelastic materials. For this thesis research, parallel plate oscillatory shear rheology was used. Figure 24 shows the setup of a parallel plate rheometer. The pressure transducer reads

both vertical force and torque, as well as phase shift amplitudes, which indicate whether a material is behaving as a liquid-like or solid-like material, as well as the stiffness, viscosity, and many other properties of the material being tested. Radius (R) refers to the plate size. Larger plates will shear solutions more significantly, meaning that the transducer will read higher forces and torques. This is desirable when testing a thinner material, as higher forces will also yield more sensitivity in measurements. The gap between plates (H) will affect the vertical force, which also affects the sensitivity of the measurements. Rotation speed (ω) refers to the cycles per second (Hz) that the bottom plate of the rheometer rotates. Rotation amplitude can be varied in the software settings.

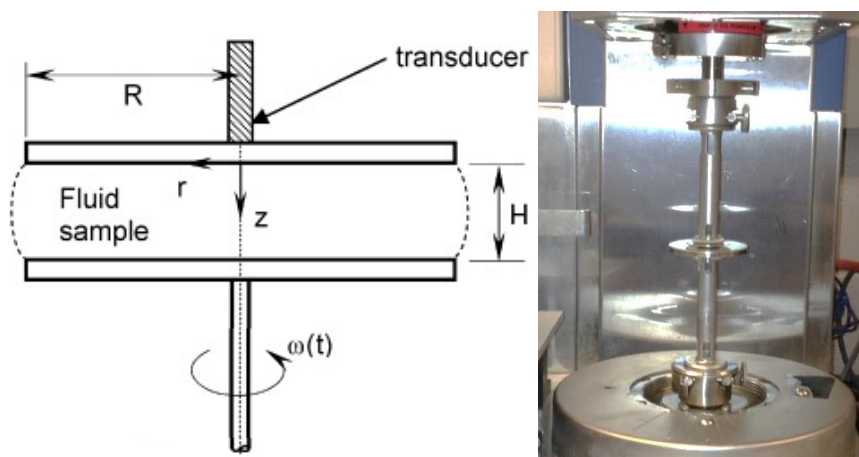


Figure 24: Rheometer setup and mechanisms [67].

The bottom plate is driven by a brushless DC motor, which can be set to rotate in a variety of ways. For this application, a frequency sweep was determined to be the most useful test. This means that the bottom plate oscillates at increasing frequencies, while the amplitude of the oscillation remains the same. Amplitudes can be defined by an initial strain sweep test, which will show that at a certain strain rate, properties will shift and will no longer exhibit linear behaviors. While

rotating, the rheometer has the capacity to measure many different variables. Those used primarily for this research are the storage and loss moduli (G' and G'' , respectively), the dynamic viscosity (η), the damping ratio (ζ) and the complex shear modulus (G^*). Storage and loss moduli (Pascals), indicate the shear modulus of the liquid-like portion and solid-like portion of a viscoelastic material. The damping ratio (Equation 3) is merely the ratio of loss modulus to storage modulus. A lower damping ratio indicates a more solid-like material, while a higher ratio indicates a more liquid-like material. Dynamic viscosity (Pascal-seconds) is derived purely from the liquid-like portion (loss modulus (G'')) of a material (Equation 4), as it is directly dependent on the loss modulus. Complex shear modulus (Equation 3 and (Equation 5) is a conjugate of the storage and loss modulus, and measured in units of Pascals. For comparison of values, the magnitude of the complex modulus is taken. This allows us to compare a value similar to stiffness in order to gauge differences in how a certain material will augment the vocal fold. Damping

$$\zeta = G''/G' \text{ (Equation 3)}$$

$$\eta = G'' / \omega \text{ (where } \omega = \text{frequency) (Equation 4)}$$

$$G^* = G' + iG'' \text{ (Equation 5)}$$

$$|G^*| = \sqrt{((G')^2 + (G'')^2)} \text{ (Equation 6)}$$

Each silk material format was tested for G^* , G' , η , and ζ , and the results were then plotted and compared with other silk constructs, and with vocal fold mucosal tissue, the rheological properties of which were found in literature. Parallel plate rheology was performed using a TA Ares-LS2 parallel plate rheometer (TA Instruments, New Castle, DE). All rheological testing was performed using the

same equipment and protocols unless otherwise indicated. For RSF solutions, 50 mm plates were set to a 0.5 mm gap. Initially, a strain sweep was performed to determine the strain cutoff for physical changes in the silk structure (indicated by a significant drop in the storage modulus of the material above a certain % strain). In the case of RSF solution and hydrogels, strain sweeps indicated that this cutoff value was higher than 100%. Due to this complication, it was determined that the best method of choosing a % strain value at which to run frequency sweeps was to choose a lower end value at which all properties recorded were linear. The region from 1-10% strain is both linear and highly correlated for all tested parameters. An intermediate value of 4% strain was chosen for all RSF solution and hydrogel oscillatory shear rheology frequency sweeps. Frequency sweeps were performed from 0.1 to 100 rad/s, at 4% strain, taking 10 measurements per decade. All samples were tested at room temperature. It is necessary to note that rheological measurements are not performed under physiological conditions (37 °C, semi-hydrated), and thus there may be some discrepancy between in-vivo rheological properties and those determined by this experimental testing.

3.4 Degradation Studies

In vitro degradation studies were performed using Protease XIV from *Streptomyces Griseus*. Protease XIV concentrations were set to 0.5 U/mL. Protease was mixed with Dubelco's Phosphate Buffered Saline Solution (Invitrogen), and the resulting supernatant was used to hydrate samples. 3 mm biopsy punches were used to harvest samples, which were placed in Falcon

MULTIWELL™ 24 well polystyrene plates with one sample per well, and 2 mL of supernatant per sample. Samples were incubated at 37 °C, and solutions were changed daily.

3.5 Post-Processing Methods

3.5.1 Vortexed Gels

RSF solution was placed in a conical tube and vortexed at 3200 rpm (amplitude of 2.45 mm) using a vortex mixer (Fisher Scientific). The same volume of solution was used for each sample to minimize variability. Samples were allowed to rest for 150-180 minutes post-vortexing to ensure completed phase transitions. Limits were chosen based on previously published data (Yucel, et al., 2009 [32]). Varying concentrations of RSF solution were vortexed for a range of times, and rheological testing was performed on all constructs as previously described.

3.5.2 Sheared Gels

Preliminary testing was performed with sheared gels to gain a sense of the viability of the construct for this application. Ideally, an RSF solution could be injected directly into the vocal fold through the needle and catheter system. The small diameters of the needle and catheter as well as the length of the catheter will apply significant amounts of shear to the material, likely causing an increase in β -Sheet content. In order to perform accurate rheological testing of this material, 7% w/w RSF solutions were injected directly onto the bottom plate of the parallel plate TA Ares-LS2 rheometer through various gauge needles by hand. Injecting

solutions by hand means that input force on the syringe will vary widely. This fact, coupled with viscosity altered by shear forces, means that both the inputs and solution properties will be varying during each injection, resulting in high levels of error between rheological measurements. Secondary testing was performed to explore effects of the needle and catheter setup used for trans-nasal injections.

3.5.3 Silk Electrogels

Figure 25 shows the setup used throughout this project for electrogelation of silk. Electrogels (E-Gels) were formed using an Agilent E3634A DC power supply connected to two platinum electrodes, which were submerged in a bath of silk solution. Voltage was set to 25 V +/- 0.1 V, and monitored for accuracy during gelation. The positive platinum electrode, which serves as the collection surface for any silk hydrogel formed during electrogelation, is an 11x37 mm platinum plate (Surepure Chemetals, Inc., Florham Park, NJ), soldered to a copper wire that connects to the positive port of the power supply. The negative electrode is made from a 0.4 mm diameter x 37 mm platinum wire (Surepure Chemetals, Inc., Florham Park, NJ), soldered to a copper wire that connects to the negative port of the power supply. A setup for gelation was prototyped using a Trotec Speedy 300™ Laser Cutter to cut ¼” clear acrylic sheets (McMaster-Carr), the pieces of which were welded together to form a fixture using Plastruct General Purpose Plastic Solvent Cement. 20 mL syringes with the tops removed served as baths for silk solution, allowing the volume of the remaining solution to be measured after removal of any hydrogel that may have formed during electrogelation.

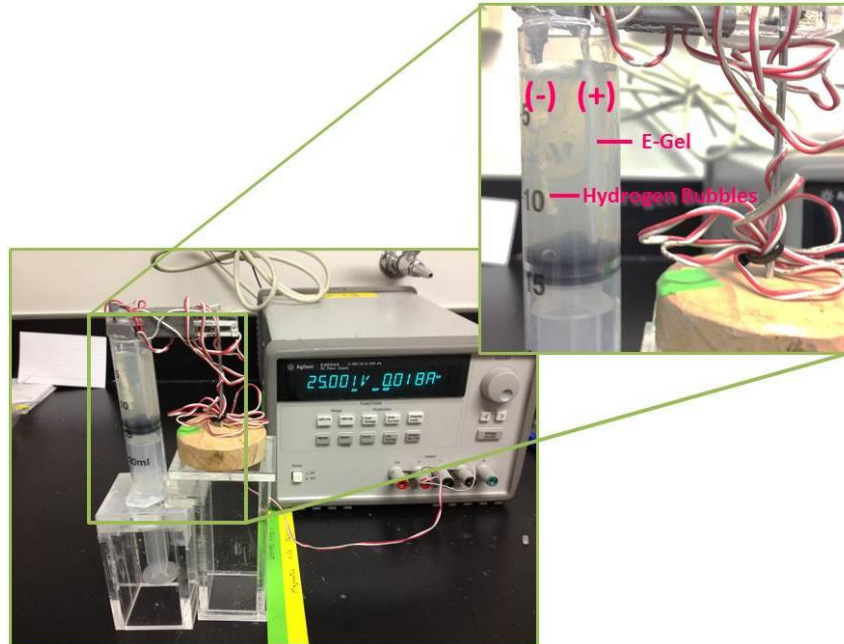


Figure 25: E-Gelling setup.

E-Gels were initially created from 10, 15, and 30mb RSF solutions, and rheological testing was performed as previously described. In order to investigate the role of silk solution age on the quality of E-Gels, a study was conducted taking rheological measurements of silk solutions and E-Gels weekly (for 15 and 30mb RSF solutions) or bi-weekly (for 10mb RSF solutions) until natural self-assembly occurred. Data from this study was also used to determine that 15mb RSF was the best solution to use in electrogelation of silk constructs for this application. After the decision to use 7%w/w 15mb RSF (for injectability reasons), E-Gels were tested for enzymatic degradation using the methods previously described. A minimum of 3 samples were collected at each time point.

3.5.4 Silk Electrogels with additives

There are near infinite substances that have the potential to cause cross-linking, accelerated assembly, or solidification of RSF solution. Each additive will have

different effects on the solution, some macromolecular, some chemical, and some physical. Because of the nature of this process as an *in vivo* gelation mechanism, additives are limited to body-friendly substances, which greatly reduces the number of usable additives. A few additives were tried and tested to improve the properties of E-Gels, described below.

Salinated Electrogels

Increasing the ionic content of a silk solution proved to decrease assembly time and encourage gelation in silk solutions. The constraints of this project require that any solutions injected into the vocal fold be of physiological salinity (0.90% w/v NaCl) or lower [1]. Increasing the salinity of the RSF solution also increases the conductivity, thus allowing electrogelation to occur more quickly due to increased current flow. As mentioned previously, the addition of ionic content also encourages protein assembly. Electrogelation of silk solutions with varying levels of salinity were tested for acceleration of gelation and higher solution to gel conversion percentages.

It was noted that during electrogelation, the temperature of the solution increased significantly when RSF solution was doped with NaCl. Tests were conducted to quantify thermal effects of added salt. Omega 0.01" diameter, glass-insulated type T thermocouples were immersed in RSF baths under applied voltage. Thermocouples output to a National Instruments cDAQ-9172 chassis with an NI 9219 Module, which connected to a computer via USB port. Raw data was read by NI Measurement and Automation software, which was interfaced

with LabVIEW, where data was processed and exported to a usable file format.

Figure 26 shows the NI DAQ/Thermocouple setup used for this experiment.

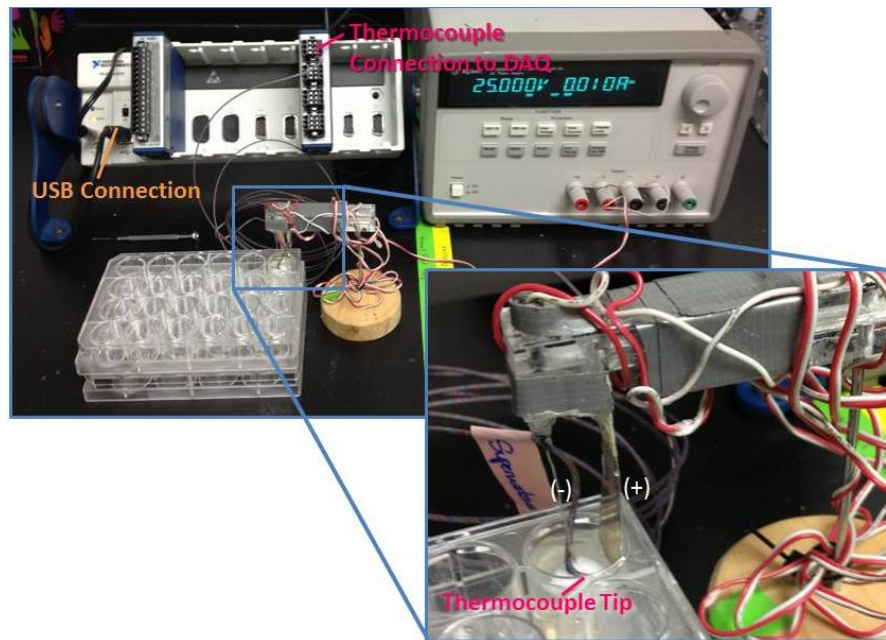


Figure 26: NI-DAQ and thermocouple setup.

Measurements were taken every two seconds and recorded into a text file using a LabVIEW code. Data was plotted and compared to determine the maximum salinity of RSF under applied voltage such that burning of the tissue would not occur and there would be limited patient discomfort. As a preliminary temperature limit, the maximum temperature reached in a natural physiological environment was chosen, and was found to be 42 °C [68]. Temperature testing was performed using 3 mL RSF solution with an applied voltage of 25 V. Based on this, a two-minute time limit was imposed by the consulting otolaryngologist as an acceptable time frame for having a needle in the patient's vocal fold. Voltage was applied to the RSF solution for two minutes, and temperature measurements were

continued for one minute after applied voltage was removed in order to monitor cooling rates.

Thermocouple and rheological measurements (performed as previously described) were taken at salinity levels of 0.90% w/v NaCl, 0.45% w/v NaCl, and 0.225% w/v NaCl, and the results were compared. During testing, the percentage of remaining RSF solution after gelation was monitored for each sample.

Physical Reinforcements

While chemical additives may increase the temperature to dangerous levels for *in vivo* gelation, physical reinforcements will not. Many silk constructs use other silk formats as reinforcements to obtain better mechanical properties, such as microfiber reinforcements, particle reinforcements, and various silk composite constructs [26, 69]. Chopped lyophilized silk foam, milled silk powder, and a combination of the two were added to RSF solution prior to the application of voltage in ratios of 0.5 g reinforcement media to 3 mL RSF solution. Degradation testing was performed as previously described to compare properties between constructs.

Cross Linkers

Ethanol was added to RSF solution and mixed gently prior to electrogelation. It is unclear what concentrations of ethanol are safe when injected locally, so a wide range of concentrations were tested to determine the effects on electrogelation. 0.1, 1, and 10% Ethanol 7% w/w RSF solutions were prepared and electrogelated. Rheological and degradation studies were performed as previously described.

3.5.5 Additive Gels

As with acceleration of electrogelation, there are many substances that have the potential to cause accelerated assembly of silk proteins without a secondary gelation mechanism. Ionic additives are one of the most commonly used for the gelation of silk, as ionic content is one of the key mechanisms used to adjust silk consistency in the natural silk spinning process. In order to maintain a level of biocompatibility, only ions naturally found in the human body were investigated for use in the gelation of RSF. The additive primarily focused on for this portion of the project was sodium chloride (table salt).

Sodium Chloride

5M NaCl solution was acquired from Sigma Aldrich and mixed with 7%w/w 15mb RSF solution in various ratios. Samples were incubated at 37 °C, and results were monitored for several days. Solutions were prepared in a Falcon MULTIWELL™ 24 well polystyrene plate, and ratios ranged from 95% silk to 95% 5M NaCl solution, with samples prepared at concentration increments of 5%. The salt concentration of the mixture was later calculated to determine the salinity of each well. The best construct from this experiment was tested for degradation and rheological properties as previously described.

4. Results and Discussion

Several important factors of vocal fold augmentation materials were investigated for each silk format including rheology, degradation, *in vivo* safety, and delivery. Rheological comparisons were made between silk materials by comparing complex shear modulus (G^*) curve magnitudes. This value (related to stiffness) allows us to compare silk constructs with varying processing parameters. A typical G^* curve for a generic silk construct is shown in Figure 27, where the modulus increases with increasing frequency. Raw data from the rheometer was plotted and curve-fit using a power curve of the form $Y = kx^n$. By plotting the “k” value from these curve fits for each construct, it is easy to identify trends and compare silk formats.

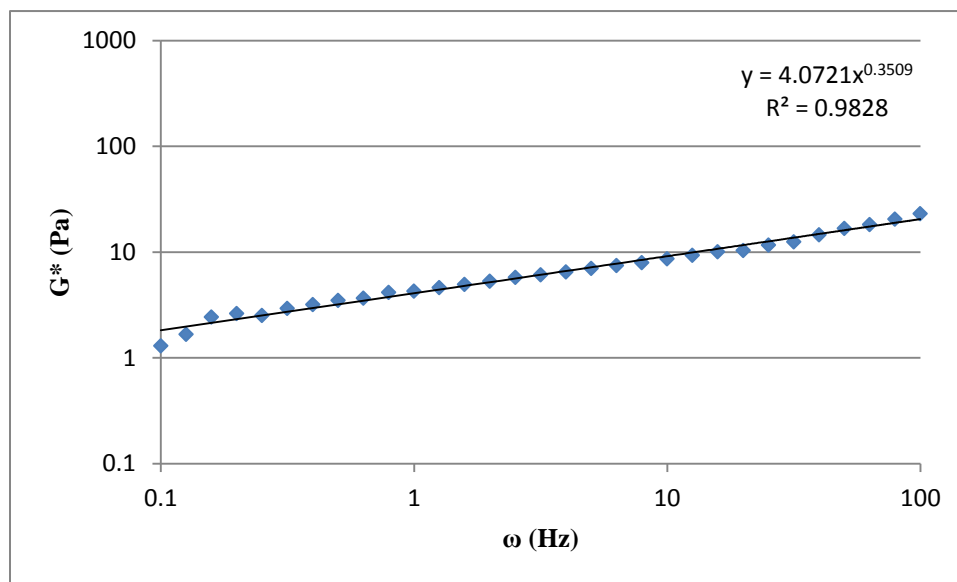


Figure 27: Typical complex shear modulus curve for silk constructs.

G^* Curve magnitude values were plotted for each silk construct to determine the effects of processing conditions. The storage modulus (G'), dynamic viscosity (η), and damping ratio (ζ) of each silk construct were then compared to rheological

data collected on the human vocal fold mucosa (Chan et al. 1999). Chan et al., 1999 explored differences in the human vocal fold mucosa between age and gender groups by investigating these three properties. By plotting data collected on silk constructs for these three properties, it is possible to gain an understanding of how closely a given construct matches the viscoelasticity of the vocal fold. Figure 28 shows typical curves for these properties (silk constructs). Storage modulus (or shear modulus) curves steadily increase with frequency. This means that at higher shear rates, the material becomes stiffer. The opposite is true of dynamic viscosity. A linear, negatively sloped dynamic viscosity curve indicates a Newtonian shear-thinning material. Slight changes in damping ratio indicate materials shifting slightly between more solid-like and more liquid-like behaviors. A higher damping ratio indicates a more liquid-like material, and a lower damping ratio indicates a more solid-like material.

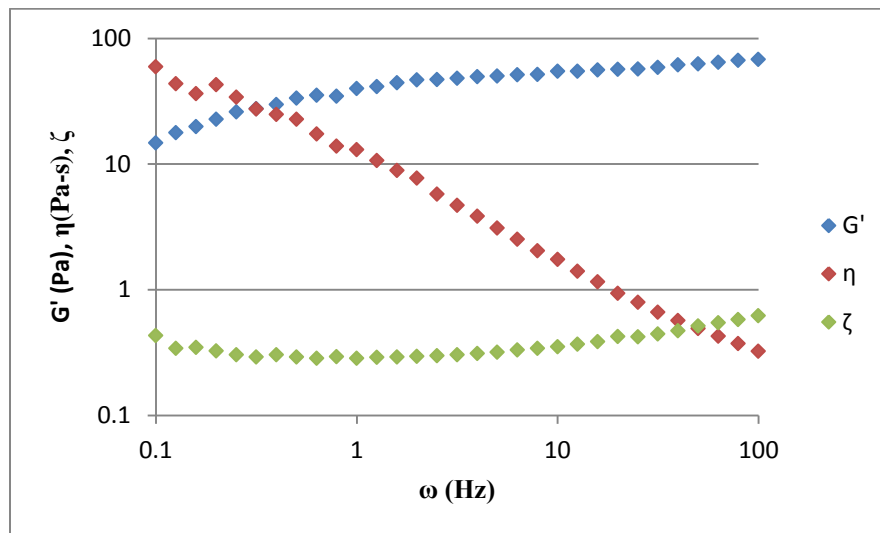


Figure 28: Standard G' , η , and ζ curves for silk

Each silk material investigated was altered by varying certain processing parameters. Table 4 shows parameters that were altered for each silk construct, as well as tests that were performed to characterize each silk material format.

Table 4: Parameters altered and tests performed for various silk constructs

	Parameters Altered	Tests Performed
Vortexed Gels	<ul style="list-style-type: none"> • Vortexing time • Post-vortex assembly time • Silk solution concentration 	<ul style="list-style-type: none"> • Rheology
Sheared Gels	<ul style="list-style-type: none"> • Needle gauge • Use of catheter 	<ul style="list-style-type: none"> • Rheology
E-Gels	<ul style="list-style-type: none"> • Silk solution concentration • Silk solution boil time • Silk solution age • Use of various additives 	<ul style="list-style-type: none"> • Rheology • Degradation • solution-gel conversion
Additive Gels	<ul style="list-style-type: none"> • Additive concentration 	<ul style="list-style-type: none"> • Rheology • Degradation
Silk Foams	--	--
Sonicated Gels	--	--
pH Gels	--	--

4.1 Vortexed Gels

Initially, rheological testing of vortexed gels was performed. Figure 29 compares the complex shear modulus between two concentrations (3 and 8%w/w RSF) and two vortexing times (V_t of 2 and 5 minutes), and post-vortex assembly times (A_t ranging from 150-180 minutes). Post-vortex assembly times must be long enough to allow full gelation of the material (since vortexing causes a time delayed gelation reaction). The values chosen were conservative, and based on the results

of testing performed to quantify the rheological properties of vortexed gels at various post-vortex assembly times [32].

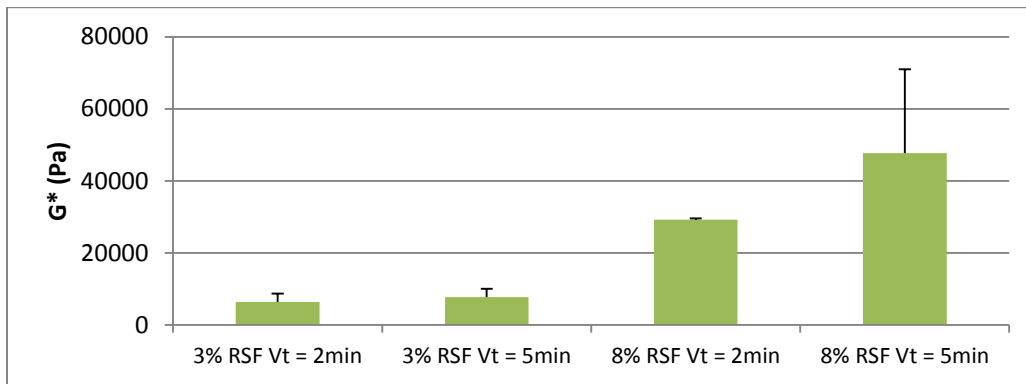
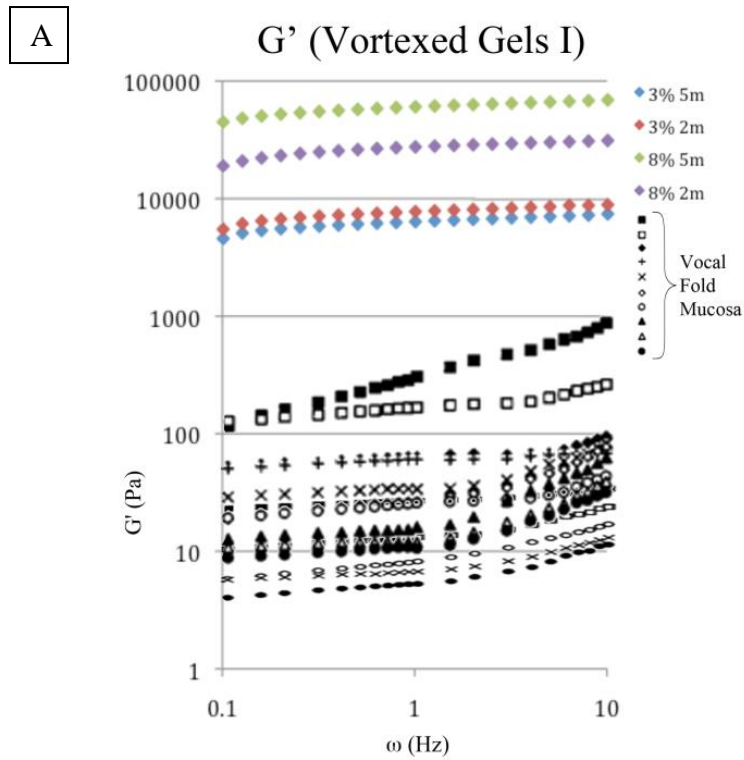


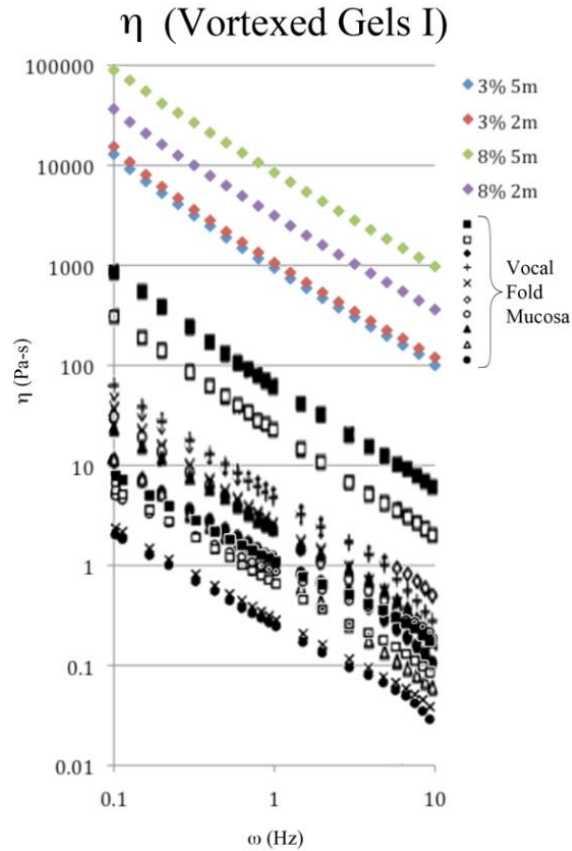
Figure 29: Vortexed gel rheology: Complex shear modulus comparisons between RSF solutions of varying concentration and V_t (3 samples per construct).

There are clear trends regarding vortexing time and solution concentration. As expected, an increase in concentration increases the stiffness of the gel, as does an increase in vortexing time. This is likely due to a higher number of inter-chain interactions. Differences in vortexing time yield more significant differences in G^* at higher solution concentrations (the complex modulus of an 8% RSF sonicated hydrogel increases by approximately 65% when vortexing time is increased from 2 to 5 minutes, whereas the complex modulus of a 3% RSF sonicated hydrogel only increases by approximately 20%). This could indicate a higher likelihood of chain interactions with higher concentrations, meaning that there is a higher maximum possible stiffness and a wider range of properties is possible. In order to compare properties accurately, plots of rheological data collected were overlaid onto existing plots of vocal fold mucosa data from the literature (Chan et al., 1999). Because of differences in equipment, data was collected on a slightly different frequency range in the two studies, meaning that

datasets had to be truncated in order to directly compare results. Figure 30 shows three plots: shear modulus (G') comparisons, dynamic viscosity (η) comparisons, and damping ratio (ζ) comparisons. Black and white data shows various vocal fold tests, and color data shows silk constructs.



B



C

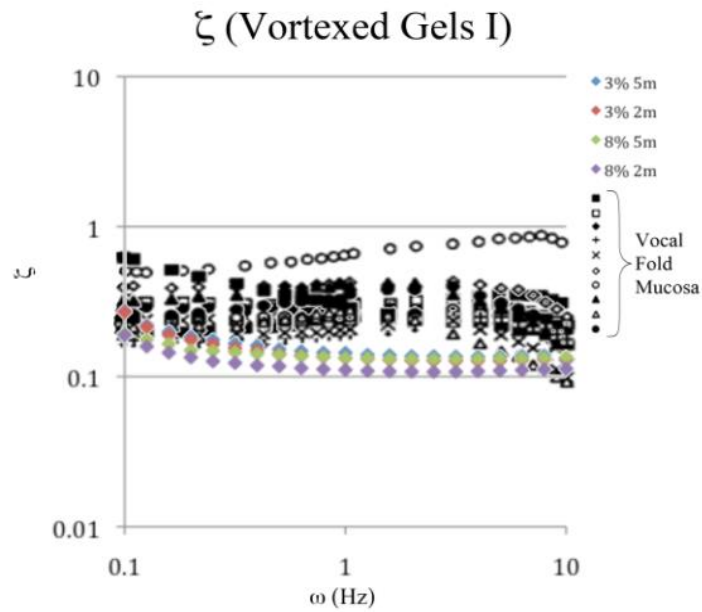


Figure 30: Rheological comparisons between initial vortexed gels and human vocal fold mucosa (3 samples per data point). (A) Storage modulus. (B) Dynamic Viscosity. (C) Damping ratio.

The magnitude of shear modulus and viscosity curves of all of these constructs are several orders of magnitude higher than those of the vocal fold mucosa. This indicates that that vortexed gels (when created using these processing parameters) are too stiff for this application. Viscosity curves do, however, match relatively well based on slope, meaning that the shear-thinning properties of the gels are similar to those of the vocal fold. The same observation can be made when looking at the damping ratio plot. Curves are of a similar magnitude, though a bit low, indicating more solid-like behavior than that of the vocal fold mucosa. This stiffness is likely due to the high levels of β -Sheet content in vortexed gels, and the high quantity of chain interactions caused when uniform vibrational shear is applied to a silk solution.

Due to the high stiffness of this material, further testing was conducted using shorter vortexing times. Complex shear modulus values for 8% RSF solutions vortexed for 10, 30 and 60 s are shown in Figure 31. Note that values are plotted on a logarithmic scale due to the orders of magnitude differences between $V_t = 10$ s and the other values.

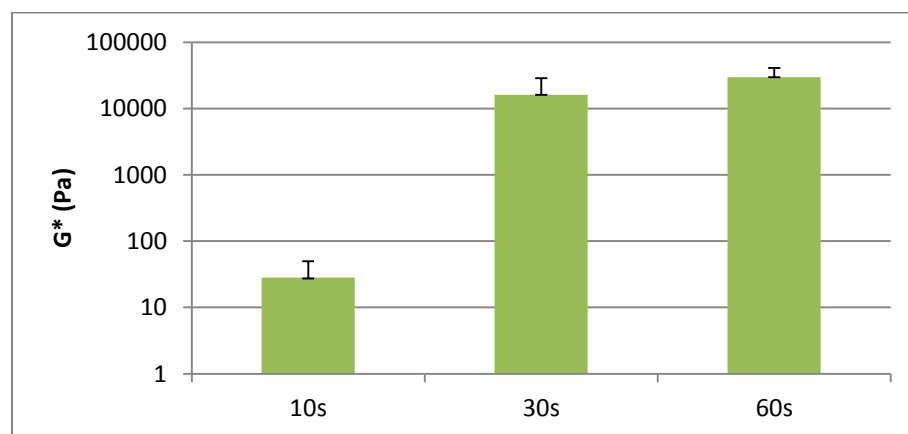
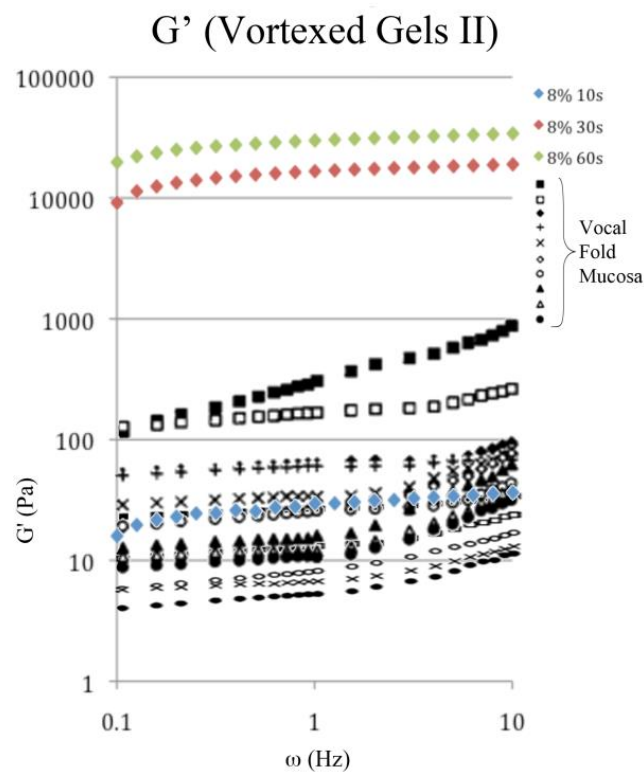


Figure 31: Vortexed gel rheology: secondary complex shear modulus comparisons of 8%w/w RSF with varying vortexing times (3 samples per construct).

As expected (and as found in previous experiments and literature), an increase in vortexing time directly correlates to an increase in stiffness. This is likely due to increased inter-chain interactions, and a higher percentage of conversion of random coil and α -Helix conformations to β -Sheet. At a certain point, G^* plateaus, and the stiffness of the gel becomes independent of vortexing time. This is due to the limited number of inter-chain interactions that can occur in a given RSF solution. Shear modulus, dynamic viscosity, and damping ratio comparisons for 8% RSF ($V_t = 10, 30, \text{ and } 60 \text{ s}$) materials and vocal fold mucosa are shown in Figure 32.

A



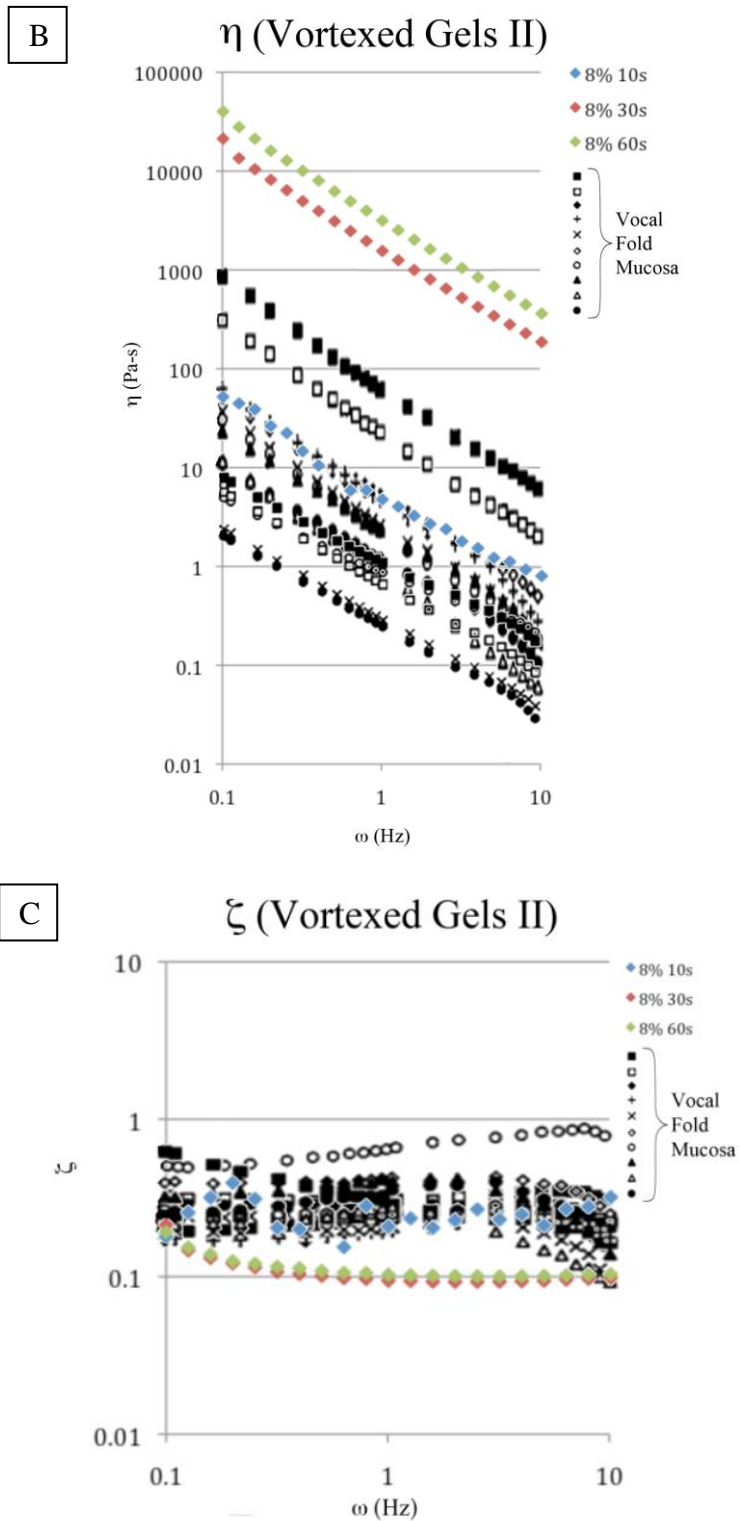


Figure 32: Rheological comparisons between secondary vortexed gels and human vocal fold mucosa (3 samples per data point). (A) Storage modulus. (B) Dynamic Viscosity. (C) Damping ratio.

As shown in Figure 31, Both 30 and 60 second vortexing times yield hydrogels with shear modulus and dynamic viscosity curves two to three orders of magnitude higher than those of the vocal fold, as well as a significantly more solid-like damping ratio curve (lower magnitude). These materials are significantly stiffer and more solid-like than the vocal fold mucosa, making them a poor choice for vocal fold augmentation. Another property to note, which may not be clear from the rheological properties shown, is that although very stiff, these gels are not particularly cohesive, and often crumble under mechanical load. The properties of RSF solutions vortexed for 10 s match well for shear modulus and dynamic viscosity, however, the solution was qualitatively solution-like in nature. This may not be evident by the damping ratio plot, as the curve appears to match the magnitude of the vocal fold curves well, but it must be noted that the data is quite scattered (lack of distinct trending in the lower frequency region). This occurs when a solution is too thin for the transducer to read properly, and indicates that measurements may be slightly inaccurate in this specific data range. This means that any data in the scattered area must be discounted (data at higher frequency ranges is often much more readable, and therefore comparisons may still be made by looking at overall responses and ignoring the lower frequency range). The solution-like properties of this material can also be noted upon handling, as it behaves more like a silk solution than a hydrogel. This indicates that the construct would likely be resorbed quickly *in vivo*, and also does not sufficiently match the rheology of the vocal fold.

Other concerns with vortexed gels are the effects of solution age and inconsistencies, which could decrease gelation time, as will temperature, humidity, and applied shear. Any errors or anomalies in an RSF solution vortexed pre-injection could either cause premature gelation, which would cause the catheter to clog, or gel too slowly, which would result in the injection being resorbed before solidification. It is more likely that problems would arise due to catheter clogging and premature gelation, as there is a larger margin for error in when looking at absorption time. In addition, the application of shear as the vortexed solution is injected increases the possibility of premature gelation and catheter clogging. Additionally, pre-injection vortexing would limit the surgeons working time, since injections would need to be completed before gelation occurred.

To avoid these inconsistencies, vortexing could be performed *in vivo*, by applying the vibration source to the skin on the outside of the larynx. Low frequency vibrations (while more noticeable) would not harm the tissues in the vocal fold, although the discomfort caused by exposure to high amplitude vibrations may be too much, depending on the patient. There is also the possibility that the vibrational energy produced by the source will not penetrate the tissues sufficiently and gelation of the silk will not occur. Damping due to cartilage, muscle, and mucosal tissues will vary between male and female patients, as well as patient to patient within those groups, as each individual has unique combinations of muscle mass, laryngeal cavity size, and tissue stiffness.

4.2 Sheared Gels

During mechanical testing (performed to determine optimal solution concentration), it was noted that 7%w/w 15mb RSF solutions tended to gel slightly when injected through the trans-nasal vocal fold augmentation needle and catheter system. Based on this, 7%w/w 15mb RSF solutions were used for testing sheared gels.

4.2.1 Rheology

Initially, before parameters had been set for needle size, rheological testing was performed on 7% 15mb RSF flowed through several different needles by hand. Figure 33 shows interpolated complex shear modulus curve magnitude values for these constructs.

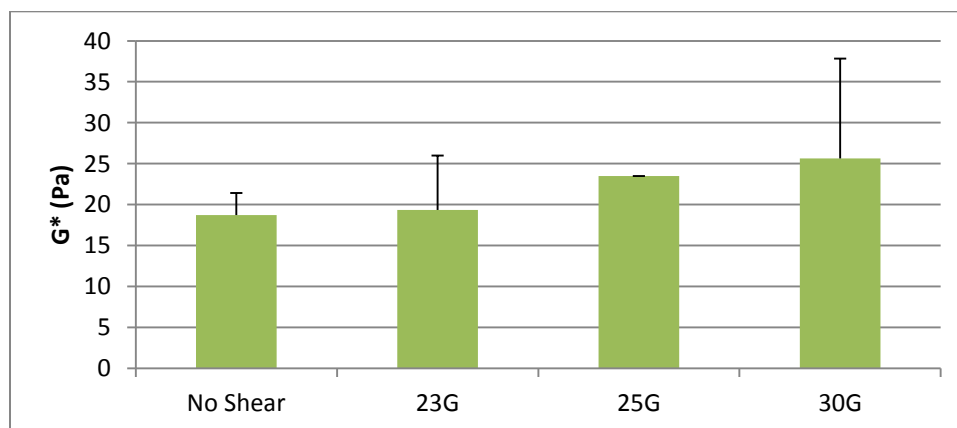
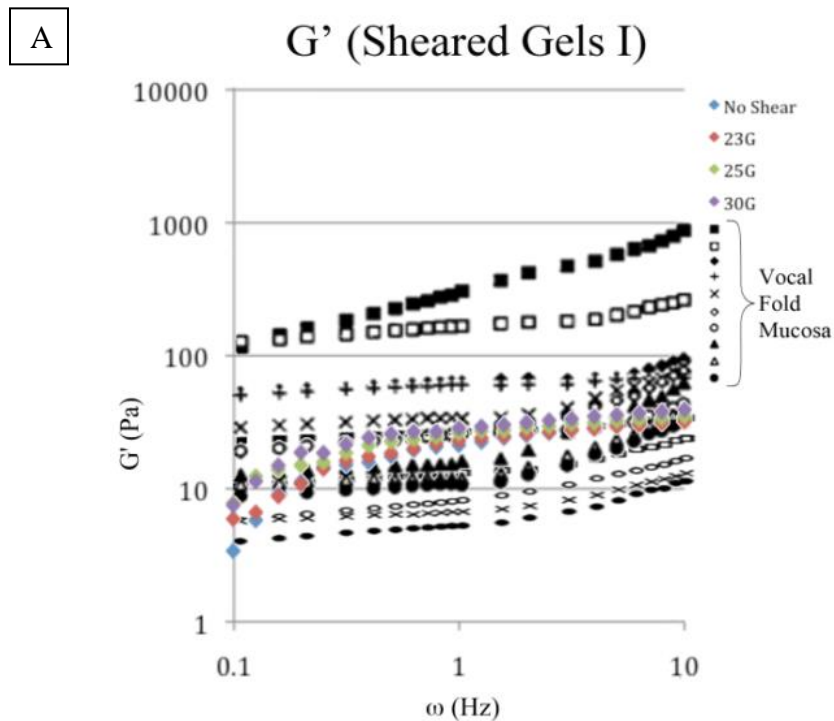


Figure 33: Sheared gel rheology: complex shear modulus comparisons between 7%RSF solutions injected through various needles (2 samples per construct).

As expected, there is some increase in stiffness with an increase in needle gauge (smaller needles), due to higher levels of shear with smaller needle diameters. While there appears to be a trend in the data, it is important to note that error is significant, and interrupts this trend. On a larger scale, these constructs are all of

very similar shear modulus. Error in these measurements is caused by variable input force (injections were performed by hand). Because injections will be performed by hand during procedures, it is important to mimic these conditions when testing construct properties. In order to better elucidate the effect of shear on silk solution properties, shear modulus, dynamic viscosity, and damping ratio are compared to data on the same variables for vocal fold mucosa (Figure 34).



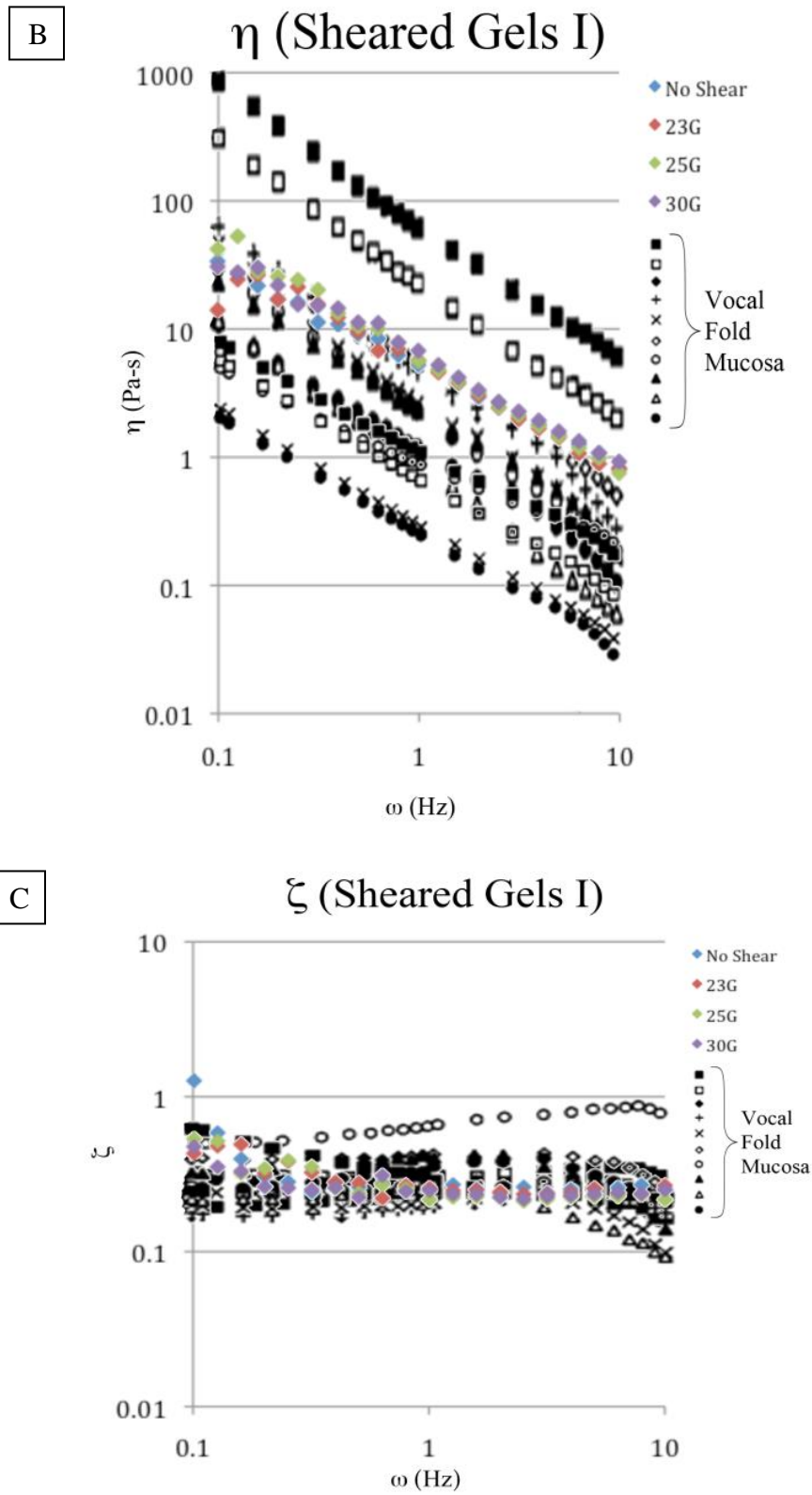


Figure 34: Rheological comparisons between sheared gels (various needles) and vocal fold mucosa (2 samples per data point). (A) Storage modulus. (B) Dynamic viscosity. (C) Damping ratio

These materials appear to match the rheological properties of the vocal fold mucosa quite well. All curves fall within acceptable ranges. It must be noted, however, that the material properties of sheared gels line up closely with those of an un-sheared RSF solution (shown in blue). One reason for this lack of distinction between constructs is that sheared gels tend to develop small clumps of very stiff material suspended in a larger quantity of unaffected solution. The rheometer has difficulty reading the properties of such an inhomogeneous solution, and the properties of these β -Sheet conformation-rich clumps of material will likely not register, meaning that only the un-sheared solution properties will be recorded.

After initial testing, when parameters had been defined for needle and catheter sizes and a model of the injection system was fabricated, secondary rheological testing was performed using 27G Needles and 10" 16G catheters (as per the project specifications). Solution was loaded into 1 mL syringes and injected through the needle and catheter system onto the plate. It was noted during this experiment that catheter flexibility played a large role in the actual shear forces applied to the solution. Using a soft polymeric catheter clearly limited the amount of force possible to input from the syringe, so that pressing the plunger all the way down and exerting as much force as possible generally achieved the same results as pressing it down slowly. Due to this complication, testing was performed with 27G needles connected directly to a syringe, as was previously performed with other needle sizes. Figure 35 shows the results of these tests.

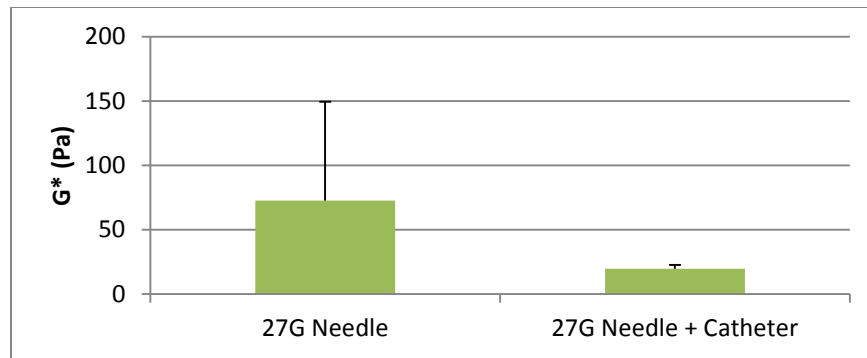
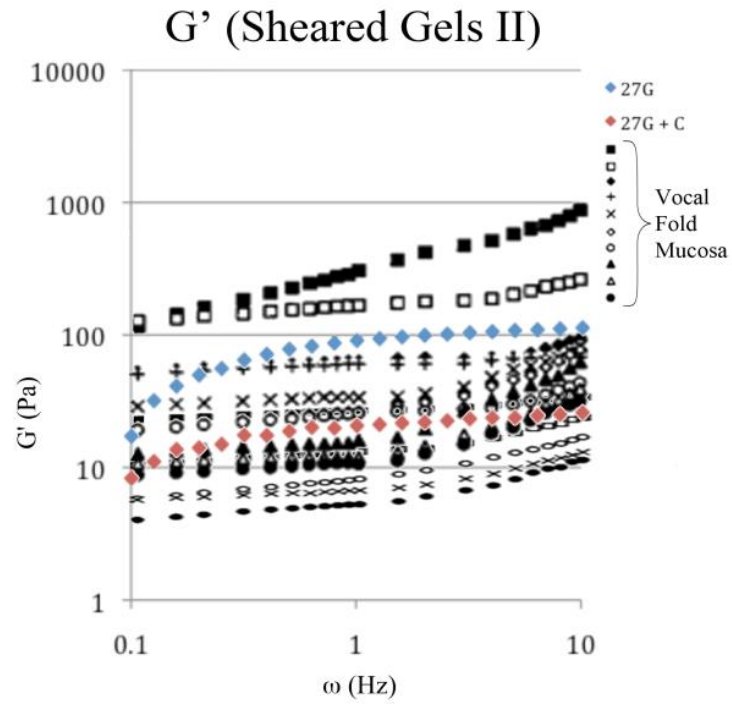


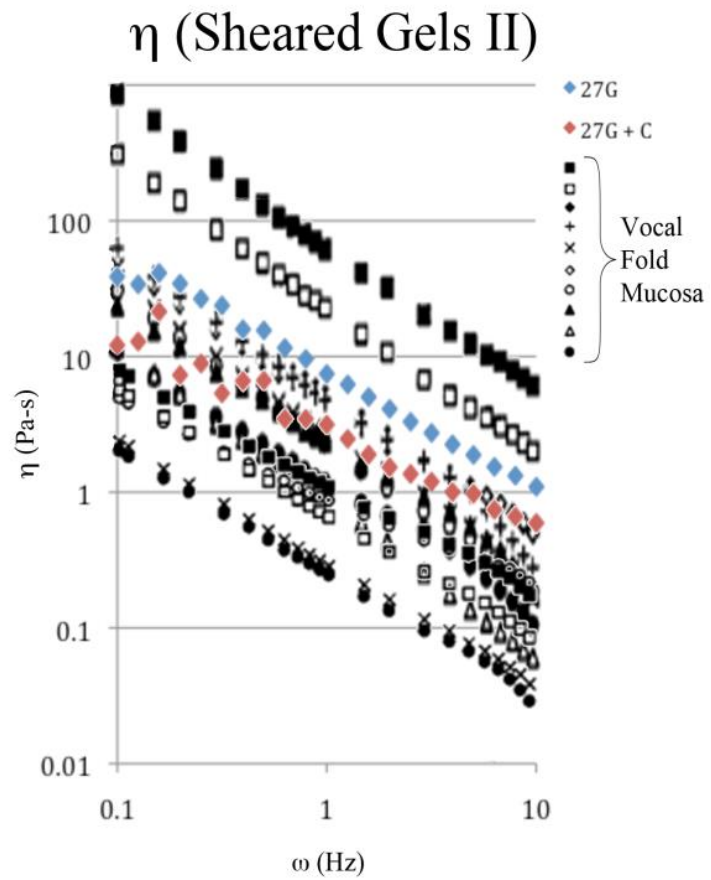
Figure 35: Sheared gel rheology: complex shear modulus comparisons of RSF solutions sheared by injection through a 27G needle with and without a catheter (3 samples per construct).

It can be seen that using a catheter composed of Tygon tubing (a slightly elastic material) lowers the shear forces applied to the solution. This is exhibited by a lower shear modulus (less shear force yields a softer material). Use of a soft catheter also generates a more consistent material, as evidenced by the significantly smaller error. This is due to the lack of rigidity in the catheter walls, or catheter extensibility. This result can be viewed as a positive and negative quality. Balancing out forces applied by the surgeon will result in more repeatable results (smaller error bars), however it also eliminates any sense of feedback for the surgeon performing the injection. Pressing the syringe down a measured amount does not necessarily directly correlate to an amount of material extruded through the needle. In order to further investigate the effects of various needle and catheter setups, rheological comparisons between these sheared gels and vocal fold mucosa were investigated (Figure 36).

A



B



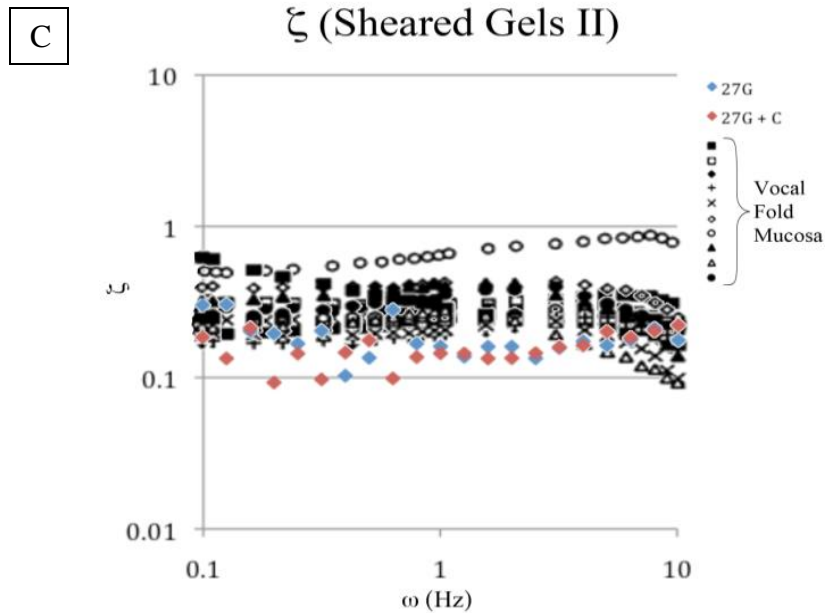


Figure 36: Rheological comparisons between 27G needle sheared gels (with and without a catheter) and vocal fold mucosa (3 samples per data point). (A) Storage modulus. (B) Dynamic viscosity. (C) Damping ratio.

As with the initial sheared gel testing, all rheological properties match reasonably well: curve magnitudes for shear modulus, dynamic viscosity, and damping ratio all fall within the limits of the vocal fold rheology, and curve slopes match those of the vocal fold mucosa well. Injecting solution without a catheter clearly results in a higher viscosity, stiffer material than when an extensible catheter is used (as anticipated based on complex shear modulus results). When examining the damping ratio plot, it must be noted that both materials exhibit erratic rheological testing response (as with other thin materials) indicating that the solution was too liquid-like to accurately characterize due to the limited sensitivity of the transducer. Sheared Gels (as processed currently) would likely offer partially successful augmentation. β -Sheet clumps would likely remain strong in the vocal fold, however the solution in which these clumps are suspended would be resorbed. With the current system, over-injection of the material would be

necessary, and further rheological testing would need to be done to determine if the β -Sheet rich clumps would match the rheological properties of the vocal fold correctly or not.

4.2.2 Delivery

Shear can be applied to the solution in many ways, however the most convenient method for this application is to inject the silk solution through the needle and catheter system already in place for trans-nasal vocal fold augmentation injections (as shown in Figure 37). The parameters of the solution can then be altered to achieve the desired hydrogel quality.

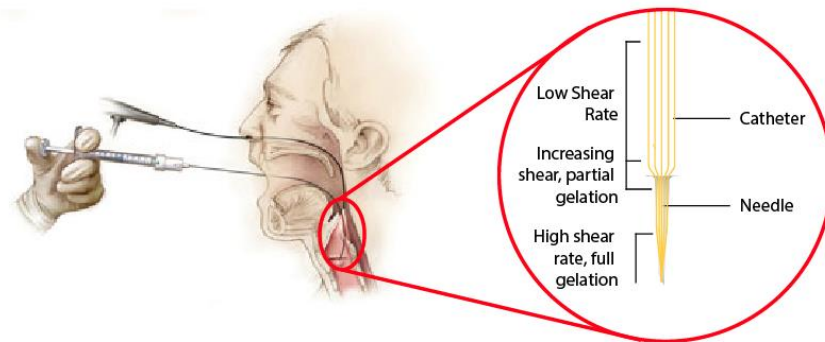


Figure 37: Proposed sheared gel delivery mechanism.

While this is an attractive option due to the lack of preparation, extra hardware, and overall simplicity, there are many constraints for this process. pH and ionic content cannot fall outside the physiological range (pH 5 – pH 8), meaning that only the solution concentration can be widely varied to achieve desirable properties. RSF solution concentration must also be constrained, however, as changes in concentration directly correlate to changes in viscosity. High viscosity solutions will be too difficult for the surgeon to inject, while very low viscosity

solutions will be difficult to control. The most important challenge associated with this delivery mechanism is the input force. Because the pressure applied to the plunger of the syringe is applied by a human, the input force will vary widely. This means that even a homogenous silk solution that is consistent between samples will not gel the same way every time, and the results of the procedure will be highly inconsistent. This begs the use of a mechanical pressure assistive device, however, such a device would decrease or eliminate tactile feedback for the surgeon, which is a critical for correct placement and quantity of the augmentation material.

4.3 Silk Electrogels

Initially, E-Gels were tested for dependence on RSF solution age. E-Gels were created and tested using aged solution to identify the effects of solution age on rheological properties of E-Gels. Solution rheology was also recorded. This testing was performed primarily as part of a study investigating the influence of silk age on various constructs, but data collected is also useful for this application, as it gives a wide range of data for solutions and E-Gels that can be compared to the vocal fold mucosa.

4.3.1 Time Dependent Rheology

Average complex shear modulus (G^*) was plotted for each time point, the results of which can be seen in Figure 38. Note that curve labels are abbreviated by boil time and construct type (10mbS refers to a 10 minute boil solution, and 10mbE refers to a 10 minute boil E-Gel).

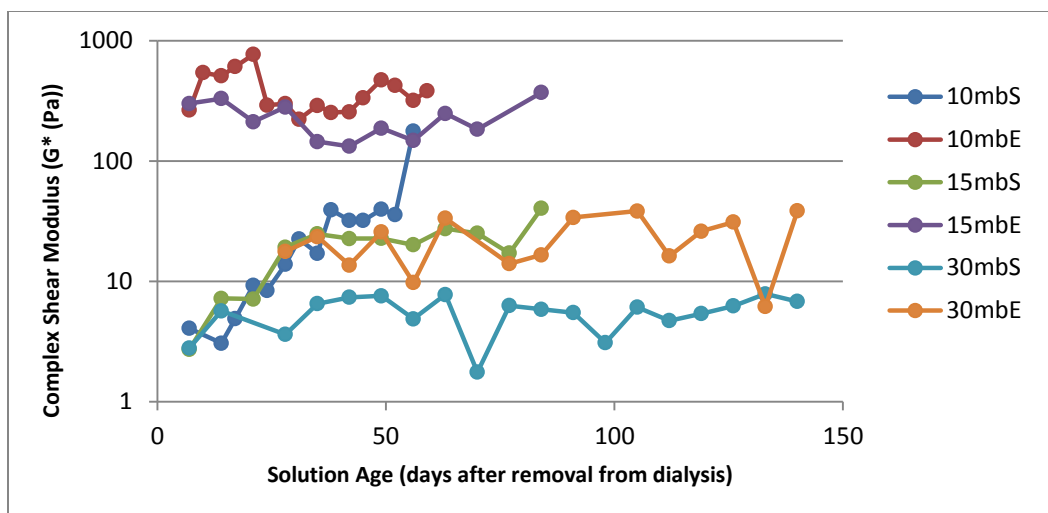


Figure 38: E-Gel rheology: complex shear modulus of RSF solutions and E-Gels as a function of solution age (3 samples per construct per time point).

Looking at each curve, there is a wide variety of results. The stiffness of 10mb solution increases steadily and rapidly until self-assembly occurs after 56 days. Similar behavior can be noted in 15mb solution and E-Gel, though on a much more gradual scale. 10mb E-Gel exhibits odd behaviors, and actually decreases in shear modulus after 21 days, then increases again slowly. The reasons behind this behavior are not well elucidated, but may be attributed to inconsistencies in the electrogelation process. 30mb solutions and E-Gels exhibit erratic behavior: data is scattered and shows significant changes in shear modulus over time without any noticeable trends. It is possible that the amount of scattering could be due to inconsistencies in the electrogelation process, or that changes in solution could be quantified more accurately by comparing another parameter. The data collected during this test was also used to compare average complex shear modulus, shear modulus, dynamic viscosity, and damping ratio curves for all results. Figure 39 shows comparisons of complex shear modulus curve magnitudes between solutions and E-Gels of different boil times.

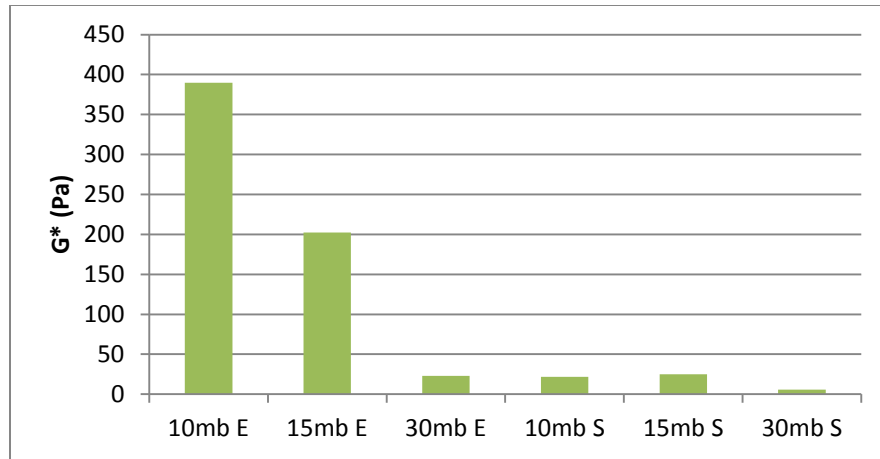
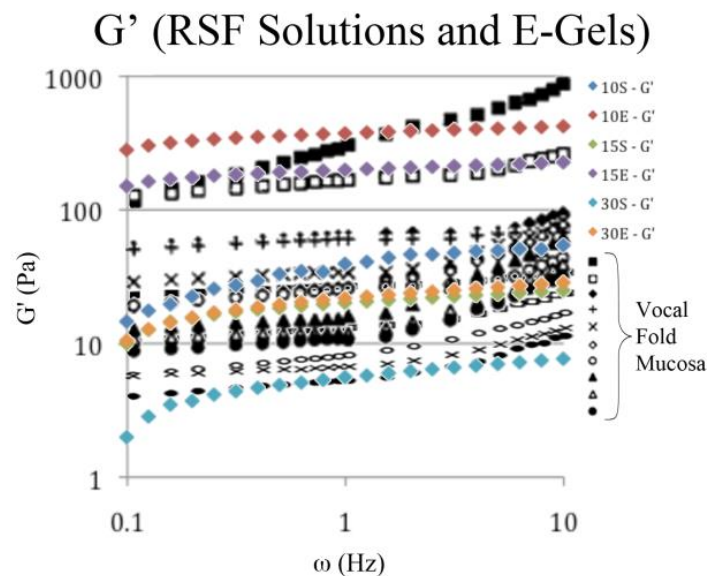


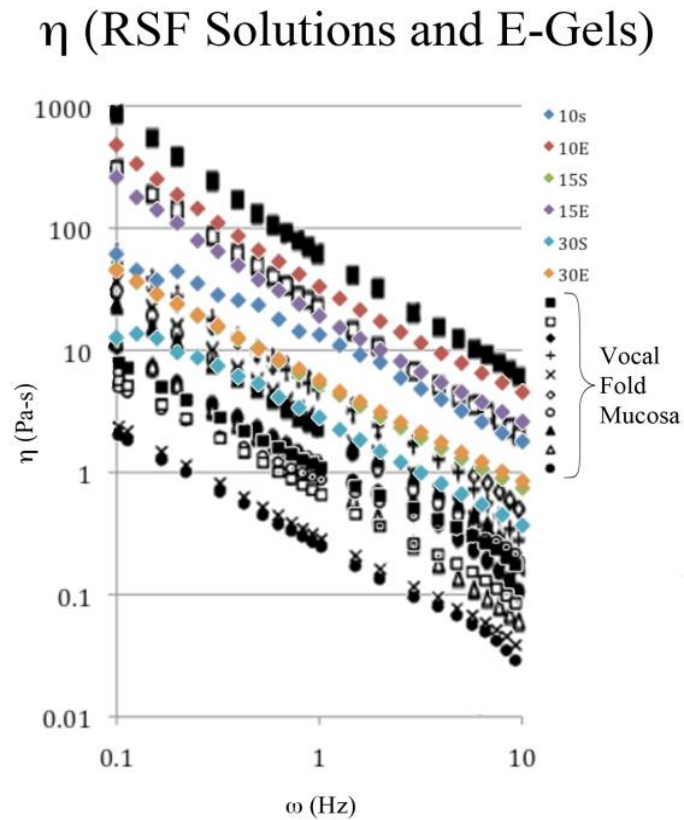
Figure 39: E-Gel rheology: complex shear modulus comparisons between E-Gels and RSF solutions of different boiling times (48 samples or more per construct).

Looking at the trends in Figure 39, it is clear that a decrease in boil time directly affects the stiffness of the construct created. This is due to the degradation of silk chains during the boiling process. Boiling cocoons for longer periods of time results in a lower overall molecular weight (which is one reason higher boil time solutions are less viscous). In order to determine the best E-Gel construct for this application, rheological comparisons were made between vocal fold mucosal tissue and 10, 15, and 30 minute boil solutions and E-Gels (Figure 40).

A



B



C

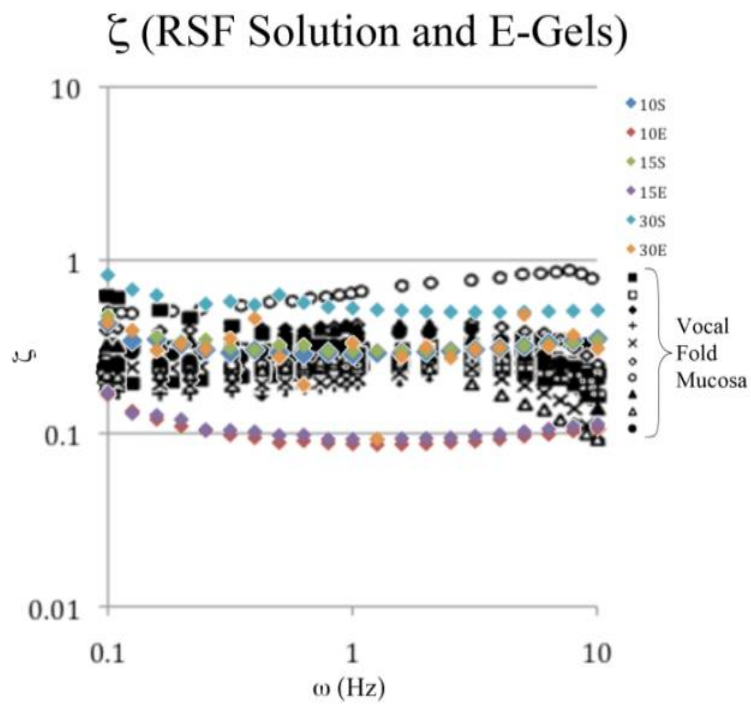


Figure 40: Rheological comparisons between RSF solutions, 10 minute - 25 volt E-Gels, and vocal fold mucosa (48 samples or more per data point). (A) Storage modulus. (B) Dynamic viscosity. (C) Damping ratio.

At first glance, all of these constructs fall within reasonable limits of vocal fold rheological matching. Upon closer inspection of the shear modulus and damping ratio plots, it can be noticed that 10mb E-Gels (red) and 15mb-E-Gels (purple) are stiffer and more solid-like than is ideal (10mb E-Gels more so than 15mb E-Gels). On the other end of the spectrum, 30mb solution (teal) is far on the liquid-like end of the spectrum, and has very low stiffness. All of these materials have dynamic viscosity curves that match the vocal fold well. 30mb E-Gels, 10mb solutions, and 15mb solutions have properties (in all categories) that fall in the middle of the spectrum for vocal fold rheology. While this seems promising, these materials all exhibit (qualitatively) solution-like behaviors, and would likely be resorbed quickly, making them ineffective implants. Of these materials, 15mb E-Gels are closest to matching vocal fold properties while remaining a gel-like material. Additionally, 10mb solutions are significantly more viscous and would be extremely difficult to inject through the vocal fold augmentation injection needle and catheter system. Based on these observations, future testing of E-Gel structures used 7% 15mb E-Gels. While the properties of this construct are promising, there is a significant drawback to the use of this material. As gelation spreads and the hydrogel grows away from the positive electrode, it begins to come closer to the negative electrode. Once the gel becomes close enough to the negative electrode, the gelation mechanism is reversed, and any gel that is formed is immediately dissolved. This means that 100% solution-gel conversion cannot be achieved using an untreated E-Gel.

Because the delivery mechanism for this silk format must be an injection of silk solution then gelation of the material *in vivo*, the process must also be relatively quick. An E-Gel made from 7%w/w 15mb RSF solution can take up to 10 minutes to form a volume of gel sufficient to augment the vocal fold. This time frame is unreasonable when a needle is embedded in the patient's vocal fold.

These two drawbacks to E-Gels prompted the use and testing of several additives. It was speculated that additives such as sodium chloride, ethanol, silk powder, and chopped silk foam had the potential to improve the yield of an electrogelation process.

4.3.2 Silk Electrogels with Sodium Chloride

Salinated 7%w/w 15mb RSF solutions were created at 0.9%w/v NaCl, 0.45%w/v NaCl, and 0.225%w/v NaCl and a 25V charge was applied across each solution. Gelation rate rapidly increased when compared to untreated E-Gels, and large volumes of hydrogen and oxygen bubbles were formed. It was noted that at 0.9%w/v salinity significant heating occurred during gelation. At this concentration of NaCl, it was possible to see yellow discolorations appear on the silk if the voltage was applied for an extended period of time, possibly due to overheating. Thermocouple testing was performed in order to quantify the correlation between NaCl concentration and peak solution temperature. Initially, two thermocouples were placed in within the well of silk solution being gelled to determine which electrode reached the highest temperature, and to gain some insight into what the mechanism of heating might be. One thermocouple was

placed on the negative electrode, and one on the positive. Figure 41 shows the results of temperature testing performed on a 7%w/w 0.9%w/v Salinity E-Gel.

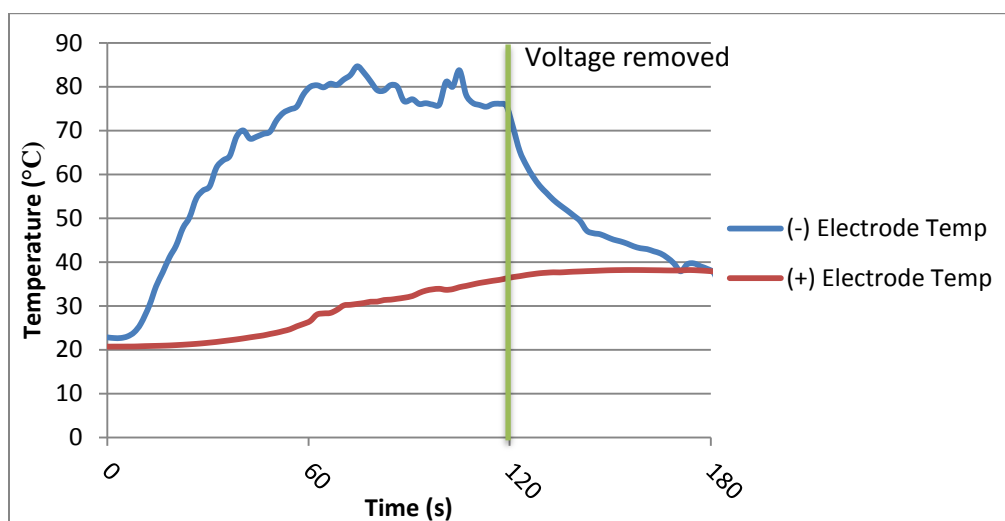


Figure 41: Initial temperature testing for salinated E-Gels: 7 %w/w 15mb RSF + 0.9%w/v NaCl temperature over time during electrogelation (average of 3 trials).

It can be seen on this plot that temperatures reach near boiling temperatures on the negative electrode. Based on the plot, the temperature plateaus after approximately one minute of gelation, and drops off steeply once the applied voltage is removed. Increased temperature is likely due to electrical heating occurring because of low solution resistivity (connecting the two electrodes with a low resistance material essentially short circuits the power supply). The negative electrode is significantly hotter than the positive, although the same amount of current flows through both electrodes. This is likely due to the difference in electrode size (wire resistivity is highly dependent on diameter, so the thin negative electrode is subject to much higher levels of resistive heating than the large plate that acts as the positive electrode).

Based on this test, all future temperature testing was done with one thermocouple in direct contact with the negative electrode. Temperature tests

were conducted a minimum of 3 times per sample, and were conducted for 0.90, 0.45, and 0%w/v NaCl solutions for comparison. Figure 42 shows a plot of maximum temperature vs. salinity.

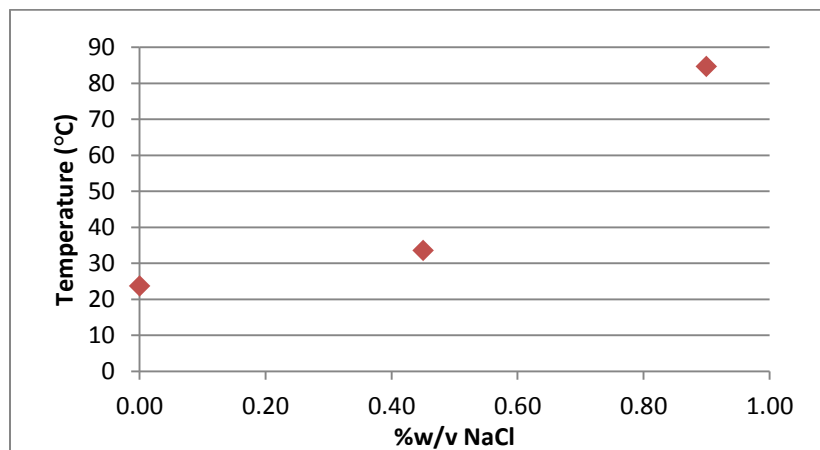


Figure 42: Maximum temperature (over a two-minute gelation period) vs. salinity for salinated E-Gels (average over 3 trials per data point).

This plot indicated a correlation between increases in temperature and increases in salinity. This correlation indicates that the original hypothesis of reduced electrical resistance leading to electrical heating is likely correct. A polynomial curve was fit to the data, resulting in (Equation 7):

$$T = 102(\%NaCl)^2 - 23.97(\%NaCl) + 23.635 \text{ (Equation 7)}$$

By extrapolating on these results to find ideal values, it was possible to determine a reasonable salinity for safe use *in vivo*. As explained previously, an extremely conservative temperature limit was defined to be 42 °C. Substituting this number into (Equation 7 yields a salinity of approximately 0.7%w/v NaCl.

In order to gauge the effect of increased salinity on hydrogel stiffness, rheological measurements were taken as previously described. Figure 43 shows the results.

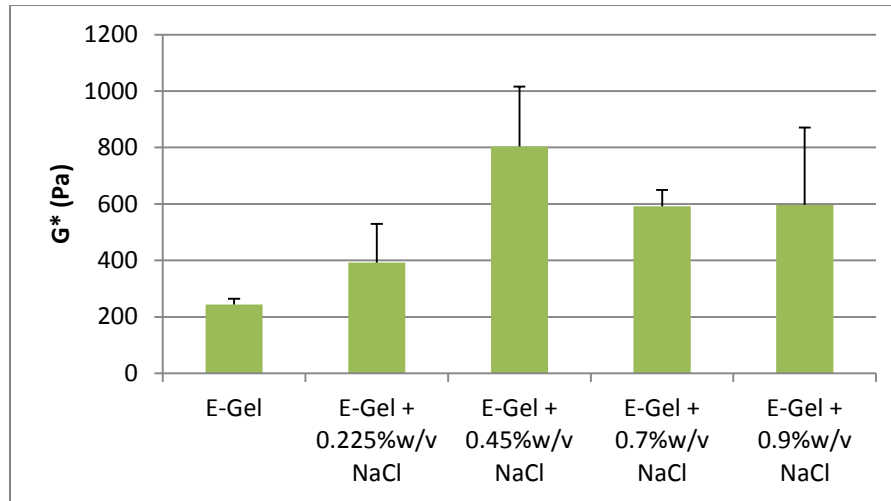
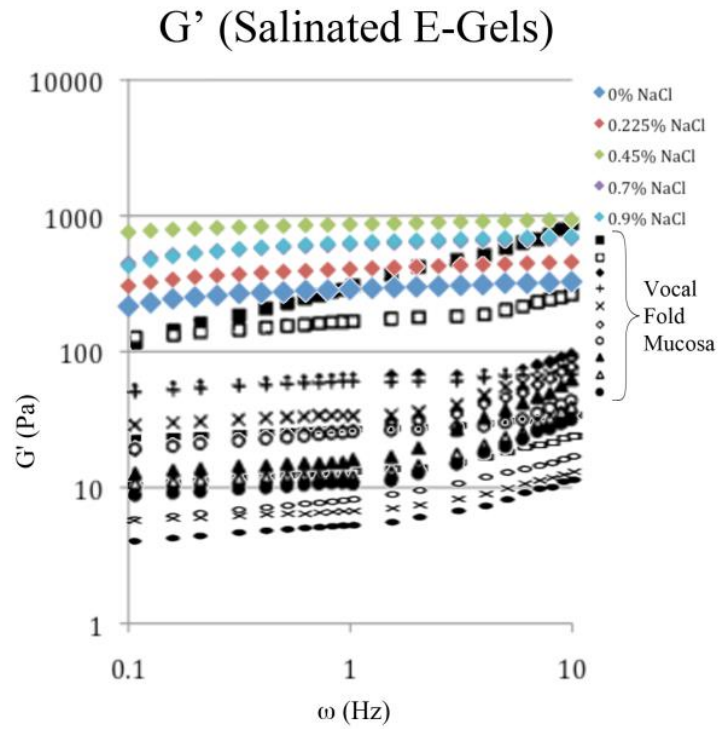


Figure 43: Salinated E-Gel rheology: complex shear modulus comparisons between different levels of salinity in E-Gels (3 samples per construct).

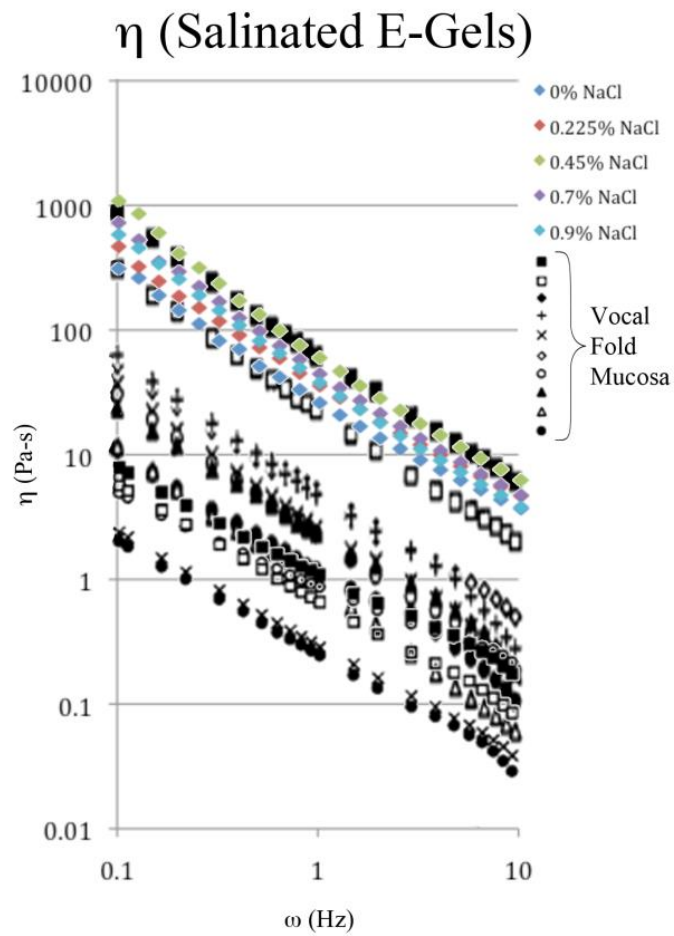
Maximum hydrogel stiffness for this set of E-Gels is achieved at 0.45% salinity. Drops in stiffness at higher concentrations might be attributed to an increased rate of gelation. This more kinetic process will decrease the clarity of the boundary between high and low pH portions of the solution, meaning that high and low pH areas of the silk may mix, locally reversing the gelation process. The speed of gelation improves the yield of the gelation process and lowers the amount of time the needle must be left in the patient's vocal fold, but does so at the expense of mechanical stiffness.

It can also be noted from Figure 43 that salinated E-Gels are slightly stiffer than untreated E-Gels. In order to ensure that the rheological properties of salinated E-Gels do not exceed the limits set by vocal fold rheology, further rheological comparisons were made. Shear modulus, dynamic viscosity, and damping ratio for each construct were compared with those of the vocal fold mucosa.

A



B



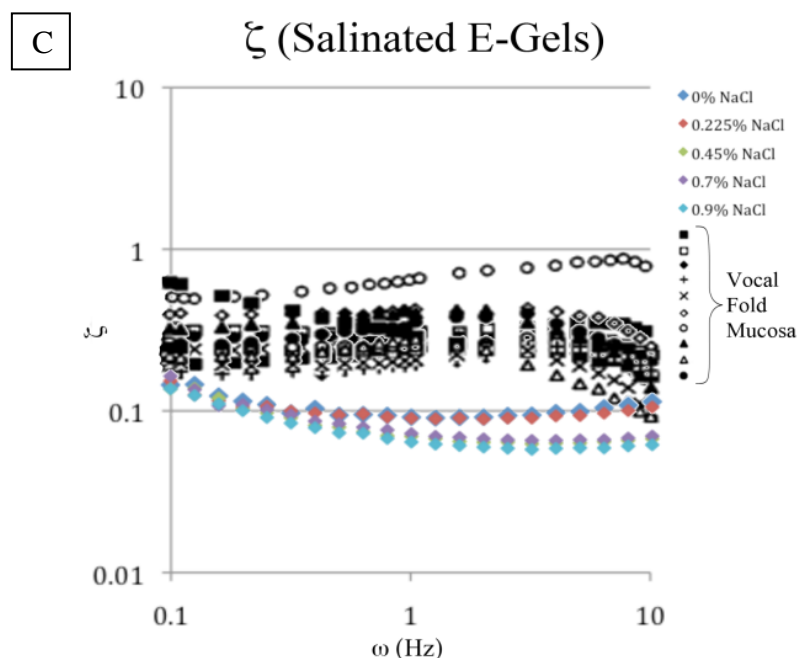


Figure 44: Rheological comparisons between salinated E-Gels and vocal fold mucosa (3 samples per data point). (A) Storage modulus. (B) Dynamic viscosity. (C) Damping ratio.

Figure 44 indicates that in general, salinated E-Gels are stiffer, more solid-like, and more viscous than E-Gels with no additive (corroborating the results of complex shear modulus comparisons), however the properties of these materials are not unreasonable for this application, especially at lower salinity levels. Stiffness is slightly higher than is ideal for all constructs, and the slopes of the curves are less steep. This indicates that E-Gels are less frequency (or shear rate) sensitive than the vocal fold mucosa. Dynamic viscosity curves for all constructs fit nicely on the upper range of vocal fold mucosa values, and curve slopes are nearly identical. While shear modulus and dynamic viscosity data matches reasonably well, distinct differences between these E-Gels and the vocal fold mucosa can be noted when examining the damping ratio curves. E-Gels exhibit a more solid-like behavior than the vocal fold, significantly so at higher salinities.

These properties indicate that salinated E-Gels would be an acceptable (but not ideal) augmentation material for this application.

During rheological testing, the percentage of silk solution converted to a gel was also recorded. Because the gelation of this material is meant to occur *in vivo*, it is important that all RSF solution injected be completely gelled, otherwise there will be excess solution and the surgeon will either have to over-inject, or the lasting augmentation results will be insufficient. The percentage of RSF solution gelled by the application of voltage was calculated for each test by measuring the volume of RSF solution before gelation, and after the E-Gel had been removed (post-gelation). The results can be seen in Figure 45.

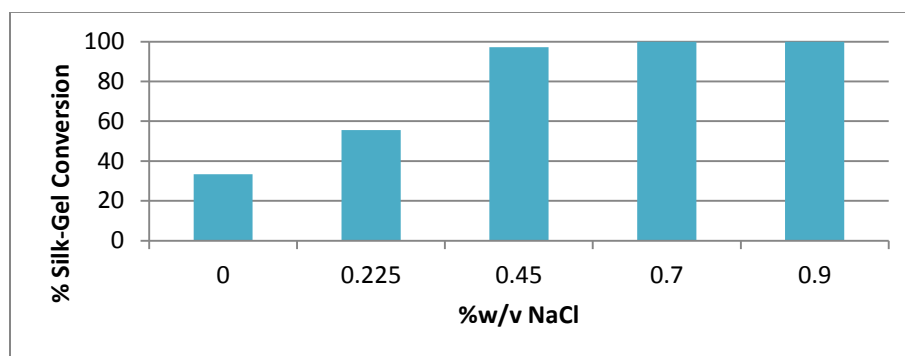


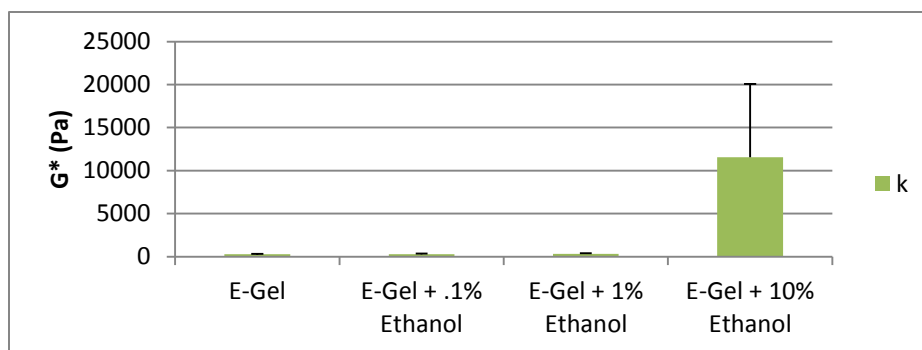
Figure 45: Percentage of silk solution converted to a hydrogel upon electrogelation with various concentrations of salt (3 samples per construct).

At higher salinity levels, full solution-gel conversion was achieved consistently. There is also a clear trend relating salinity and percent solution-gel conversion. A 0.45%w/v NaCl gel seems to be the most reasonable choice among these materials. As the rheological, temperature, and percent solution-gel conversion characteristics all satisfy customer needs. This full conversion response is likely due to the combination of removing electronegative repulsion mechanisms

(through electrogelation), and adding ionic content, both of which allow silk to create intermolecular bonds and inter-chain interactions more easily.

4.3.3 Silk Electrogels with Ethanol

Preliminary degradation studies of electrogelated silk in a Protease XIV solution provided concerns with construct robustness over time in a heated, hydrated environment. In order to improve degradation properties in E-Gels, ethanol was explored as a possible silk cross-linking agent. Because it is unclear what concentrations of ethanol can be injected directly into a small area of the body without detrimental effects, ethanol was only added at low concentrations to improve the properties of E-Gels. Rheological testing was performed at ethanol concentrations of 0.1, 1 and 10%v/v. The results are shown below in Figure 46. For scale, the first plot shows complex shear modulus curve magnitudes on a standard base-10 scale, however due to large differences between construct properties, a second plot shows these values on a logarithmic scale.



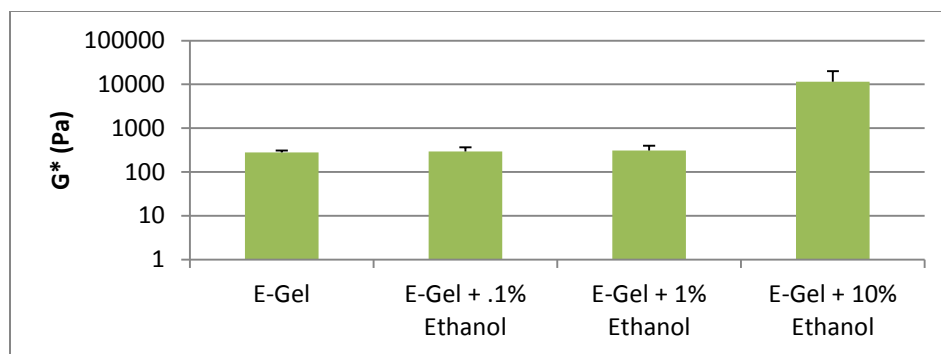
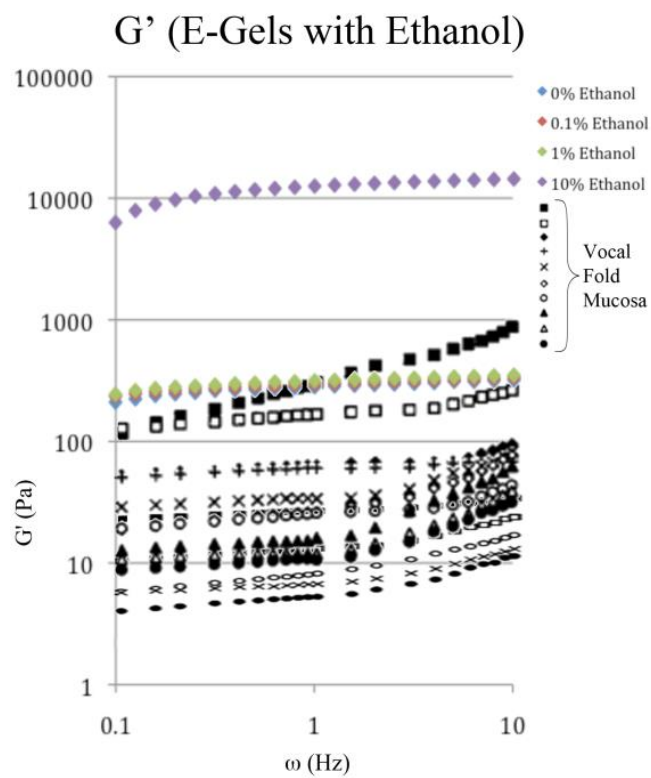


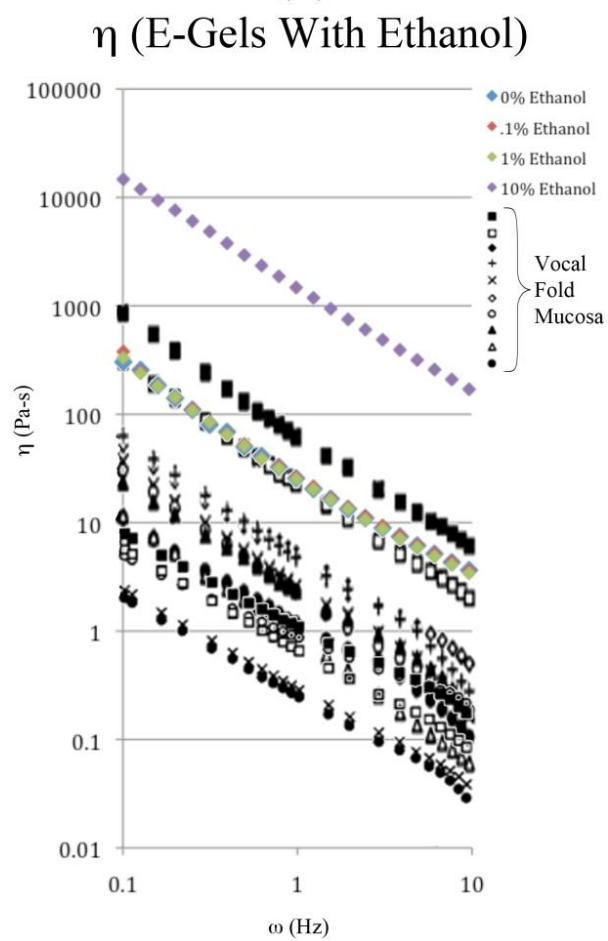
Figure 46: E-Gels with ethanol: complex shear modulus comparisons (3 samples per construct).

Based on these results, additions of low levels of ethanol have little or no effect on gel stiffness, however adding higher levels of ethanol (10%v/v) increases stiffness substantially. When examined on a smaller scale, low concentrations do appear to cause an increase in stiffness, however increases are minimal. In order to get a better sense for the impact of varying levels of ethanol in silk, comparisons with vocal fold materials were made (Figure 47).

A



B



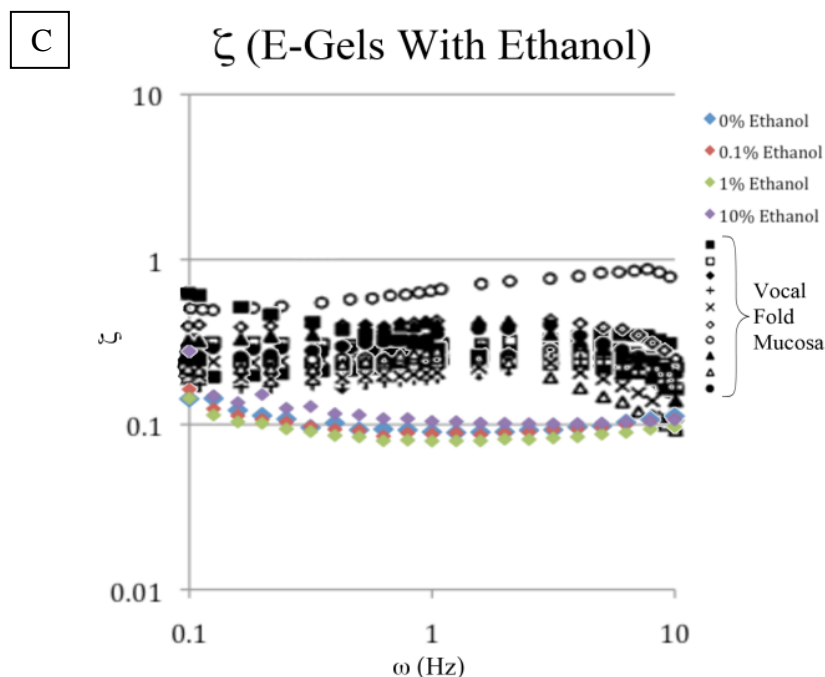


Figure 47: Rheological comparisons between E-Gels with ethanol and vocal fold mucosa (3 samples per data point). (A) Storage modulus. (B) Dynamic viscosity. (C) Damping ratio.

As expected, shear modulus and dynamic viscosity of E-Gels with 10% ethanol are orders of magnitude higher than the vocal fold mucosa, indicating that these constructs are not a good choice of material for vocal fold augmentation. Lower concentrations of ethanol exhibit very similar behavior to untreated E-Gels for all properties.

Measurements were taken in the same fashion as for salinated E-Gels to quantify the amount of silk gelled by applied voltage gelation. Figure 48 shows the results. At higher ethanol concentrations, rapid oxygenation occurred on the positive electrode caused deterioration of the hydrogel. This resulted in a lower percentage of silk that was gelled.

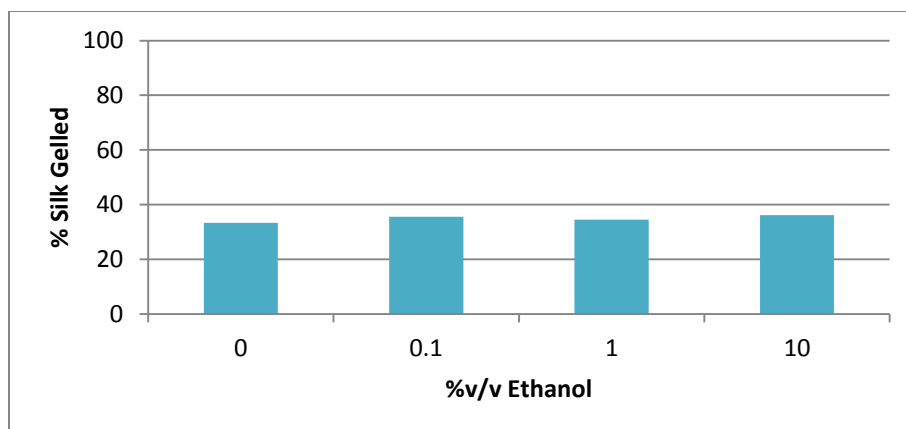


Figure 48: Percentage of silk solution converted to a hydrogel upon electrogelation with various concentrations of ethanol (3 samples per construct).

Generally, the addition of ethanol did not increase gelation rate or quantity. These results indicate that the addition of ethanol at lower concentrations only marginally affect silk E-Gels in terms of rheological and percent conversion properties. Effects on degradation are discussed in the next section.

4.3.4 Degradation

In vitro degradation studies were performed for all electrogelated constructs. Another attempted method of improving E-Gels (after initial degradation testing proved cause for concern) was to include physical reinforcements in the solution (added prior to electrogelation). Two types of physical reinforcements (silk powder and chopped silk foam) were added to silk solution in an effort to improve degradation rates. The results of degradation testing of all silk E-Gels are shown in Figure 49, which displays how many hours each construct lasted in a 0.5 U/mL Protease XIV/PBS bath when incubated at 37°C.

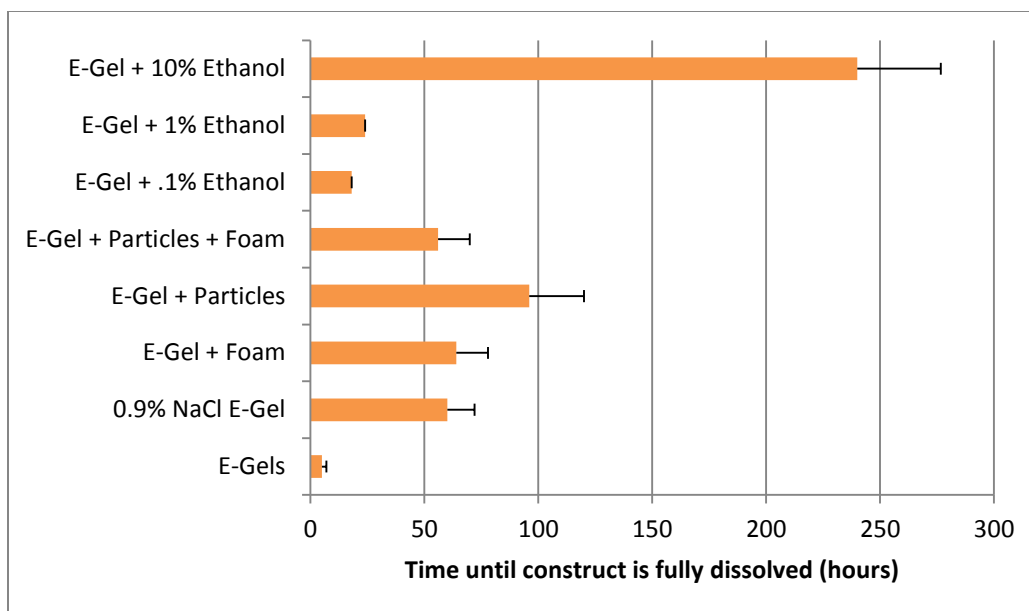


Figure 49: Enzymatic degradation of E-Gels (3 samples per construct).

The results of degradation show that there is an intrinsic link between stiffness and degradation rate. The stiffest construct (E-Gels with 10% ethanol) also exhibits the longest degradation time, and the softest (untreated E-Gels) the shortest. This is a reasonable result, since tighter chain packing and stronger bonds tend to resist enzymatic degradation. E-Gels without any additives dissolve extremely quickly in Protease XIV solution, and will even degrade over time when submerged in PBS. Additions of low concentrations of ethanol increased degradation time (as well as stiffness) slightly, however degradation rates in these constructs are still relatively fast for this application. The addition of physical reinforcements improved properties significantly, however finding a delivery mechanism for injecting solid additives would be highly difficult, making these constructs a non-ideal augmentation material. Increased salinity also proved to slow degradation rates a reasonable amount, meaning that these materials have

properties that acceptably meet customer needs for rheology, percent solution-gel conversion, and degradation, making salinated E-Gels one of the most promising constructs for this application.

4.3.5 Delivery

Electrogelation of silk is a dependable method of creating homogenous, consistent hydrogels with rheological properties that match those of the vocal fold relatively well. This gel, however, is too thick to inject through a trans-nasal catheter system once formed. When heated, E-Gels return to a low viscosity solution state and reconstitute themselves to a hydrogel state once cooled, however, the temperatures necessary to induce this response would cause serious burns if put in contact with the mucosal tissues in the vocal fold. An alternative option is to create an E-Gel *in vivo* using an electrified needle tip. Because the path of the current is directly from the positive electrode to the negative, electrical safety is not a concern unless the equipment is damaged or shorted. Care must be taken in designing such a system to avoid these hazards. Another concern with E-Gels is the inherent drop in localized pH. A pH as low as those found in E-Gels (4.2) would cause acid burns if put in contact with the skin, meaning that pH would require neutralization. Other things to consider in designing such a system are needle and electrode geometry, electrode spacing, materials, wiring geometry, and power supply methods.

In order to perform an *in vivo* electrogelation of RSF solution, a custom syringe, catheter and needle must be designed to apply a voltage across the solution, as shown in Figure 50. Simply, the needle must contain two electrodes,

which are wired along the catheter and out the cannula of the trans-nasal scope in order to connect to a battery or plug. In order to avoid the necessity of extra equipment for the hospital to buy, the ideal setup would have a short lived battery pack on each syringe that applies the correct DC voltage to the needle. In order to maintain the ability of the catheter to fit through the cannula, very thin wire must be used to connect the electrodes to the battery.

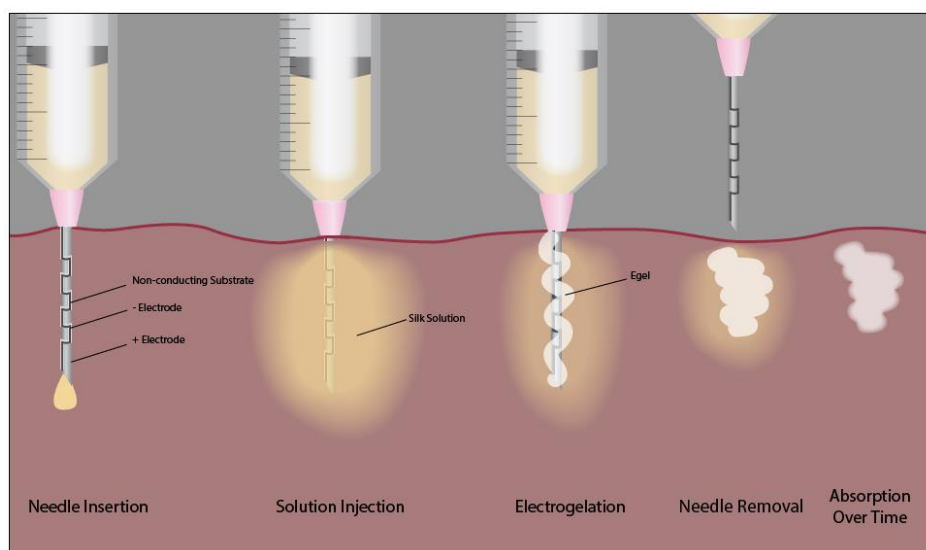


Figure 50: Proposed *in vivo* gelation mechanism for E-Gels.

Needle Design

There are many different ways to apply a voltage to the RSF solution once injected. When using a method such as the one described in Figure 50, needle geometry will be critical to success. Electrode spacing, separation, and surface area are all critical when designing such mechanisms. Figure 51 shows various designs for possible needle geometries that were developed for this application.

A patterned electrode design would only gel silk on the external surface of the needle. It would also be possible to use a non-conductive needle, with metal-

coated interior and exterior surfaces, which remain separate and act as electrodes. Another method would be to have the needle act as one electrode, while a coiled section of wire placed in the luer fitting of the needle acts as the second. By carefully choosing needle geometry it is also possible to eliminate various problems with E-Gels. If the gel is formed in the upper portion of the needle then extruded out, there will be significantly less excess solution injected into the vocal fold. It is also possible that a coating at the tip of the needle could locally buffer the pH of the extruded E-Gel. Figure 51 shows various designs for possible needle geometries that were developed for this application.

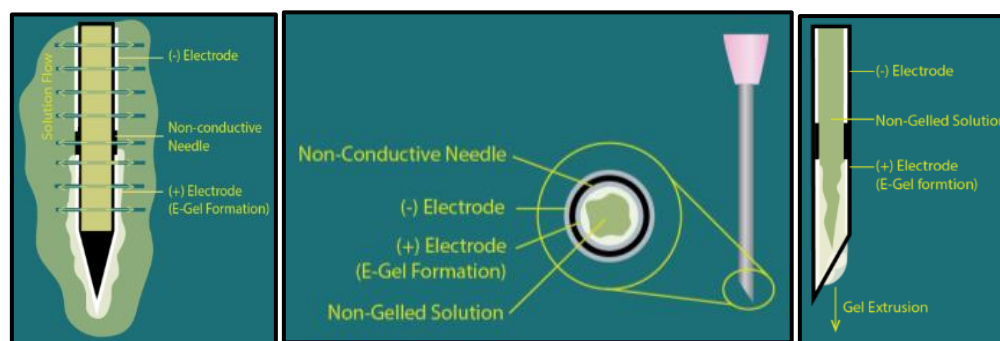


Figure 51: Proposed E-Gel delivery mechanism: needle geometries.

Syringe Design

For E-Gels with additives, syringe geometry is also an important factor. Solutions must be kept separate from additives until just before injection to avoid any possibilities of accelerated gelation, and to extend storage time and improve solution stability. Commercially available or custom mixing syringes can be used for these applications. If necessary, a custom syringe could be designed such that the optimal ratio of materials is injected without any calculations or adjustments from the surgeon.

4.4 Additive Gels

5M NaCl was added to 7% RSF solution in different ratios and incubated at 37 °C for several days. Ratios of silk to 5M NaCl were prepared in a Falcon MULTIWELL™ 24-well plate in ratios of 5%-100% silk at 5% increments. All solutions gelled upon contact to varying degrees when the two solutions were initially mixed. After several hours, some of the gels re-dissolved. Self-assembly of the proteins occurred over the next few days at varying rates, depending on salt concentration. Figure 52 shows the response over time of a select few samples. By this test, it was determined that a ratio of 55% RSF to 45% 5M NaCl (highlighted in blue) was (qualitatively) the best construct, due to the consistency of the gel quality over time. As the figure shows, mixing 45% 5M NaCl with 55% silk causes immediate gelation upon contact, and retains a high percentage of gel until full assembly occurs. All other constructs did not remain gelled through the duration of the experiment, therefore 55% silk 45% 5M NaCl was used for all further experimentation. There are many different ions that could potentially cause gelation of RSF solutions, but only NaCl was fully characterized.

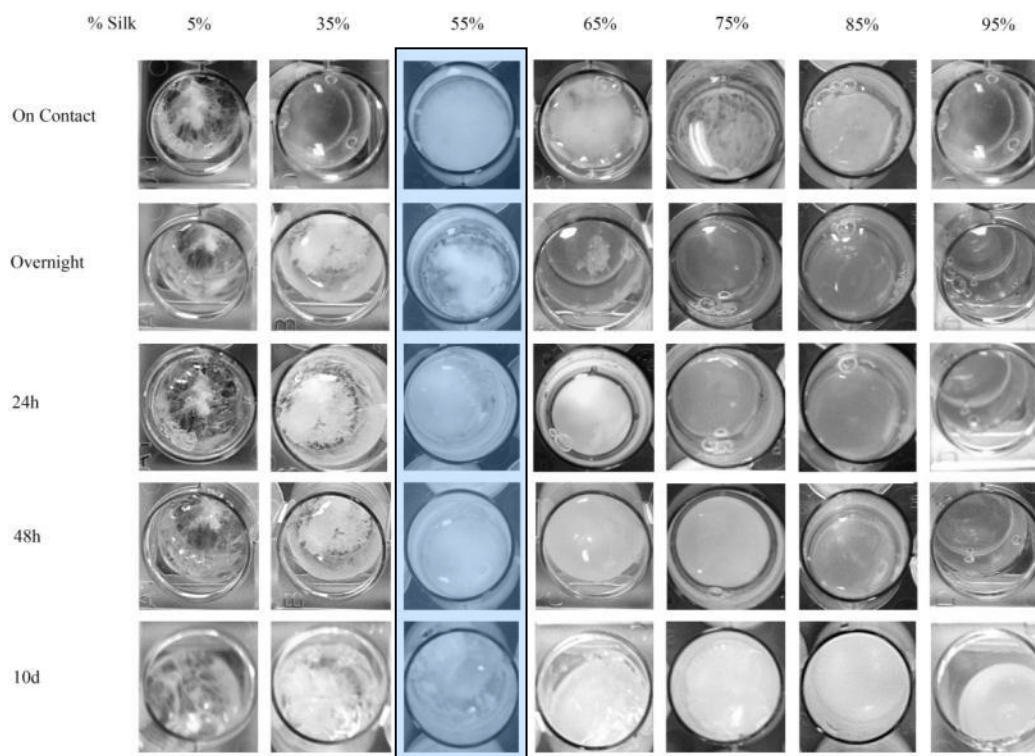


Figure 52: Progression of salt gels over time (2 samples per construct).

4.4.1 Rheology

Unfortunately, the concentration of salt necessary to gel silk is significantly higher than the acceptable physiological limits (0.9% w/v). Despite the ineligibility of this construct for in-vivo gelation due to unsafe salinity levels, rheological and degradation testing was continued in order to further characterize the constructs for use as a control in characterizing salinated E-Gels. Rheological testing was conducted over four days in order to determine how the rheology of the material developed over time, and degradation testing was performed for comparison with other silk constructs.

Rheological testing was performed to quantify the development of the gel by running a test immediately upon gelation, then once daily until results

stabilized. Data collected on complex shear modulus, shear modulus, dynamic viscosity and damping ratio testing was skewed, and concrete conclusions could not be drawn. Initially, the gel formed was qualitatively similar to a 7%w/w 15mb E-Gel, however after 24 hours of incubation at 37 °C the gel became extremely stiff. Qualitatively, stiffness of these gels was higher than any other construct tested in this research. Difficulty with rheological testing was due to the stiffness of the gel, which prevents the top plate of the rheometer from fully contacting the construct. Despite the lack of quantitative data, it is clear that this material is significantly too stiff for use in vocal fold augmentation.

4.4.2 Degradation

Enzymatic degradation of salt gels was performed in parallel with E-Gels. Salt gels proved to last significantly longer than E-Gels *in vitro*. This is an expected result, as the constructs are significantly stiffer and more cohesive. Figure 53 shows the result of degradation testing on salt gels.

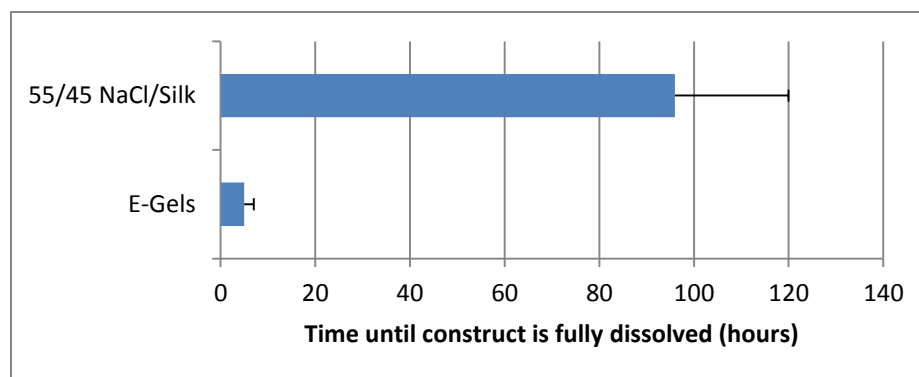


Figure 53: Enzymatic degradation of salt gels (average of 3 samples).

4.5 Injectable Silk Foams

Several injectable forms of porous silk foams have been investigated by researchers for various applications, however success has been limited to injections through large gauge needles. Even with a large needle, injection requires significant input force and in some cases a pressurized syringe. Because of the nature of the material as a solid, compressible construct, the thickness of the pore walls and number of pores per inch limits the compressibility of the injectable, meaning that it may be impossible to achieve injection through the small gauge needle and catheter system required for a trans-nasal injection. Although this material was initially considered as a possible augmentation material, needle gauge constraints were too severe and this material format was not investigated further for this application.

4.6 Sonicated Gels

When injecting a time-delayed gelation material, care must be taken to avoid premature gelation. Such a complication which would lead to clogging in the needle and catheter system, which would complicate procedures and increase cost (both in money and time). It is also critical that gelation occur before silk in a solution form is reabsorbed by the body, and that gelation occur on a very predictable time table, allowing the surgeon to slightly over inject to compensate for any material resorbed before self-assembly of the protein occurs. Because of the nature of the procedure, it is difficult to approximate the exact time necessary to place an implant. It is undesirable to place time constraints on the surgeon

performing the procedure, which could lead to detrimental effects on augmentation quality. Another concern with this procedure is that the gelation time is intrinsically dependent on silk solution quality, which varies greatly due to silk solution shelf life and processing inconsistencies. To circumnavigate this problem, the sensible direction to take would be to sonicate the solution once placed in the vocal fold for a time that will induce gelation within seconds. Unfortunately, *in vivo* sonication of RSF is impossible, as the ultrasonic waves are harmful to tissue at close range and can cause severe damage to the inner ear (the processing alone requires hearing protection).

4.7 pH Gels

Any silk gel formed *in vivo* by the addition of acidic material would have to reach a stable, β -Sheet conformation-rich state before the natural systems in the body neutralized the acid injected. Additionally, the overall pH of silk solution necessary to induce gelation is significantly lower than the acceptable limits defined by the project specifications. It is possible that a mechanism could be used to locally buffer the solution where it comes into contact with tissue, but any failure in such a mechanism could result in pain or significant burns in the vocal fold mucosa. Based on this problem, pH gels were not investigated beyond hypothetical discussions for this application.

5. Conclusions

Taking a comprehensive look at all silk constructs created, the most promising processing parameters were chosen for each silk format and the results compared. Comparisons were made between silk formats, currently used materials, and ideal or hypothetical values for rheology, degradation, safety, and delivery. It should be noted for all rheological data that for an *in vivo* delivery, RSF solution will have been slightly sheared prior to gelation. This would likely result in a slightly stiffer construct than tests using non-sheared solutions have yielded.

5.1 Rheology

The best processing parameters were chosen for each construct, and plots were constructed to compare the dynamic viscosity of each of these constructs, existing vocal fold materials, and vocal fold mucosa (Figure 54). Any materials that were considered viable for implantation are plotted.

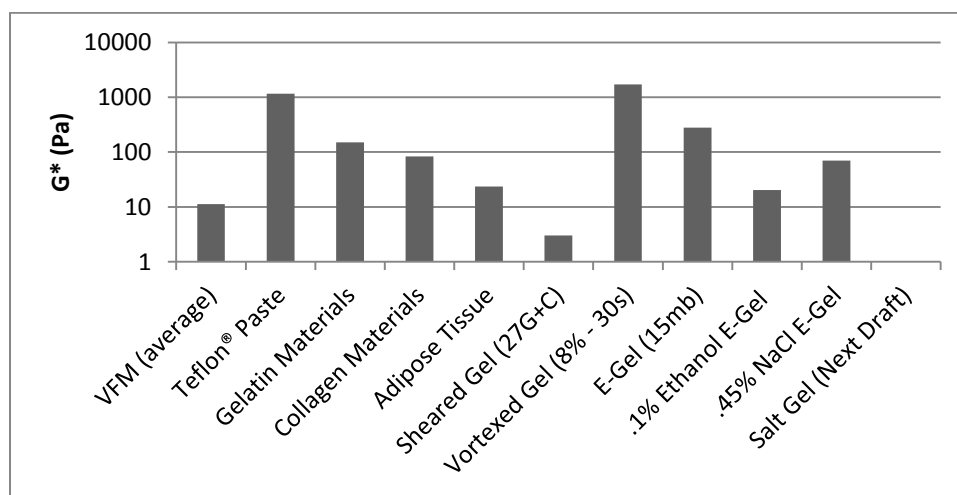
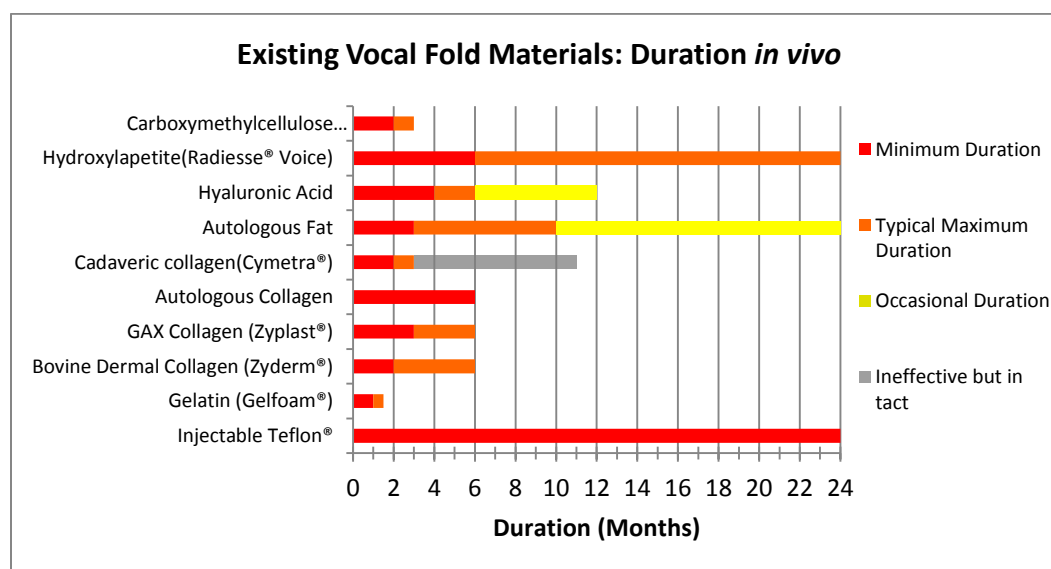


Figure 54: Rheological comparisons between current materials, silk materials and vocal fold mucosa.

While many of these materials exceed the stiffness and viscosity of the vocal fold, a construct which is on the stiffer end of the acceptable limits might be an advantage. Over time, constructs will degrade, slowly losing volume and physical robustness. Materials will soften over time, meaning that a construct that is slightly stiffer than the vocal fold initially will soon soften slightly and fit the vibratory properties of the tissue well. Ideally, implanted materials would act as a tissue scaffold for regeneration of damage tissue.

5.2 Degradation

Figure 55 shows *in vivo* degradation of existing vocal fold materials and *in vitro* degradation of silk hydrogels. Silk hydrogels degraded extremely rapidly in Protease XIV. The figure shows the number of hours until constructs were completely dissolved in Protease XIV/PBS solutions. These values are not directly correlated to *in vivo* degradation, but allow us to compare degradation rates between silk materials.



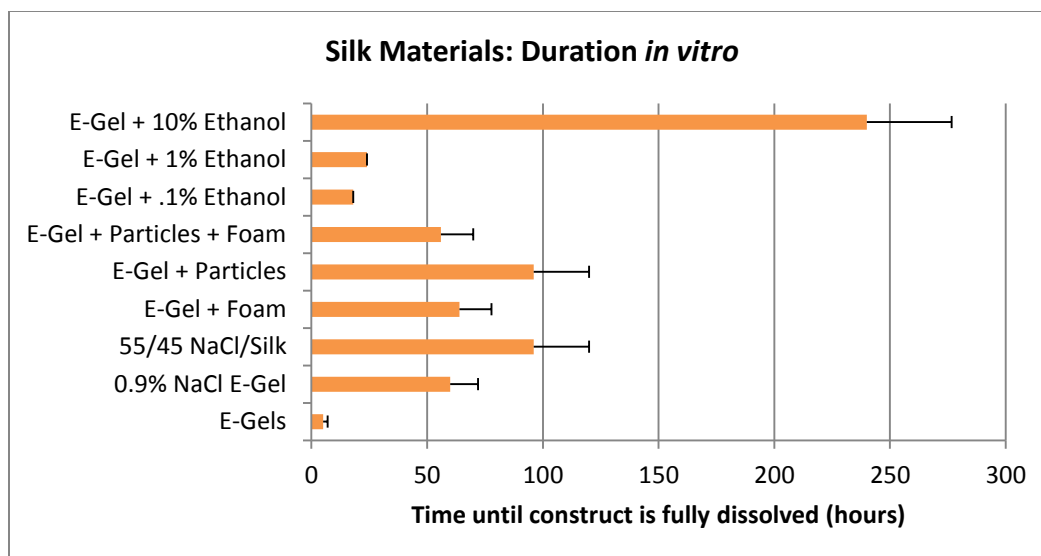


Figure 55: *In vivo* degradation of existing vocal fold materials and *in vitro* degradation of silk materials.

It is clear from this table that (as discussed previously), stiffness correlates to degradation rate. As found in comparisons between materials based on shear modulus, dynamic viscosity, and damping ratio, stiffness also correlates to solid-like behavior. In living tissue, such as the vocal fold mucosa, a material can be rheologically liquid-like without exhibiting solution-like behaviors (on a practical level). Because of molecular differences between silk materials and living tissue, these correlations indicate that a trade-off between properties will be necessary, however, certain silk materials (such as E-Gels), match closely enough that an optimal value will be within an acceptable range for all properties investigated.

5.3 Delivery

Silk material formats were compared based on ease of delivery. There are many aspects of delivery mechanisms that could be compared, and eight categories were created with rating scales to quantify the quality of each material. The first

category, consistency, refers to the ability of an injection to behave exactly the same way twice. This includes solution homogeneity (within a small volume of solution and between batches), changes in input force, and ability of the material and injection mechanism to adapt to changing environments (patient to patient). The next category is ease of injection, which simply refers to the amount of force or dexterity required to inject the material. Tactile feedback is also a critical category, and each mechanism is rated by how well the surgeon can feel what is happening at the tip of the needle. The number of steps to prepare the solution is quantified, counting any preparation steps including plugging in devices, applying a charge, or treating the solution pre-injection. Assembling syringe and catheter setups do not count toward steps, as all injections require these preparations. Full silk gelation is a yes or no category, and simply indicates whether or not it is possible to gel all silk injected. Custom needles and syringes are defined as any non-commercial setup or commercially available setup that must be altered (essentially, anything that increases the cost of the injection). Extra equipment refers to anything the hospital must purchase and have on hand for all injections provided (non-disposable equipment). Storage time is defined as the amount of time a solution remains viable for use in vocal fold augmentation injections after removal from dialysis. Table 5 shows ratings for each of these categories. Consistency, ease of injection and tactile feedback are rated on a scale of 1-5, where 5 is ideal and 1 is unacceptable.

Table 5: Comparisons for different silk formats based on ease of delivery.

	Consistency	Ease of Injection	Tactile Feedback	# Steps to Prepare	Full Silk Gelation?	Custom Needle or Syringe	Extra Equipment	Storage Time
E-Gels	3	3	4	1	No	Yes	No	<3 Months
E-Gels + NaCl	2	3	4	1	Yes	Yes	No	<3 Months
E-Gels + Ethanol	3	3	4	1	No	Yes	No	<3 Months
E-Gels + Reinforcements	2	2	4	1	No	Yes	No	<3 Months
Salt Gels	5	5	5	0	Yes	Yes	No	<3 Months
Vortexed Gels	5	variable	variable	3+	Yes	No	Yes	--
Sheared Gels	1	5	1	0	Yes	No	No	<1 Month
Injectable Silk Foams	4	0	--	0	Yes	No	No	∞

5.4 Comparisons of All Properties

In order to compare the results of Table 5 with other properties outlined in the project specifications, the scores in each category were summed for each silk format, resulting in an overall delivery score (15 possible points). The results are shown, along with comparisons of other properties, in Table 6. Rheological matching, safety and consistency are rated on a scale of 1-5, again, 5 is the best, and 1 is unacceptable.

Table 6: Comparisons between silk material formats based on customer needs.

	Rheological Matching	Delivery (Out of 15)	Degradation (Days)	Safety	Consistency
E-Gels	5	4	.5	2	5
E-Gels + NaCl	4	6	2	2	3
E-Gels + Ethanol	3	4	10+	--	5
E-Gels + Physical Reinforcements	--	2	3	2	1
Salt Gels	1	13	5	1	5
Vortexed Gels	1	5	--	5	1
Sheared Gels	4	4	--	5	1
Injectable Silk Foams	--	5	5	5	5

Rheological matching of silk materials to vocal fold mucosa was relatively good, with the exception of a few silk formats. Vortexed gels were thus far unable to match the properties correctly, and although E-Gels with ethanol crosslinking lasted longer, it was difficult to achieve a significant difference without comprising the rheological properties. Another concern with ethanol crosslinking is the fact that acceptable localized *in vivo* ethanol concentrations are not yet elucidated. Salt gels, though initially well matched, stiffened quickly over time in a 37 °C environment, and therefore are not suitable for this application based on rheology.

Enzymatic degradation tests performed showed that all silk constructs submerged in protease XIV mixed with PBS dissolved within one week. While this seems unreasonably fast, and like a significantly shorter time period than we

are looking for, these tests do not necessarily correlate to *in vivo* degradation. *In vitro* degradation is significantly harsher, and the fully hydrated environment increases the rate that constructs break down. *In vivo* conditions are quite different: the environment is only partially hydrated, and there is little fluid flow in the mucosal tissue. These factors will significantly decrease the rate of degradation when compared with enzymatic degradation studies *in vitro*. *In vitro* studies are useful, however, to conduct comparative tests between constructs. This allows us to compare silk formats and previously tested materials.

From a safety standpoint, several constructs were taken off the table, due to levels of additives not tolerable inside the body. pH gels (due to pH levels too low to implant), Salt gels (due to salinity too high to implant), and certain types of accelerated and cross-linked E-Gels were all eliminated as possible constructs for this application. E-Gels also carry the concern of pH levels too low for *in vivo* work, however since gelation is not purely dependent on pH, it is possible that a localized buffer could be used at the edges of the solution bath where it comes into contact with the tissue to avoid any burns that may occur. Additive gels are possible, however the additive primarily explored so far (NaCl) is not safe to use at the concentrations necessary for gelation, and the rheological properties do not match those of the vocal fold mucosa. If gelation of silk by the addition of particles is pursued, it should be noted that particles of a certain size will likely cause some irritation, as well as an immunogenic response that will sequester and break down the particles, causing the material to degrade more quickly and

causing discomfort for the patient, therefore only nanoparticles should be used for this application.

In terms of delivery, the only materials with unacceptable methods are E-Gels with particle reinforcements (injecting a powder would be extremely difficult), and vortexed gels (too many preparation steps, expensive equipment, and variable solution viscosity). Many of the other delivery mechanisms have challenges associated with them as well, and do not work perfectly yet, but work could be done to improve these systems. Certain *in vivo* gelation devices require complex systems, however, resulting in a higher cost per injection than something that uses a simple gelation mechanism. For example, the needle, syringe and catheter system necessary to create an *in vivo* E-Gels would need a built in battery pack and wiring (along with the high precision fabrication necessary on the needle electrodes). This will be much more costly to produce than a system that doesn't require power, driving up the cost of the procedure for the hospital and the patient.

This leaves a select few materials to be investigated further. Salinated E-Gels (or E-Gels with yet unexplored additives), sheared gels (with stabilization efforts), additive gels (liquid or nano-particle additives only), and combinations of various gelation methods can be researched further to find a good system for this application.

6. Future Work

While none of these constructs currently satisfy all customer needs, it is probable that other additives could be tried, or techniques could be modified to improve various properties.

6.1 Further Testing of Established Constructs

In order to judge the efficacy of implants created for this application, it is important to explore how well a given material ‘augments’ the vocal fold. In this case, augmentation is defined as the ability of a material to medialize the true vocal cords. This ability primarily stems from the *in vivo* compressive strength of the material implanted. Once a material has been shown to reasonably fulfill the rheological, delivery, and safety needs for this application, compressive strength can be explored by performing mechanical tests. Materials would be delivered into human or porcine cadaver vocal folds by whatever delivery mechanism was designed for each material. Compressive tests would be performed on the tissue before and after augmentation to gauge the effect of the implant, and if deemed necessary, cyclic loading tests could be performed to determine longer term responses.

It is also necessary to explore *in vivo* degradation, as the *in vitro* degradation studies described above are not necessarily accurate to responses in the body. The first study to be performed would be subcutaneous implantations of promising materials on a rat or mouse model to gauge immunogenic response and degradation in a semi-hydrated environment (defined by mass loss and changes in

compressive strength). If degradation *in vivo* proved to be significantly better than the *in vitro* results have established so far, a secondary study could be performed on a larger animal model to explore the properties of the material when implanted in the vocal fold tissue. This test would use the same implantation techniques used by the otolaryngologist on humans, and mechanical testing would be performed on the constructs pre and post implantation to assess the efficacy of the augmentation injections over time.

Each of the materials that have not been eliminated is promising in one category or another. Further testing and experimentation can be done to attempt to improve the properties in which each material is lacking. The following sections outline steps that could be taken to improve the necessary properties of each material investigated.

6.1.1 Silk Electrogels

Silk E-Gels with added saline have been shown to have excellent rheological properties, cohesion, and solution to gel conversion. While the syringe and catheter system necessary to implant the constructs could be somewhat expensive, it would be possible to produce a relatively low cost, disposable version once out of the prototyping phase of the design process. Current concerns with using E-Gels for this application are mainly limited to a localized pH drop near the positive electrode. This is a serious concern, and a buffering system must be put in place to ensure no materials of pH levels lower than pH 5 will come into contact with the patient's tissues. In the case of an extrusion style electrogelation needle, it would be relatively simple to incorporate a buffering agent at the tip of

the needle. This, however, carries the risk of causing a reversed reaction and returning the extruded hydrogel back to liquid form. Various methods of applying such a mechanism would need to be explored before any further experimentation with these materials, as a safety concern that involves possible tissue damage is of the highest priority when choosing a construct.

Should the pH of E-Gels be stabilized, methods for improving the degradation rate of E-Gels should be explored. One method to achieve such material properties could be to use a 30mb E-Gel, (injectable through the needle and catheter based on mathematical modeling and rheological comparisons to 15mb RSF solution) with a secondary gelation mechanism such as the application of shear. In this case, increased salinity would not be required, as E-Gels would be pre-formed and not require a short gelling time that achieves full silk gelation (as an *in vivo* gelation does). Applying shear to a 30mb E-Gel by injecting it would cause an increased concentration of β -Sheet conformation-rich silk, improving the degradation properties and increasing the stiffness of the material.

Some benefits of using 30mb E-Gels include a longer shelf life (due to a lower molecular weight, and fewer chain interactions in a solution state, which lead to longer natural self-assembly times) and potentially easier injection (depending on the injection method). On the other hand, the low molecular weight of 30mb RSF could lead to less stable constructs and faster degradation, but ideally this issue could be easily rectified via use of the appropriate additive.

Another way to improve E-Gels would be to add metallic nano-particles to the RSF solution before gelation. It has been noted by students working with

magnetic silk E-Gels that when added to silk in the right concentrations, Ferro fluid (a suspension of iron oxide nanoparticles in a surfactant) will cause a silk solution to gel. When added in lower concentrations, the ferrous silk solution can be electrogelated by the usual methods. Gelation is slightly accelerated, and 100% solution-gel conversion can be achieved with the right parameters. The resulting construct lasts significantly longer than untreated E-Gels in enzymatic degradation tests, and is also significantly stiffer, though no rheological data is available at this time. Similar results could likely be achieved using a gold nanoparticle suspension. Gold, due to its higher level of nobility, would be less reactive *in vivo*, and thus less likely to cause irritations or immunogenic responses.

Other E-Gel improvement methods to explore include ionic additives, such as the ones naturally found in high concentrations in the body (Ca^{2+} , Mg^{2+} , K^{+} , etc.) and collagen or elastin additives, which tend to have both plasticizing and strengthening effects on natural copolymers [70].

6.1.2 Additive Gels

Any of the additives used to improve the properties of E-Gels also have the potential to work on their own if added in the appropriate quantities. In the same way that Ferro fluids and saline solutions of various concentrations can be used to gel silk, it is likely that the right quantity of gold or silk nanoparticles would achieve the same effect.

Larger scale particles can also be used to gel silk. Silk microspheres can be created in a multitude of ways, including milling of degummed fibers or

lyophilized constructs [69] and chemical precipitation [26]. Precipitation of silk particles can also yield nano-spheres if the processing parameters are correct [26, 29, 30]. Micron sized particles have a higher likelihood of causing irritation in the body [71], so it would be prudent to run an *in vivo* study before investing significant time or resources in achieving ideal physical properties.

6.1.3 Sheared Gels

Shear induced gelation of silk is a promising method for this application. If input force can be normalized (in order to even out the force applied to the syringe, and hence the shear forces on the silk) without decreasing the amount of tactile feedback for the surgeon, the procedure would have the potential for a successful implantation with a few more alterations in processing. With a relatively even input force, the only variability found in this process comes from inconsistencies in RSF solution.

RSF processing

As it is performed now, RSF solution processing has a lot of variability, both on a large scale (batch to batch), and on a small scale (quantity of various conformations in a given volume of RSF solution). Small scale variability comes from several steps in the process. First, when dissolving silk in lithium bromide, there is human error to account for in the accuracy and precision of LiBr molarity. Next, it is necessary to stir the silk-LiBr mixture at least once during the 4 hour incubation period, meaning that solution (which is highly viscous at this stage) will be unevenly sheared in different areas in the beaker of solution. In the next stage of processing, this viscous silk-LiBr mixture is injected through 18G

needles into dialysis cassettes. Injections are performed using a pressure assist device in order to generate enough force to flow the solution through the needle. This causes a high rate of shear to be applied to the solution, and if care is not taken to inject slowly, it is possible to see small rings of silk high in β -Sheet content extruding from the needle. On a larger scale, silk varies batch to batch in molecular weight (due to small differences in degumming time, stirring, or sodium carbonate concentration), RSF concentration (due to differences in the volume of solution injected into cassettes for dialysis), and relative concentrations of various silk conformations.

Eliminating some of this variability by automating certain aspects of silk solution processing could greatly improve the success of sheared gels for this application, as well as all other silk constructs sensitive to environmental factors such as films, foams, and other silk hydrogels.

Catheter Compliance

As noted in the previous section, a semi-compliant catheter can regulate the force exerted on the syringe by the surgeon, greatly reducing variability in sheared gel rheology. The system used for experimentation during this project proved to be too compliant, as a correlation between plunger compression and gel extrusion was almost completely non-existent, eliminating tactile feedback for the surgeon. The rigidity of the catheter could be varied to achieve the ideal combination of material stiffness and tactile feedback in order to have controlled shear level and consistent material properties.

With more consistent solution and the force-limiting effect of an extensible catheter, it would be possible to construct a more accurate model of shear forces applied to the solution when passed through the needle and catheter. It is also possible that various additives could be used to increase plasticity (such as collagen or elastin materials) or stiffness (such as NaCl, Ethanol or nanoparticles) to achieve a slightly more controllable gelation method that will yield a construct with the desired properties.

6.1.4 Hybrid Materials

It is possible that a combination of many of these processes could work together to create a gel *in vivo*. For example, an RSF solution could be co-injected with a slightly acidic (pH>5), 0.9%w/v salinity (or lower) solution in a mixing syringe. The mixture would be sheared slightly in the catheter and needle system, causing some aggregation of micelles that may have formed immediately upon exposure to the additive solution. Upon entering the body, the temperature of the mixture would be slightly elevated, causing further acceleration of silk protein assembly. As long as assembly occurs before resorption, the material will successfully augment the vocal fold. The processing parameters of the silk solution used, as well as the quantities of each additive mixed in could be adjusted to achieve ideal mechanical properties. This silkworm-like gelation process seems quite promising, however results will still be subject to the high levels of variation in RSF solution, as well as solution age and syringe input force. By understanding the behaviors of silk under the influence of each of these mechanisms, it would be possible to model reactions and predict the behavior of any mixtures created. This

would allow for a wide range of variables to be explored without spending significant time and resources trying each combination of processing parameters individually.

6.2 Alternative Approach

Ideally, a more stable and longer lasting material could be used for augmentation. One possible solution to this problem is to use a silk material in a more solid, metastable state, such as HFIP processed silk to augment the vocal fold from outside the laryngeal cavity. As detailed in Figure 56, the procedure would combine the aspects of an injection laryngoplasty and a thyroplasty procedure, by injecting a small silk stent through the cartilage, which then applies a medializing force to the muscles behind the vocal fold. This would minimize the risk of infection by eliminating the need for an incision (as there is in a thyroplasty), reduce the amount of pain for the patient, and maintain a longer term augmentation than most vocal fold augmentation injection materials.

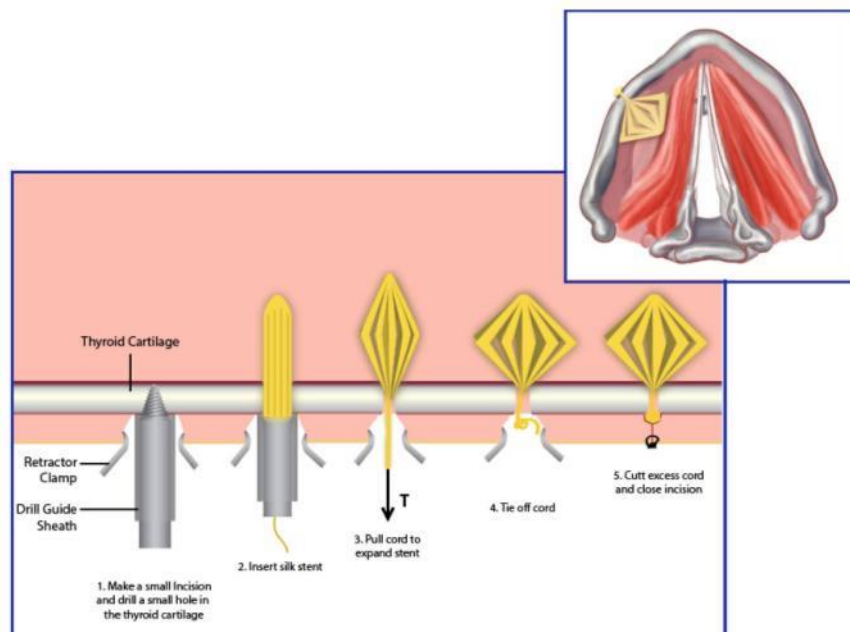


Figure 56: Alternative approach for using silk in vocal fold augmentations.

Appendix

Appendix I: Shear Flow Calculations

Hagen-Poiseuille Equation:

$$\Delta P = 8\mu \frac{LQ}{\pi r^4}$$

3 Sections: Needle, Syringe, Catheter.

Constants:

$$D_{Needle} = .210mm$$

$$D_{Catheter} = 1mm$$

$$D_{Syringe} = 4.5mm$$

$$L_{Needle} = 12.7mm$$

$$L_{Catheter} = 254mm$$

$$L_{Syringe} = 38mm$$

$$v = 8mm/s$$

Constraints:

$$F = 15-20N \text{ (Goal)}$$

$$\mu_{7\% \text{ 15mb RSF}} = 21.627 \text{ Pa-s}$$

Assumptions:

- incompressible fluid
- extensibility in the system is negligible
- constant force
- Fluid dependencies on applied shear are negligible

Syringe Calculations

$$Q = v * A = 8.5 \frac{mm}{s} * \left(\frac{\pi}{4} (4.5mm)^2 \right)$$

$$Q = 135.19mm^3/s$$

$$\Delta P = 8 * 21.627(pa - s) * \frac{38mm * 135.19mm^3/s}{\pi(2.25)^4}$$

$$\Delta P = 11039 \text{ Pa}$$

$$F = P * A = 11039(Pa) * \pi(2.25mm)^2$$

$$F = .1756N$$

Catheter Calculations

$$Q = 135.19mm^3/s \text{ (Flow rate remains constant due to continuity)}$$

$$\Delta P = 8 * 21.627(pa - s) * \frac{254mm * 135.19mm^3/s}{\pi(.5mm)^4}$$

$$\Delta P = 30.26 \text{ MPa}$$

$$F = P * A = 30.26(MPa) * \pi(.5mm)^2$$

$$F = 23.8N$$

Needle Calculations

$$Q = 135.19\text{mm}^3/\text{s} \text{ (Flow rate remains constant due to continuity)}$$

$$\Delta P = 8 * 21.627(\text{pa} - \text{s}) * \frac{12.7\text{mm} * 135.19\text{mm}^3/\text{s}}{\pi(.105\text{mm})^4}$$

$$\Delta P = 777.9 \text{MPa}$$

$$F = P * A = 777.9(\text{MPa}) * \pi(.105\text{mm})^2$$

$$F = 26.94 \text{N}$$

References

1. Carroll, T., E.F. Rosario Friedman, Gary Leisk, Personal Communication.
2. Carroll, T.L. and C.A. Rosen, *Trial vocal fold injection*. *Journal of Voice*, 2010. **24**(4): p. 494-498.
3. Martini, F., *Anatomy & Physiology*. 1st ed 2005, Singapore: Pearson Education Inc. as Prentice Hall.
4. Kahle, W., H. Leonhardt, and W. Platzer, *Color Atlas and Text of Human Anatomy - Internal Organs*. Vol. 2. 1993.
5. Thurnher, D., et al., *The glottis and subglottis: an otolaryngologist's perspective*. *Thoracic Surgery Clinics*, 2007. **17**(4): p. 549-560.
6. Institute, N.C. *The Larynx*. 2011.
7. Institute, N.C., *Laryngeal Anatomy*, 2011.
<http://visualsonline.cancer.gov/details.cfm?imageid=9257>
8. Antranik, *The Respiratory System*, 2011.
<http://antranik.org/the-respiratory-system/>
9. Chan, R.W. and I.R. Titze, *Dependence of phonation threshold pressure on vocal tract acoustics and vocal fold tissue mechanics*. *The Journal of the Acoustical Society of America*, 2006. **119**: p. 2351.
10. Seikel, J.A., D.W. King, and D.G. Drumright, *Anatomy and Physiology for Speech, Language, and Hearing*, 2010, Cengage Learning: Clifton Park, NY 12065-2919. p. 243-259.
11. Benninger, M.S., et al., *Vocal fold scarring: current concepts and management*. *Otolaryngology-Head and Neck Surgery*, 1996. **115**(5): p. 474-482.
12. *Operative Techniques in Laryngology* 2008: Springer Berlin Heidelberg.
13. Mallur, P.S. and C.A. Rosen, *Vocal fold injection: review of indications, techniques, and materials for augmentation*. *Clinical and experimental otorhinolaryngology*, 2010. **3**(4): p. 177-182.
14. Bruce Tan, M., *Vocal Fold Augmentation*, M. Sofia Lyford-Pike, Editor 2008.
15. Mertz Aesthetics, I. *Radiesse Voice Treatment Options*. 2011.
<http://www.radiesse-voice.com/pages.php?id=10&type=1>
16. Franco Jr, R.A., *Adduction arytenopexy, hypopharyngoplasty, medialization laryngoplasty, and cricothyroid sublaxation for the treatment of paralytic dysphonia and dysphagia*. *Operative Techniques in Otolaryngology-Head and Neck Surgery*, 2012. **23**(3): p. 164-172.
17. Remacle, M. and H.E. Eckel, *Surgery of Larynx and Trachea* 2010: Springer.
18. Thomas Carroll, M., *Current Management of Unilateral Vocal Fold Paralysis and Paresis*, 2012, Tufts Medical Center: Center for Voice and Swallowing.
19. Gray, H., *Gray's Anatomy*, W.H. Lewis, Editor 2000: Bartleby.com.

20. Chan, R.W. and I.R. Titze, *Viscosities of implantable biomaterials in vocal fold augmentation surgery*. The Laryngoscope, 2009. **108**(5): p. 725-731.
21. Rubin and Sataloff, *Vocal Fold Paresis and Paralysis*. Otolaryngology, 2007. **40**: p. 1109-1131.
22. O'Leary and G. M. Grillone, *Injection Laryngoplasty*. Otolaryngology, 2006. **39**: p. 43-54.
23. Chan, R.W. and I.R. Titze, *Viscoelastic shear properties of human vocal fold mucosa: measurement methodology and empirical results*. The Journal of the Acoustical Society of America, 1999. **106**: p. 2008.
24. Carroll, T.L. and C.A. Rosen, *Long-term results of calcium hydroxylapatite for vocal fold augmentation*. The Laryngoscope, 2011. **121**(2): p. 313-319.
25. Vepari, C. and D.L. Kaplan, *Silk as a biomaterial*. Progress in polymer science, 2007. **32**(8): p. 991-1007.
26. Rockwood, D.N., et al., *Materials fabrication from Bombyx mori silk fibroin*. Nature protocols, 2011. **6**(10): p. 1612-1631.
27. Kim, U.J., et al., *Three-dimensional aqueous-derived biomaterial scaffolds from silk fibroin*. Biomaterials, 2005. **26**(15): p. 2775-2785.
28. Meinel, L. and D.L. Kaplan, *Silk constructs for delivery of musculoskeletal therapeutics*. Advanced Drug Delivery Reviews, 2012.
29. Wang, X., et al., *Silk nanospheres and microspheres from silk/pva blend films for drug delivery*. Biomaterials, 2010. **31**(6): p. 1025-1035.
30. Wang, X., et al., *Silk microspheres for encapsulation and controlled release*. Journal of controlled release, 2007. **117**(3): p. 360-370.
31. Omenetto, F.G. and D.L. Kaplan, *New opportunities for an ancient material*. Science, 2010. **329**(5991): p. 528-531.
32. Yucel, T., P. Cebe, and D.L. Kaplan, *Vortex-induced injectable silk fibroin hydrogels*. Biophysical journal, 2009. **97**(7): p. 2044-2050.
33. Etienne, O., et al., *Soft tissue augmentation using silk gels: an in vitro and in vivo study*. Journal of periodontology, 2009. **80**(11): p. 1852-1858.
34. Sofia, S., et al., *Functionalized silk-based biomaterials for bone formation*. Journal of biomedical materials research, 2000. **54**(1): p. 139-148.
35. Wang, Y., et al., *In vivo degradation of three-dimensional silk fibroin scaffolds*. Biomaterials, 2008. **29**(24): p. 3415-3428.
36. Nagarkar, S., et al., *Structure and gelation mechanism of silk hydrogels*. Phys. Chem. Chem. Phys., 2010. **12**(15): p. 3834-3844.
37. Pritchard, E.M. and D.L. Kaplan, *Silk fibroin biomaterials for controlled release drug delivery*. Expert Opinion on Drug Delivery, 2011. **8**(6): p. 797-811.
38. Karageorgiou, V., et al., *Bone morphogenetic protein-2 decorated silk fibroin films induce osteogenic differentiation of human bone marrow stromal cells*. Journal of Biomedical Materials Research Part A, 2004. **71**(3): p. 528-537.

39. Karageorgiou, V., et al., *Porous silk fibroin 3-D scaffolds for delivery of bone morphogenetic protein-2 in vitro and in vivo*. Journal of Biomedical Materials Research Part A, 2006. **78**(2): p. 324-334.
40. Li, C., et al., *Electrospun silk-BMP-2 scaffolds for bone tissue engineering*. Biomaterials, 2006. **27**(16): p. 3115-3124.
41. Lu, S., et al., *Stabilization of enzymes in silk films*. Biomacromolecules, 2009. **10**(5): p. 1032-1042.
42. Lu, Q., et al., *Stabilization and release of enzymes from silk films*. Macromolecular bioscience, 2010. **10**(4): p. 359-368.
43. Altman, G.H., et al., *Silk-based biomaterials*. Biomaterials, 2003. **24**(3): p. 401-416.
44. Xia, X.-X., et al., *Tunable self-assembly of genetically engineered silk-elastin-like protein polymers*. Biomacromolecules, 2011. **12**(11): p. 3844-3850.
45. Wang, Y., et al., *Stem cell-based tissue engineering with silk biomaterials*. Biomaterials, 2006. **27**(36): p. 6064-6082.
46. Jin, H.J. and D.L. Kaplan, *Mechanism of silk processing in insects and spiders*. Nature, 2003. **424**(6952): p. 1057-1061.
47. Lee, Y.-W., *Silk reeling and testing manual*. Vol. 136. 1999: Food & Agriculture Organization of the UN (FAO).
48. Li, G., et al., *The natural silk spinning process*. European Journal of Biochemistry, 2002. **268**(24): p. 6600-6606.
49. Kim, U.J., et al., *Structure and properties of silk hydrogels*. Biomacromolecules, 2004. **5**(3): p. 786-792.
50. Valluzzi, R., et al., *Silk: molecular organization and control of assembly*. Philosophical Transactions of the Royal Society of London. Series B: Biological Sciences, 2002. **357**(1418): p. 165-167.
51. Matsumoto, A., et al., *Mechanisms of silk fibroin sol-gel transitions*. The Journal of Physical Chemistry B, 2006. **110**(43): p. 21630-21638.
52. Partlow, B., *Optimization of Silk Processing for Enhanced Mechanical Properties*, in *Mechanical Engineering 2012*, Tufts University. p. 76.
53. Li, M., et al., *Study on porous silk fibroin materials. I. Fine structure of freeze dried silk fibroin*. Journal of applied polymer science, 2001. **79**(12): p. 2185-2191.
54. Li, M., et al., *Study on porous silk fibroin materials. II. Preparation and characteristics of spongy porous silk fibroin materials*. Journal of applied polymer science, 2001. **79**(12): p. 2192-2199.
55. Nazarov, R., H.-J. Jin, and D.L. Kaplan, *Porous 3-D scaffolds from regenerated silk fibroin*. Biomacromolecules, 2004. **5**(3): p. 718-726.
56. Lv, Q. and Q. Feng, *Preparation of 3-D regenerated fibroin scaffolds with freeze drying method and freeze drying/foaming technique*. Journal of Materials Science: Materials in Medicine, 2006. **17**(12): p. 1349-1356.
57. Nam, J. and Y.H. Park, *Morphology of regenerated silk fibroin: Effects of freezing temperature, alcohol addition, and molecular weight*. Journal of applied polymer science, 2001. **81**(12): p. 3008-3021.

58. Matsumoto, A., et al., *Silk fibroin solution properties related to assembly and structure*. Macromolecular bioscience, 2008. **8**(11): p. 1006-1018.
59. Lotz, B. and F. Colonna Cesari, *The chemical structure and the crystalline structures of *Bombyx mori* silk fibroin*. Biochimie, 1979. **61**(2): p. 205-214.
60. Jin, H.-J., et al., *Bioprocessing of silk proteins-controlling assembly*. Bionanotechnology, 2006: p. 189-208.
61. Wang, X., et al., *Sonication-induced gelation of silk fibroin for cell encapsulation*. Biomaterials, 2008. **29**(8): p. 1054-1064.
62. Zhang, W., et al., *The use of injectable sonication-induced silk hydrogel for VEGF and BMP-2 delivery for elevation of the maxillary sinus floor*. Biomaterials, 2011. **32**(35): p. 9415-9424.
63. Foo, C.W.P., et al., *Role of pH and charge on silk protein assembly in insects and spiders*. Applied Physics A: Materials Science & Processing, 2006. **82**(2): p. 223-233.
64. Terry, A.E., et al., *pH Induced Changes in the Rheology of Silk Fibroin Solution from the Middle Division of *Bombyx mori* Silkworm*. Biomacromolecules, 2004. **5**(3): p. 768-772.
65. Kojic, N., et al., *Ion electrodiffusion governs silk electrogelation*. Soft Matter, 2012.
66. Yucel, T., et al., *Non-equilibrium silk fibroin adhesives*. Journal of structural biology, 2010. **170**(2): p. 406-412.
67. Hatzikiriakos, S.G., *Wall slip of molten polymers*. Progress in polymer science, 2012. **37**(4): p. 624-643.
68. Mackowiak, P.A. and J.A. Boulant, *Fever's glass ceiling*. Clinical infectious diseases, 1996. **22**(3): p. 525-536.
69. Rajkhowa, R., et al., *Reinforcing silk scaffolds with silk particles*. Macromolecular bioscience, 2010. **10**(6): p. 599-611.
70. Hu, X., et al., *Biomaterials derived from silk-tropoelastin protein systems*. Biomaterials, 2010. **31**(32): p. 8121.
71. Gelb, H., et al., *In vivo inflammatory response to polymethylmethacrylate particulate debris: effect of size, morphology, and surface area*. Journal of orthopaedic research, 2005. **12**(1): p. 83-92.